

การศึกษากลไกการทำงานของเอนไซม์ทรานส์กลูโคซิเดส OS9BGLU31



นางสาวจุฑามาส คำวงษา

วิทยานิพนธ์นี้เป็นส่วนหนึ่งของการศึกษาตามหลักสูตรปริญญาวิทยาศาสตรดุษฎีบัณฑิต

สาขาวิชาชีวเคมี

มหาวิทยาลัยเทคโนโลยีสุรนารี

ปีการศึกษา 2557

**FUNCTIONAL CHARACTERIZATION OF OS9BGLU31
TRANSGLUCOSIDASE**

Juthamath Komvongsa



**Thesis Submitted in Partial Fulfillment of the Requirements for the
Degree of Doctor of Philosophy in Biochemistry
Suranaree University of Technology
Academic Year 2014**

FUNCTIONAL CHARACTERIZATION OF OS9BGLU31 TRANSGLUCOSIDASE

Suranaree University of Technology has approved this thesis submitted in partial fulfillment of the requirements for the Degree of Doctor of Philosophy.

Thesis Examining Committee

(Assoc. Prof. Dr. Jatuporn Wittayakun)

Chairperson

(Prof. Dr. James R. Ketudat-Cairns)

Member (Thesis Advisor)

(Prof. Dr. Norman G. Lewis)

Member

(Assoc. Prof. Dr. Mariena Ketudat-Cairns)

Member

(Assoc. Prof. Dr. Polkit Sangvanich)

Member

(Asst. Prof. Dr. Panida Khunkaewla)

Member

(Prof. Dr. Sukit Limpijumnong)

Vice Rector for Academic Affairs
and Innovation

(Assoc. Prof. Dr. Prapun Manyum)

Dean of Institute of Science

จุฑามาส คำวงษา : การศึกษากลไกการทำงานของเอนไซม์ทรานส์กลูโคซิเดส S9BGLU31
(FUNCTIONAL CHARACTERIZATION OF OS9BGLU31 TRANSGLUCOSIDASE)

อาจารย์ที่ปรึกษา : ศาสตราจารย์ ดร.เจมส์ เกตุทัต-คาร์นส์, 116 หน้า.

เอนไซม์ข้าว Os9BGLu31 เป็นทรานส์กลูโคซิเดสในตระกูล Glycoside hydrolase family 1 (GH1) ที่มีความสามารถในการย้ายหมู่น้ำตาลกลูโคสให้กับสารในกลุ่มของกรดพีนอลิก ฟลาโวนอยด์ และสารกลุ่มฮอร์โมนพืช เอนไซม์ Os9BGLu31 มีความจำเพาะเจาะจงต่อพีนอลิก 1-O-β-กลูโคสเอสเทอร์ที่ทำหน้าที่เป็นตัวให้ (Donor) ได้ดีกว่าไกลโคไซด์ (Glycoside) นอกจากนี้กรดพีนอลิกอิสระของเอสเทอร์นี้ยังทำหน้าที่เป็นตัวรับ (Acceptor) ที่ดีอีกด้วย จากการศึกษาโครงสร้างของเอนไซม์โดย homology model พบว่ากรดอะมิโนที่อยู่รอบๆ บริเวณเร่งปฏิกิริยาของเอนไซม์ Os9BGLu31 ตัวนี้มีส่วนที่ไม่ชอบน้ำอยู่มากจึงได้ทำการสร้างตัวกลายพันธุ์ I172T L183Q L241D และ W243N พบว่าตัวกลายพันธุ์ W243N มีประสิทธิภาพสูงสุด และการกลายพันธุ์ที่ตำแหน่ง W243 (A D M N F และ Y) มีอัตราส่วนในการเติมกลูโคสให้กับแนฟทอล และ 1-แนฟทาลีนอะซิติกแอซิด อย่างน้อยสองเท่าในการทำปฏิกิริยาทรานส์กลูโคซิเลชันเมื่อเทียบกับ wild type จึงทดลองใช้เคมีเฟอร์อล ซึ่งเป็นสารในกลุ่มฟลาโวนอยด์ที่มีหมู่ไฮดรอกซิลในโมเลกุลอยู่ 4 ตัว มาใช้เป็นสารตั้งต้นตัวรับกลูโคส พบว่าตัวกลายพันธุ์ W243N มีประสิทธิภาพสูงกว่า wild type เอนไซม์ ดังนั้นตำแหน่งจำเพาะเจาะจงของการเติมหมู่กลูโคสให้กับเคมีเฟอร์อล จึงถูกนำมาเปรียบเทียบกับ wild type Os9BGLu31 และตัวกลายพันธุ์ W243 อื่นๆ ผลปรากฏว่า wild type Os9BGLu31 สามารถผลิตเคมีเฟอร์อล 7-O-กลูโคไซด์ได้เพียงหนึ่งชนิดเท่านั้น ในขณะที่ตัวกลายพันธุ์ W243 สามารถผลิตเคมีเฟอร์อล โมโนกลูโคไซด์ ได้ถึงสามชนิด และเคมีเฟอร์อล ไดกลูโคไซด์ อีกสามชนิด การศึกษาดำเนินการเติมน้ำตาลกลูโคสให้เคมีเฟอร์อลถูกวิเคราะห์โดยเทคนิคการใช้ประจุ Tandem mass spectrometry เพื่อแยกชนิดของเคมีเฟอร์อล โมโนกลูโคไซด์ ที่ตำแหน่ง 3-O 7-O และ 4'-O กลูโคไซด์ และเคมีเฟอร์อล ไดกลูโคไซด์ ที่ตำแหน่ง 3-O 7-O และ 4'-O ไดกลูโคไซด์ ตามหลักความเสถียรของการทำให้เกิดอนุมูลอิสระหลังการเสียหมู่กลูโคส ตัวกลายพันธุ์ Os9BGLu31 W243 ยังสามารถใช้ เคมีเฟอร์อล 3-O-กลูโคไซด์เป็นสารตั้งต้นตัวให้กลูโคสได้ดีกว่า นอกจากนี้ยังสรุปได้ว่า W243F และ W243Y ให้ผลคล้ายกับ wild type จากผลดังกล่าวนี้พบว่าตัว W243 มีความจำเพาะอย่างยิ่งต่อสารตั้งต้นและสารผลิตภัณฑ์ของ Os9BGLu31

เอนไซม์ทรานส์กลูโคซิเดส Os9BGLu31 มีบทบาทในเมตาบอลิซึมของพืชรวมทั้งในข้าว ด้วยจากการศึกษาด้วยเครื่อง Ultra performance liquid chromatography-mass spectrometry (UPLC-MS) ในการคุมเมตาบอลิโพรไฟล์ของสารสกัดจากใบของข้าว พบว่าสารสกัดจากใบของข้าว

ประกอบด้วย ฟลาโวนอยด์สโกลโคน และสโกลโคไซด์ โดยมีการเปรียบเทียบสารสำคัญระหว่างข้าวปกติ wild type กับข้าวที่ยับยั้งการแสดงออกของยีน Os9BGlu31 โดยวิธี homologous T-DNA และ Tos17/2 ซึ่งเป็นการทำให้การแสดงออกของยีน Os9BGlu31 ลดต่ำลงจนถึงไม่มีการแสดงออกของยีนนี้อีกเลย เพื่อศึกษาการเพิ่มขึ้นหรือการลดลงของสารที่เกิดจากการขาดเอนไซม์ Os9BGlu31 จากการศึกษาพบว่า มีสารหนึ่งชนิดที่มีปริมาณเพิ่มขึ้นในข้าวที่เป็น homologous knockout Os9BGlu31 คือ 1-*O*-feruloyl β -D-glucoside (FAG) ซึ่งเป็นสารตั้งต้นตัวให้กลูโคสของ Os9BGlu31 ที่มีรายงานการศึกษาแบบ *in vitro* มาก่อนแล้ว การศึกษานี้พบว่าในใบธงของข้าว knockout Os9BGlu31 มี FAG อยู่ในปริมาณมากและยังพบการลดลงของสารที่เทียบเป็น Tricin 4'-(guaiacylglyceryl)ether 7-*O*-glucoside ที่สามารถใช้เป็นสารตั้งต้นตัวให้กลูโคสของ Os9BGlu31 ในการทดลองแบบ *in vitro* ครั้งนี้ด้วย สารนี้อาจเป็นสารตั้งต้นหรือผลิตภัณฑ์ที่สำคัญของข้าว งานวิจัยนี้เป็นงานวิจัยชิ้นแรกที่ทำการศึกษาการทำงานของ Os9BGlu31 ในข้าว



JUTHAMATH KOMVONGSA : FUNCTIONAL CHARACTERIZATION
OF OS9BGLU31 TRANSGLUCOSIDASE. THESIS ADVISOR : PROF.
JAMES R. KETUDAT-CAIRNS, Ph.D. 116 PP.

Rice Os9BGlu31 is a glycoside hydrolase family 1 (GH1) transglucosidase that can transfer glucose to phenolic acids, flavonoids, and phytohormones. Os9BGlu31 displays broad specificity, with phenolic 1-*O*- β -D-glucose esters acting as better glucosyl donors than glucosides, whereas the free phenolic acids of these esters are also excellent acceptor substrates. Based on homology modeling of this enzyme, we made single point mutations of residues surrounding the acceptor binding region of the Os9BGlu31 active site, including I172T, L183Q, L241D, and W243N. The most active variant produced was W243N, and all variants with mutations at W243 (to A, D, M, N, F and Y) had at least a 2-fold higher ratio of naphthol to naphthalene acetic acid transglucosylation compared to wild type Os9BGlu31. Kaempferol is a flavanol containing 4 hydroxyl groups, on which the Os9BGlu31 W243N mutant activity was considerably higher than that of wild type recombinant enzyme. Therefore, the regioselectivity for kaempferol glucosylation was compared between Os9BGlu31 wild type and its W243 mutants. The wild type Os9BGlu31 recombinant enzyme produced only 7-*O*-glucoside in significant amounts, while the W243 variants produced up to 3 kaempferol monoglucosides and 3 diglucosides. Fragmentation analysis by negative ion electrospray ionization tandem mass spectrometry identified the kaempferol mono-*O*-glucosides as 3-*O*, 7-*O*, and 4'-*O* glucosides and di-*O*-glucosides as 3,7-*O*, 4'7-*O*, and 3,4'-*O* kaempferol diglucosides, based on the expected stability of different radical products of glucosyl group loss. The Os9BGlu31 W243 mutants were also better able

to use kaempferol 3-*O*-glucoside as a donor substrate, although the W243F and W243Y variants were similar to wild type. Therefore, the W243 residue was found to be critical to the substrate and product specificity of Os9BGlu31.

The role of Os9BGlu31 transglucosidase in rice plant metabolism has only been speculated to date. We tentatively identified various compounds in rice flag leaf extracts, including flavonoid aglycones and glycosides, by ultra performance liquid chromatography-mass spectrometry (UPLC-MS)-based metabolite profiling. Extracts of homologous T-DNA and Tos17/2 insertion *os9bglu31* knockout lines were compared to those of paired homozygous *Os9BGlu31* wild type lines to identify compounds that accumulated or are decreased in the absence of Os9BGlu31. One compound that accumulated in the homozygous knockout lines, was 1-*O*-feruloyl- β -D-glucoside (FAG), which has been reported as a glucosyl donor substrate of Os9BGlu31 *in vitro*. We discovered that FAG is the substrate for Os9BGlu31 *in vivo*, since FAG is accumulated in flag leaves of Os9BGlu31 knockout lines. Certain compounds in the rice flag leaf extracts, including one with a mass matching tricetin 4'-*O*-(guaiacylglyceryl)ether 7-*O*-glucoside, could also serve as Os9BGlu31 donor substrates in an *in vitro* assay, suggesting they may also be potential substrates or products in the plant. This work provides the first experimental evidence for the function of Os9BGlu31 *in planta*.

School of Biochemistry

Academic Year 2014

Student's Signature _____

Advisor's Signature _____

ACKNOWLEDGEMENTS

First, I would like to express my sincere gratitude to my thesis advisor, Prof. Dr. James R. Ketudat-Cairns, for providing me the opportunity to study towards my Ph.D. degree in Biochemistry and his excellent guidance, caring, patience and encouragement.

I am very grateful to Assoc. Prof. Dr. Mariena Ketudat-Cairns for her valuable guidance, advice on plant β -glucosidase work, and mental support. I am also deeply grateful to Prof. Dr. Norman G. Lewis for providing me a chance to do some part of my research at Institute of Biological Chemistry, Washington State University, Pullman, WA, USA and his advice on the metabolite analysis.

I would like to thank Dr. Joaquim V. Marque for training, advising, and his excellent guidance on UPLC-MSMS with metabolite profiling. I thank Dr. Sukanya Luang for cloning and constructing of pET32a/*Os9BGlu31* and designing some of the mutations. Mr. Bancha Mahong is gratefully acknowledged for isolation and breeding of rice T-DNA insertion lines and providing me both wild type and knockout *Os9BGlu31* rice flag leaf specimens.

I sincerely thank Assoc. Prof. Dr. Jatuporn Wittayakun, Prof. Dr. Norman G. Lewis, Assoc. Prof. Dr. Mariena Ketudat-Cairns, Assoc. Prof. Dr. Polkit Sangvanich, and Asst. Prof. Dr. Panida Khunkeawla for patiently reading this dissertation and providing helpful comments.

Special thanks are extended to all my friends in the School of Biochemistry, Suranaree University of Technology for their help, and to all my friends at Institute of

Biological Chemistry, Washington State University, WA, USA for their help, advice, and guidance.

Finally, I would like to express my deepest gratitude to my family. They were always supporting me, encouraging me and cheering me up with their best wishes.

This work was supported by the Thailand Research Fund, the Royal Golden Jubilee Scholarship Ph.D. Program and the National Research University Project to Suranaree University of Technology from the Commission on Higher Education of Thailand.

Juthamath Komvongsa



CONTENTS

	Page
ABSTRACT IN THAI	I
ABSTRACT IN ENGLISH.....	III
ACKNOWLEDGEMENTS	V
CONTENTS	VII
LIST OF TABLES	XI
LIST OF FIGURES.....	XII
LIST OF ABBREVIATIONS AND SYMBOLS	XVI
CHAPTER	
I INTRODUCTION.....	1
1.1 General introduction.....	1
1.2 Research objectives	6
1.3 Research scope.....	7
II LITERATURE REVIEW.....	8
2.1 Glycoside hydrolases, glycosyltransferase, and transglucosidases	8
2.1.1 Glycosyltransferase	8
2.1.2 Glycoside hydrolases	9
2.1.3 Transglucosidase	12
2.1.4 Classification by function and E.C. number	13
2.1.5 Glycoside hydrolase and glycosyltransferase families	13

CONTENTS (Continued)

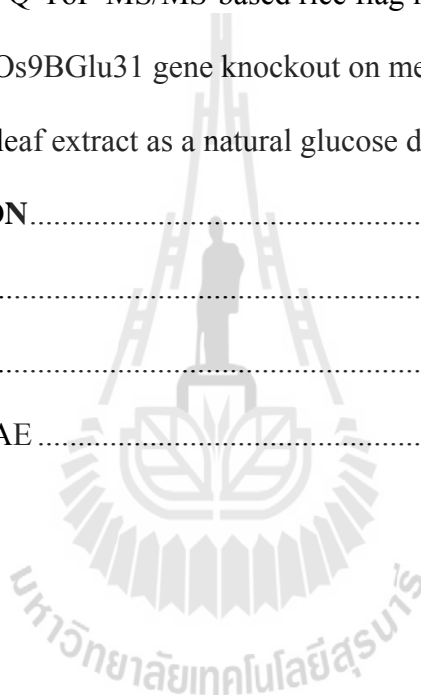
	Page
2.2 Glycosyltransferase, glycoside hydrolase, and transglycosidase mechanisms.....	14
2.3 Catalytic nucleophile and acid/basic mutants.....	18
2.3.1 Rescue of catalytic nucleophile mutants.....	18
2.3.2 Rescue of catalytic acid/base mutants.....	20
2.4 β -Glycoside hydrolase and GH family 1	22
2.5 GH1 transglycosidases.....	24
2.6 Role of GH1 enzyme in rice	25
2.7 Site-directed mutagenesis and directed evolution	27
2.8 Mass spectrometry	29
2.9 Metabolite profiling of glycoconjugates.....	31
2.10 Flavonoids.....	33
III MATERIALS AND METHODS	36
3.1 General materials	36
3.1.1 Plasmid and bacterial strain	36
3.1.2 Oligonucleotide and mutagenesis primers	37
3.1.3 Phenolic compounds and flavonoids.....	38
3.1.4 Freeze-dried rice flag leaves	39
3.2 General methods	39
3.2.1 Competent cell preparation	39
3.2.2 Bacterial transformation.....	40

CONTENTS (Continued)

	Page
3.2.3 Site-directed mutagenesis.....	40
3.2.4 SDS-PAGE.....	41
3.2.5 Extraction of wild type and Os9BGlu31 knockout rice flag leaves.....	42
3.3 Protein expression and purification	43
3.4 Relative activities of Os9BGlu31 wild type and mutants.....	44
3.5 Evaluation of transglucosylation of kaempferol with 4NPGlc and kaempferol 3- <i>O</i> -glucoside	45
3.6 Rice flag leaf extracts as natural substrate for Os9BGlu31 enzyme assay.....	46
3.6.1 UPLC G2 Q-ToF mass spectrometry analysis system.....	46
3.6.2 UPLC triple quadrupole mass spectrometry analysis system	47
IV RESULTS AND DISCUSSION	49
4.1 Os9BGlu31 expression and purification.....	49
4.2 Effect of mutations of W243, L183, and I172 on Os9BGlu31 activity....	51
4.3. Substrate specificity for transglucosylation of Os9BGlu31 W243 mutants.....	54
4.4 Determination of the glucosylation position and fragmentation patterns of kaempferol mono- <i>O</i> -glucosides.....	59
4.5 Fragmentation behavior of kaempferol di- <i>O</i> -glucosides.....	66

CONTENTS (Continued)

	Page
4.6 Kaempferol 3- <i>O</i> -glucoside as acceptor and donor for Os9BGlu31	
W243 mutants.....	71
4.7 UPLC G2 Q-ToF-MS/MS-based rice flag leaf metabolite profiling.....	75
4.8 Effect of Os9BGlu31 gene knockout on metabolite profile	80
4.9 Rice flag leaf extract as a natural glucose donor	89
V CONCLUSION	93
REFERENCES.....	96
APPENDIX.....	114
CURRICULUM VITAE.....	116



LIST OF TABLES

Table	Page
2.1 Accumulation of flavonoids in rice flag leaves	33
3.1 Oligonucleotide primers for site-directed mutagenesis.....	37
4.1 Parameters of kaempferol glucosides observed in UPLC G2-Q-ToF-MS ^E	61
4.2 Putative identification of compounds from wild type rice flag leaves extracted in 70% methanol in water	77
4.3 Putative compounds extracted from wild type rice flag leaves in 5% methanol in water	79
4.4 The 1- <i>O</i> -feruloyl- β -D-glucoside (FAG ester) peak areas in UPLC G2-Q- ToF-MS for homozygous knockout Os9BGlu31 lines <i>bglu31-4</i> , <i>bglu31-1</i> , <i>bglu31-2</i> , and <i>bglu31-3</i> and corresponding wild type segregation lines	87
4.5 1- <i>O</i> -feruloyl- β -D-glucopyranoside concentration in 70% methanol in water extracts of rice flag leaves determined by UPLC triple quadrupole- MSMS.....	88
4.6 1- <i>O</i> -NAA-glucosyl (NAA-Glc) ester produced by Os9BGlu31 in <i>in vitro</i> enzymatic reactions with rice flag leaf extracts.....	91

LIST OF FIGURES

Figure	Page
2.1 Glycosyltransferases catalyze glycosyl group transfer with either inversion or retention of the anomeric stereochemistry with respect to the donor sugar ...	9
2.2 General catalytic mechanism of glycoside hydrolase activity	10
2.3 Endo/exo-acting glycoside hydrolases	10
2.4 Retaining and inverting glycoside hydrolase mechanisms	11
2.5 Glycosidase mechanisms for hydrolysis.	16
2.6 Unusual glycosidase mechanisms	18
2.7 Rescue of catalytic activity in the nucleophile mutant of <i>Sulfolobus solfataricus</i> β -glucosidase by formate.....	19
2.8 Mechanism of transglycosylation with a glycosynthase	20
2.9 Rescue of catalytic activity in the acid/base mutants by azide utilizes ascorbate as a general base catalyst	21
2.10 A natural version of chemical rescue with <i>Sinapis alba</i> myrosinase.....	22
2.11 β -Glucosidase structure from various GH families.....	23
3.1 Diagram of the protein-coding sequence of recombinant pET32a (+)/DEST with the <i>Os9bglu31</i> cDNA inserted after the enterokinase cleavage site by directional Gateway recombination cloning.....	36
4.1 Silver staining SDS-PAGE of Os9BGlu31 W243N throughout purification	50

LIST OF FIGURES (Continued)

Figure	Page
4.2	Superposition of a homology model of Os9BGlu31 transglucosidase on the x-ray crystal structure of the Os3BGlu6 β -glucosidase covalent intermediate with 2-fluoro- α -D-glucoside (PDB code 3GNR).52
4.3	Relative activities of Os9BGlu31 and its active site cleft mutants with various acceptors53
4.4	Activity versus curves of Os9BGlu31 W243 mutants55
4.5	Chromatograms of reaction mixtures of Os9BGlu31 W243 variants transfer of glucose to phenolic acid acceptors56
4.6	Chromatograms of products from kaempferol transglycosylation by wild type and W243N variants of Os9BGlu31 using 4NPGlc as a glucosyl donor62
4.7	The fragmentation pathways of kaempferol mono- <i>O</i> -glucoside: 3- <i>O</i> -glucoside63
4.8	[M-H] ⁻ product ion spectra of compounds 4, 5, and 6 in negative ion mode64
4.9	Kaempferol structural diagram representing radical delocalization positions from homolytic cleavage ions of glucose65
4.10	[M-H] ⁻ product ion mass spectra of compounds 1, 2, and 3 in negative ion mode67

LIST OF FIGURES (Continued)

Figure	Page
4.11 The fragmentation pathways of kaempferol 3,7-di- <i>O</i> -glucoside and the possible mechanism for the formation of radical ions observed in the MS/MS spectra.....	68
4.12 The fragmentation pathways of kaempferol 4',7-di- <i>O</i> -glucoside and the possible mechanism for the formation of radical ions observed in the MS/MS spectra.....	69
4.13 The fragmentation pathways of kaempferol 3,4'-di- <i>O</i> -glucoside and the possible mechanism for the formation of radical ions observed in the MS/MS spectra.....	70
4.14 Chromatograms of reaction solutions of Os9BGlu31 wild type and W243N mutant using kaempferol 3- <i>O</i> - β -D-glucoside alone as substrate	73
4.15 Comparison of reaction products for glycosylation of kaempferol by Os9BGlu31 WT and W243 variants.	74
4.16 The chromatogram of rice flag leaf extracts in in positive (A) and negative ion mode (B) from extraction with 70% methanol in water	76
4.17 The chromatogram of rice flag leaf extracts in positive (A) and negative ion mode (B) from extraction with 5% (v/v) methanol in water.....	78
4.18 The UPLC G2 Q-ToF-MS total ion chromatogram of 70% methanol extracts of wild type (A) and the homologous Os9BGlu31 knockout line <i>osbglu31-2</i> (B) rice flag leaves	82

LIST OF FIGURES (Continued)

Figure	Page
4.19	The specific selected ion (m/z 355.1035) UPLC G2 Q-ToF-MS chromatogram showing the accumulation of 1- <i>O</i> -feruloyl- β -D-glucose (m/z 355.1035) in knockout line.....83
4.20	The standard curve of specific fragment ion response for ferulic acid concentration at m/z 134.....84
4.21	The standard curve of specific fragment ion response to 1- <i>O</i> -feruloyl- β -D-glucose concentration.....85
4.22	The chromatogram from UPLC ESI MRM triple quadrupole mass spectrometer showing the selected precursor ion at m/z 35586
4.23	The chromatogram of 1- <i>O</i> -naphthalene acetic acid β -D-glucose ester (NAA-glucosyl ester) production from Os9BGlu31 reaction using rice flag leaf extracts as the glucose donor source.....90
4.24	Mass spectra of 1- <i>O</i> -naphthalene acetic acid- β -D-glucoside (NAA-glucosyl ester) m/z of 347.1136 (A) and the putative triclin 4'- <i>O</i> -(guaiacylglyceryl)ether 7- <i>O</i> -glucoside m/z of 687.1925 (B)92

LIST OF ABBREVIATIONS AND SYMBOLS

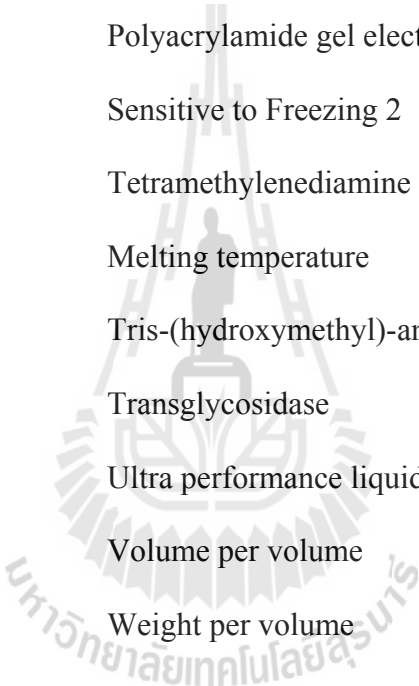
(m, μ)l	(milli, micro) Liter
(m, μ)g	(milli, micro) Gram
(m, μ)M	(milli, micro) Molar
(μ)mol	(micro) Mole
AAGT	Acyl-glucose-dependent anthocyanin glucosyl transferase
bp	Base pair(s)
BSA	Bovine serum albumin
CV	Column volume(s)
DMSO	Dimethyl sulfoxide
DNA	Deoxyribonucleic acid
DNase	Deoxyribonuclease
DTT	Dithiothreitol
ESI	Electrospray ionization
FA	Ferulic acid
FAG	1- <i>O</i> -feruloyl- β -D-glucose ester
GGGT	Galactolipid-galactosyltransferase
GH	Glycoside hydrolase
GH1	Glycoside hydrolase family 1
GT	Glycosyltransferase
h	Hour

LIST OF ABBREVIATIONS AND SYMBOLS (Continued)

HPLC	High performance liquid chromatography
4HBA	4-hydroxybenzoic acid
IMAC	Immobilized metal affinity chromatography
IPTG	Isopropyl thio- β -D-galactoside
kDa	Kilo Dalton
l	Liter
LC	Liquid chromatography
LC-MS	Liquid chromatography-mass spectrometry
M	Molar
MES	2-morpholinoethanesulfonic acid
min	Minute
MRM	Multiple reaction monitoring
MS ^E	Data independent acquisition multiplexed MS/MS
MSMS	Tandem mass spectrometry
MWCO	Molecular weight cut off
NAA	1-naphthalene acetic acid
NAA-Glc	1-naphthalene <i>O</i> - β -D-glucose ester
NBT	<i>p</i> -nitrobenzenethiol
nm	Nanometer
NMR	Nuclear Magnetic Resonance
4NP	4-nitrophenyl
4NPGlc	4-nitrophenyl- β -D-glucopyranoside

LIST OF ABBREVIATIONS AND SYMBOLS (Continued)

OD	Optical density
PMSF	Phenyl methylsulfonyl fluoride
rpm	Revolutions per minute
SDS	Sodium dodecyl sulfate
SDS-PAGE	Polyacrylamide gel electrophoresis with SDS
SFR2	Sensitive to Freezing 2
TEMED	Tetramethylethylenediamine
T _m	Melting temperature
Tris	Tris-(hydroxymethyl)-aminoethane
TG	Transglycosidase
UPLC	Ultra performance liquid chromatography
v/v	Volume per volume
w/v	Weight per volume



CHAPTER I

INTRODUCTION

1.1 General introduction

Glycosylation is an important mechanism involved in controlling the bioactivity of many plant metabolites, including phytohormones and defense compounds (Bowles *et al.*, 2006; Wei *et al.*, 2013). The formation and cleavage of glycosyl linkages in these conjugates can be mediated by glycosyltransferases (GTs), glycoside hydrolases (GHs), and transglycosidases (TGs) (Lairson and Withers, 2004). The enzymatic formation of glycosidic bonds can be performed by both glycosyltransferases, which use nucleotide or phospholipid sugars as donor substrates, and transglycosidases, which transfer sugars from other donor substrates.

Although GH family GH1 enzymes have long been known to catalyze transglycosylation in addition to hydrolysis, natural TGs belonging to GH1 have only recently been described (Moellering *et al.*, 2010; Matsuba *et al.*, 2010). Galactolipid-galactolipid galactosyl transferase (GGGT), a chloroplast membrane remodeling enzyme, was recently found to correspond to the GH1 protein SFR2 (Moellering *et al.*, 2010). GH1 enzymes were also found to be acyl-glucose-dependent anthocyanin glucosyl transferases (AAGT, which in fact are TGs), responsible for the adding a second glucosyl moiety on anthocyanidin 3-*O*-glucoside in certain flowers (Matsuba *et al.*, 2010). AAGT were subsequently demonstrated to collaborate with acyl-glucose dependent acyl transferases to build up large anthocyanin complexes by a series of sugar

and acyl transfers to the anthocyanin backbone (Nishizaki *et al.*, 2013). The Arabidopsis GH1 enzyme AtBGLU10 was shown to play a similar anthocyanin TG role (Miyahara *et al.*, 2013).

The transfer and hydrolysis of glycosyl moieties on glycoconjugates can occur with retention or inversion of the configuration of the anomeric carbon in the glycosidic bond, but the TG described to date are primarily retaining enzymes (Lairson and Withers, 2004; Matsuba *et al.*, 2010; Ketudat Cairns *et al.*, 2012). There are a large number of retaining glycosidases that catalyze both hydrolysis and transglycosylation, but not much is known regarding what determines the ratio between the transglycosylation and hydrolysis reactions (Teze *et al.*, 2013). Glycosidases are abundant in nature and can be applied for transglycosylation of simple substrates. However, the hydrolysis of synthetic products results in low reaction yields. The problem of product hydrolysis can be solved by the use of glycosynthases (Mackenzie *et al.*, 1998), a class of genetically engineered glycosidases in which the catalytic nucleophile (glutamate or aspartate) residue is altered to a small, neutral amino acid, such as alanine, glycine, or serine. A number of glycosynthases derived from glycosidases belonging to different GH families have been developed and used to construct oligosaccharides (Mackenzie *et al.*, 1998; Teze *et al.*, 2013), polysaccharides, glycosides, glycosphingolipids, and glycoproteins (Wei *et al.*, 2013).

Due to the need for synthesis of glycosides and oligosaccharides for a variety of purposes and the relative expense of the nucleotide sugar substrates of GTs, significant efforts have been made to increase the transglycosylation activities of glycoside hydrolases or improve the product specificities of transglycosidases. In GH family GH16, a surface loop thought to affect acceptor substrate binding was identified to help

differentiate between a xyloglucan endohydrolase and xyloglucan endotransferase (XET, a TG) (Baumann *et al.*, 2007), but the critical determinant of transglycosylation activity is generally unclear.

β -Glucosidases are one set of enzymes of interest for both their hydrolysis and transglycosylation activities, and the broadest range of specificities of these enzymes are found in plants (Ketudat Cairns and Esen, 2010). Plant β -glucosidases are involved in the defense against pests, phytohormone activation, lignification, and cell wall degradation. Many β -glucosidases belong to glycoside hydrolase family GH1 and contain the highly conserved amino acid sequences of T(F/L)NEP at the catalytic acid/base and (I/V)TENG at the catalytic nucleophile (Ketudat Cairns *et al.*, 2012). The GH1 β -D-glycosidases have a wide range of aglycone specificities, with substrates including oligosaccharides, cyanogenic glucosides, phytohormone glycoconjugates, flavonoid and isoflavonoid glycosides, the monoterpene indole alkaloid precursor strictosidine, and benzoxanoids.

Rice Os9BGlu31 is a vacuolar transglucosidase belonging to GH1 and acts to transfer glucose between phenolic acids, phytohormones, and flavonoids (Luang *et al.*, 2013). It shows highest activity with feruloyl glucose and similar phenolic acid esters as donors, whereas the free phenolic acids of these esters are also excellent acceptor substrates. When no acceptor is present, Os9BGlu31 4-nitrophenyl- β -D-glucoside (4NPGlc) hydrolysis activity is approximately 10% of its transglycosylation activity in the presence of 0.25 mM ferulic acid, but in the presence of such acceptors insignificant amounts of glucose are released. This suggests that Os9BGlu31 may help equilibrate the free phenolic acids and phenolic acid conjugate levels in plants and thereby play

roles in plant growth and cell wall synthesis (Luang *et al.*, 2013). Although Os9BGlu31 does not transfer glucose to cyanidin 3-*O*-glucoside, the preferred acceptor substrate of acyl glucose-dependent anthocyanin transglucosidases from carnation and delphinium (Matsuba *et al.*, 2010), it is able to use apigenin 7-*O*-glucoside as a glucosyl donor and apigenin as an acceptor (Luang *et al.*, 2013).

Rice Os9BGlu31 displays an unusual lack of inhibition by mechanism-based inhibitors of GH1 β -glucosidases. However, mutagenesis showed that the E179 and E369 residues corresponding to the conserved catalytic acid-base and nucleophile in GH1 glycosidases are important for Os9BGlu31 catalysis, supporting the idea that it uses a double displacement retaining mechanism similar to GH1 β -glucosidases. The residue preceding the catalytic nucleophile is typically a threonine in plant GH1 β -glucosidases, but is a histidine (H368) in Os9BGlu31 transglucosidase. However, mutating H368 to T had no effect on the ratio of transglycosylation to hydrolysis.

Flavonoids are a widely distributed group of natural products found in plants, and have been classified according to their chemical structures. Flavones and flavonols are in the anthoxanthins group, members of which have a very similar core structure but differences in the number and position of hydroxyl and methoxyl groups. They have potential health benefits arising from antioxidant, radical scavenging, anti-inflammatory, and antiviral activities (Nijjivelt *et al.*, 2001; Rora and Nair, 1998). Kaempferol is in the flavonol subgroup with four hydroxyl groups at the 3, 5, 7, and 4' positions, and it has been found to be glucosylated at 3, 7, and 4' positions in different plant species (Gaynor *et al.*, 1988). Flavonoids have been widely characterized using LC-ESI-MS, including both glycosides and aglycones (Hvattum and Ekeberg, 2003; Wang *et al.*, 2008; Staszko *et al.*, 2011; Irakli *et al.*, 2012). Electrospray ionization

tandem mass spectrometry (ESI-MS/MS) has been used in the structural characterization of flavonoid glycosides, including aglycone structure and glycosylation pattern (Luczkiewicz *et al.*, 2004; Fabre *et al.*, 2001; Cuychens and Claeys, 2004; Sinseadka *et al.*, 2010).

In this study, I have characterized the effects of mutations of residues surrounding the aglycone/acceptor binding site of Os9BGlu31 on glucosyl transfer to different acceptors. The product regio-specificity of variants mutated at W243 was also investigated in experiments using kaempferol as a model and monitoring the production of mono- and di-glucosides, which were identified from their differential fragmentation patterns.

Metabolomics is defined as the analysis of all metabolites in an organism (Oikawa *et al.*, 2008). Metabolomics provides the possibility of clarifying gene functions directly connected to rice quality, since the metabolome, implying the varieties and amounts of all metabolites in the organism, is related to important traits of rice, such as the yield, nutrient content, and defense mechanisms (Fenie *et al.*, 2004; Jung *et al.*, 2013; Franceschi *et al.*, 2012). Plant metabolomics has a possibility to be applied to various purposes in addition to the studies exemplified above. Recently, several *Arabidopsis* studies have demonstrated that integration of transcriptomic and metabolomic datasets is a strategy for the functional identification of metabolism-related genes (Matsuda *et al.*, 2009; Matsuda *et al.*, 2012).

The methodology in metabolomics tends to converge on several analytical instruments, such as infused high-performance MS, hyphenated MS, and nuclear magnetic resonance spectroscopy (NMR) (Cuychens *et al.*, 2004; Fiehn *et al.*, 2000). Liquid chromatography-mass spectrometry (LC-MS), which couples an MS to a high

performance liquid chromatography (HPLC) or similar liquid chromatography system, has been a powerful tool for metabolite profiling of secondary metabolites (Matsuda *et al.*, 2012; Oikawa *et al.*, 2008; Chen *et al.*, 2013). However, the development of more high-throughput and high-sensitivity methods and more powerful software for analysis and standardization of methods may be expected to improve metabolomic analysis in the future. Nonetheless, LC-MS is already a powerful tool for profiling of secondary metabolites including alkaloids, flavonoids, and phenyl propanoids (Dettmer *et al.*, 2007).

In this work we have characterized rice secondary metabolites by UPLC-MSMS of wild type and Os9BGlu31 knockout rice flag leaf extracts to identify compounds found at different levels in the mutant and wild type rice, which may reflect different substrates and products or downstream metabolites. We have also used rice extract as a source of natural glucosyl donor substrates for Os9BGlu31 to transfer glucose to a synthetic acceptor in order to identify potential natural glucosyl donors. We found that Os9BGlu31 can transfer glucose from the extract components to 1-naphthalene acetic acid, in a manner similar to that seen with synthetic glucosyl donor.

1.2 Research objectives

The objectives for this research thesis are listed below.

1.2.1 To investigate the mechanism of Os9BGlu31 transglycosylation selectivity by site-directed mutagenesis, kinetic studies, and inhibition studies.

1.2.2 To apply Os9BGlu31 or its mutants to glycosylation of compounds for, e.g. production of flavonoid glucosides or other glucosylated compounds.

1.2.3 To develop a method for metabolite profiling of rice flag leaves and detection of the differences between extracts of wild type and Os9BGlu31 knockout

rice flag leaves *in vivo* by liquid chromatography and tandem mass spectrometry (LC-MSMS).

1.2.4 To identify natural glycoconjugates that are substrates of Os9BGlu31 by targeted profiling with LC-MSMS.

1.3 Research scope

The scope of this project is to characterize the Os9BGlu31 mechanism for selection of acceptor substrates by production of mutations around the active site and substrate-binding cleft to see whether it can be converted to a hydrolase. The selection of mutations was based on sequence differences in this region between Os9BGlu31 and GH1 hydrolytic enzymes. In the course of this work, the Os9BGlu31 mechanism was characterized, in terms of dependence of the ratio of transglycosylation to hydrolysis activities on active site cleft residues. Application of these mutant enzymes for production of flavonoid glucosides, such as mono- and di-glucosides of kaempferol, was performed and glycosylation positions were determined by UPLC-MSMS. The glycosylation position of these products was characterized by comparison of the relative abundance of fragment ions and those expected from homolytic cleavage theory.

A second aspect of this work was the development of a method for profiling secondary metabolite glycoconjugates in plant extracts by UPLC-MSMS, and use of this method to identify substrates and products in rice extracts and after *in vitro* reactions with the recombinant Os9BGlu31 enzyme. Wild type and knockout Os9BGlu31 were differentiated using these methods to characterize the different components in rice flag leaves provided by our colleagues in Korea.

CHAPTER II

LITERATURE REVIEW

2.1 Glycosyltransferases, glycoside hydrolases, and transglycosidases

Carbohydrates have many important functions in living organisms, including structural, storage, and signaling roles, and these functions are controlled by the enzymes that synthesize, breakdown and modify the carbohydrates. Carbohydrate active enzymes include glycoside hydrolases (GH), glycosyltransferases (GT), polysaccharide lyases (PL), and carbohydrate esterases (CE), according to the CAZY website (Cantarel *et al.*, 2009). Of these enzymes, the GHs and GTs are most responsible for the addition and removal of glucosyl residues from various complex carbohydrates, polysaccharides and glycoconjugates.

2.1.1 Glucosyltransferases

Glycosyltransferases (GTs; EC 2.4.x.y) catalyze the formation of O -, N-, S - and C-glycosidic bonds by the attachment of a sugar moiety to a range of acceptors (including small molecules, peptides, proteins, glycons and lipids) with perfect regiocontrol and stereocontrol (Lairson *et al.*, 2008; Gantt *et al.*, 2011). GTs are involved in many different cellular functions, including but not limited to energy storage, immune response, cellular structure, protein trafficking and intra- and extracellular signaling (Varki and Chrispeels, 1999; Rudd *et al.*, 2001; Zhang *et al.*, 2006; Thibodeaux *et al.*, 2008; Hart *et al.*, 2011). GTs involved in secondary metabolism are often quite promiscuous in that they can use structurally altered donors

or acceptors. There are many excellent comprehensive reviews on various aspects of GTs (e.g., mechanisms, function, structural biology and engineering) (e.g. Bowles *et al.*, 2006; Palcic and Sujino, 2011). The majority of characterized GTs are Leloir-type (sugar nucleotide-dependent) and use either nucleotide di- or monophosphate sugars as donors, in which the nucleotide phosphate plays two roles: 1) as a recognition element for the GT and 2) as a leaving group for the glycosyltransfer reaction. Compared to the sugar nucleotide-dependent GTs, the less prevalent non-Leloir GTs use alternative sugar donors, such as sucrose, glucose-1-phosphate or polyprenyl phosphate sugars and are generally more substrate specific as shown in Figure 2.1.

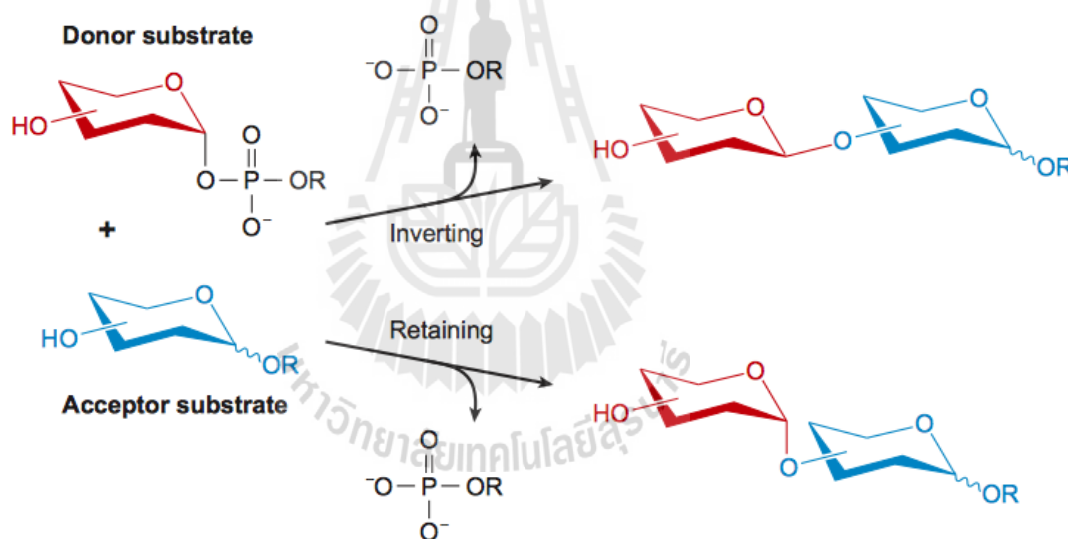


Figure 2.1 Glycosyltransferases catalyze glycosyl group transfer with either inversion or retention of the anomeric stereochemistry with respect to the donor sugar (Lairson *et al.*, 2008).

2.1.2 Glycoside hydrolases

Glycoside hydrolases (GHs; EC 3.2.x.y) are enzymes that catalyze the hydrolysis of the glycosidic linkage between sugars or between sugar and nonsugar

aglycone moieties of glycosides, leading to the formation of a sugar hemiacetal or hemiketal and the corresponding free aglycone or shortened saccharide. GHs are also referred to as glycosyl hydrolases, glycosidases, and carbohydrases. GHs can catalyze the hydrolysis of O-, N- and S-linked glycosides (Figure 2.2). GHs can be classified in many different ways, such as the specific reaction catalyzed (i.e. the Enzyme Commission, E.C., number), endo/exo acting (Figure 2.3), mechanistic classification (Figure 2.4), and sequence-based classification. From amino acid sequence similarity, these enzymes can be classified into 133 glycoside hydrolase families, which show varieties of substrate specificities and structural models (www.cazy.org; Cantarel *et al.*, 2009).

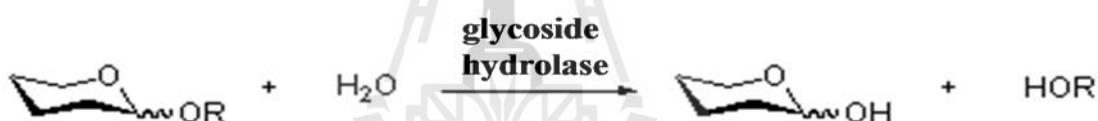


Figure 2.2 General catalytic mechanism of glycoside hydrolases activity

(www.cazypedia.org).

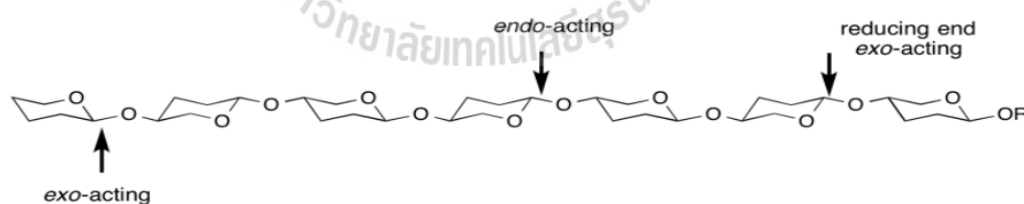
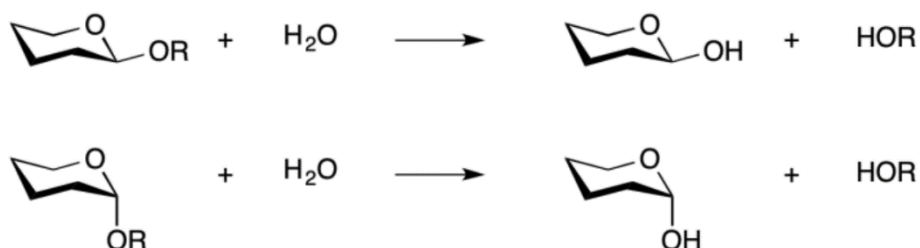
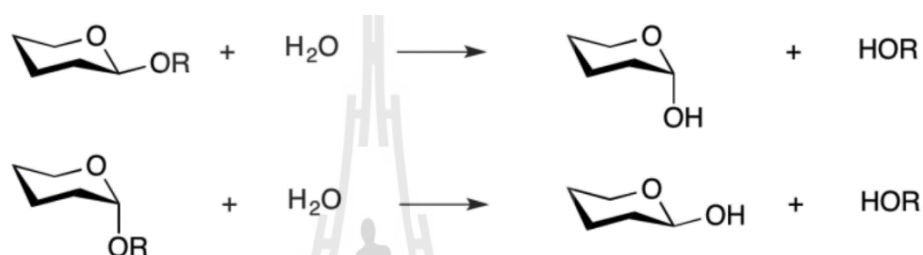


Figure 2.3 Endo/exo-acting glycoside hydrolases (www.cazypedia.org).

Retaining glycoside hydrolases:**Inverting glycoside hydrolases:****Figure 2.4** Retaining and inverting glycoside hydrolase mechanisms

(www.cazypedia.org).

GHs make up one set of gene families that are of particular interest to investigate in plants (Henrissat, 1991). Plants have a wide variety of glycosides and polysaccharides, which carry-out many functions. These include cell wall polysaccharides, which form the bulk of the structure and biomass of plants, as well as starch and other forms of storage carbohydrates. Glycosides found in plants include glycolipid components of cellular membranes and pigments, as well as many reactive or bioactive species that are blocked from their activity by sugars for storage or to allow reactions at other positions on the molecule.

In addition, GHs have great potential for biotechnological applications, such as in release of nutrients and flavor compounds in plant-derived foods and feeds, conversion of certain sugars, like lactose in milk products, to more desirable sugars, and

in biomass conversion of cellulose and other polysaccharide waste to useful products, including fuels (Sharma *et al.*, 2013). β -Glycosidases, including β -glucosidases, β -galactosidases and related enzymes, are particularly interesting in this regard.

2.1.3 Transglycosidases

The creation of glycoconjugates in nature is primarily catalyzed by GT, which are enzymes that transfer a sugar from a nucleotide phosphate sugar or phospholipid sugar donor to an acceptor to form a glycosidic ether or ester linkage (Lairson and Withers, 2004; Lairson *et al.*, 2008). For synthesis of most glucosides and glucosyl esters in plants, these enzymes use uridine diphosphate α -D-glucoside (UDP-Glc) as the donor. The vast majority of glycosylation reactions in plants are catalyzed by GTs (Bowles *et al.*, 2006), but transglycosidases (TGs) also play a role.

Transglycosidases are enzymes that catalyze the transfer of sugars from donors other than nucleotide sugars and phospholipid sugars to targeted aglycone acceptors (Lairson and Withers, 2004). The sugar donors include unprotected di-, tri-, oligo- and poly-saccharide-based donors and glycosides bearing an appropriate leaving group at the anomeric position. Those TGs that have been described are related to GHs, many of which can also catalyze transglycosylation reactions under the appropriate conditions, such as high donor and acceptor substrate concentrations.

While GHs are able to generate very regio- and stereo-specific glycosidic bonds, desired product formation is constrained by both thermodynamic parameters and competition from hydrolytic reactions (Wang and Huang, 2009). Therefore, synthetic transglycosylation reactions catalyzed by wild-type glycosidases are generally conducted under tight kinetic control to maximize reaction yields. To overcome this limitation on the use of GH in synthesis, several classes of mutated glycosidases

(glycosynthases, thioglycoligases, thio-glycosynthases and O-glycoligases) have been developed to maintain transglycosylation activity, while eliminating hydrolysis activity.

Nonetheless, nature has developed its own set of TGs to move saccharides between various donors and acceptors, such as xyloglucan endotransferases (Eklöf and Brumer, 2010), disproportionating isoenzyme 2 (DPE2, Fettke *et al.*, 2006), and galactolipid galactolipid galactosyl transferase (GGGT, Moellering *et al.*, 2010). TG catalyze mainly transglycosylation with little hydrolysis, such as in the transfer of xyloglucan linkages between strands by xyloglucan endo-transferases (XET, xyloglucan:xyloglucosyl transferase; EC 2.4.1.207 (Eklöf and Brumer, 2010)). Although XETs, which are closely related to xyloglucan hydrolases, act on polysaccharides, other TGs can act on glycolipids and small molecules.

2.1.4 Classification by Function and E.C. Number

Carbohydrate-active enzymes can be classified according to various criteria. The simplest classification is based on their substrate specificities and forms the basis of the recommendations of the International Union of Biochemistry and Molecular Biology (IUBMB), which determined an EC number for a given enzyme activity (Enzyme Nomenclature Committee, 2001). GHs are given the codes EC 3.2.1.x, where x represents substrate specificity. Similarly, GTs are described as EC 2.4.y.z, where y defines whether the sugar transferred is a pentose or a hexose and z describes the acceptor specificity.

2.1.5 Glycoside hydrolase and glycosyltransferase families

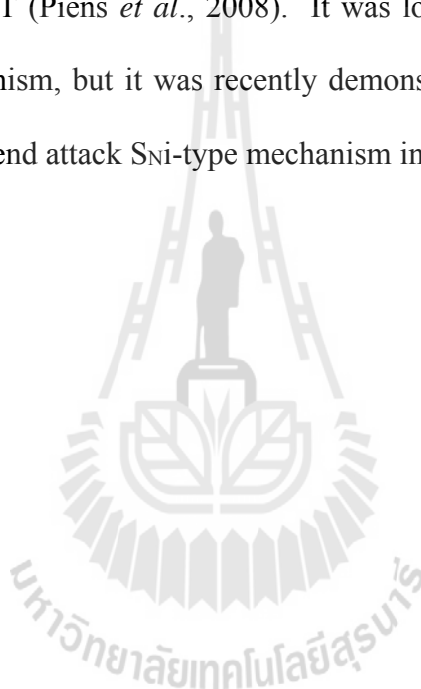
GHs and GTs have been grouped in families by sequence similarity and these families joined into clans by structural and mechanistic similarities (Henrissat *et al.*, 1991; Campbell *et al.*, 1997; Henrissat and Davies, 2000). Currently, there are 133 GH

and 96 GT families in the Carbohydrate Active eZYme online resource (<http://www.cazy.org>; Cantarel *et al.*, 2009). The TGs have been described to date fall within the GH families, for example, XET are members of GH family GH16. The families can be grouped into clans related by their 3-dimensional structures and mechanisms. GH Clan A, for instance, is made up of enzymes with $(\beta/\alpha)_8$ barrel structures with carboxylic acids that act as catalytic acid/bases and nucleophiles on the C-terminal ends of β -strands 4 and 7, respectively. This clan includes families 1, 2, 5, 10, 17, 26, 30, 35, 39, 42, 50, 51, 53, 59, 72, 79, 86, 113, and 128, which include enzymes with a wide variety of activities, despite the similar structures. Most families include many activities (E.C. numbers), and one activity can be found in multiple families. For instance, GH family 1 (GH1) has been found to include most plant β -glucosidases that have been characterized to date, although it also contains enzymes with other activities, such as β -mannosidase, disaccharidase, transglucosidase, and hydroxyisourate hydrolase, and β -glucosidase activity is found in other families as well.

2.2 Glycosyltransferase, glycoside hydrolase, and transglycosidase mechanisms

Transfer and hydrolysis of glycosyl moieties on glycoconjugates can occur with either retention or inversion of the stereochemistry at the anomeric carbon at the glycosidic bond that is broken in the process (Koshland *et al.*, 1953; Lairson and Withers, 2004). The inverting mechanism of both GHs and GTs is thought to occur through a single displacement mechanism, in which the glycosidic bond is broken while the acceptor (water in the case of hydrolysis) attacks from the opposite face of the sugar.

In GHs, the retaining mechanism is thought to occur via a double displacement mechanism (Figure 2.5), which occurs in two steps, glycosylation and deglycosylation. In the glycosylation step, the catalytic acid/base protonates the leaving group aglycone and the catalytic nucleophile (usually a nucleophilic amino acid residue side chain) attacks the anomeric carbon of the sugar to form a covalent intermediate (Withers *et al.*, 1990). Transglycosylation can occur by the same mechanism in GHs and TGs, as has been shown for a XET (Piens *et al.*, 2008). It was long supposed that retaining GT could use this mechanism, but it was recently demonstrated that trehalose phosphate synthase uses a front-end attack S_Ni -type mechanism instead (Lee *et al.*, 2011).



Inverting mechanism for a β -glycosidase:



Retaining mechanism for a β -glycosidase:

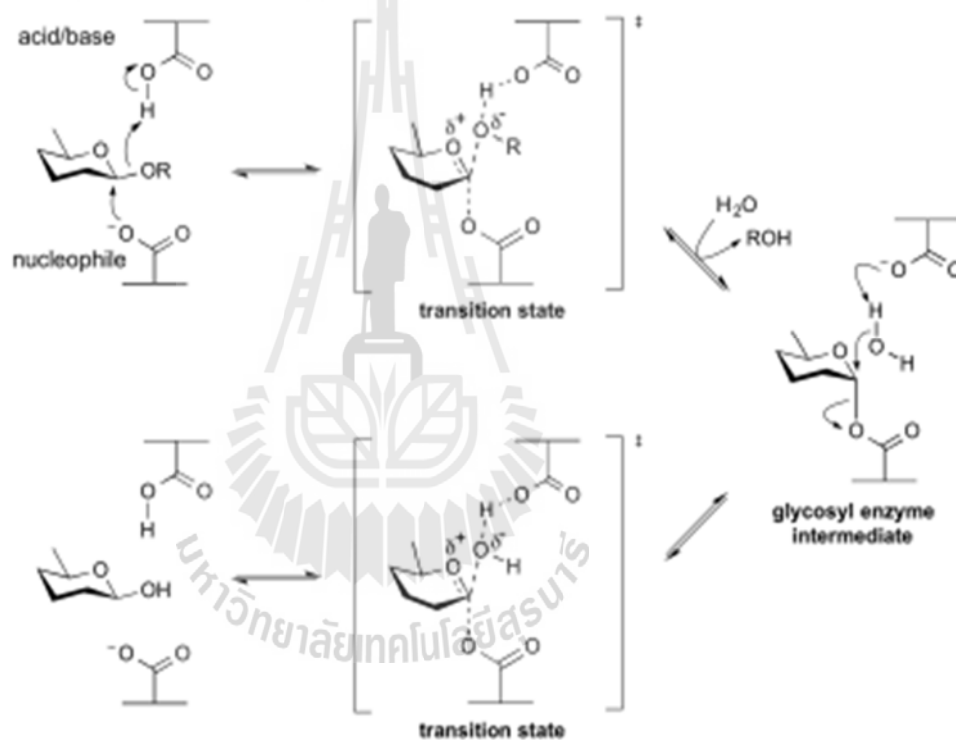


Figure 2.5 Glycosidase mechanisms for hydrolysis. Classical mechanism for inversion of stereochemistry and classical mechanism for retention of stereochemistry (Rempel and Withers, 2008).

Other mechanisms have been proposed for small sets of families of glycoside hydrolases. Gloster and Davies (2010) reviewed these other mechanisms, two of which are described below. A substrate-assisted catalytic mechanism (Figure 2.6a.) has been

proposed for glycoside hydrolases which catalyse hydrolysis of substrates containing *N*-acetylhexosamine with retention of the configuration, despite the absence of a conventional nucleophile. These enzymes are grouped into families GH18, GH20, GH25, GH56, GH84, and GH85. The catalytic nucleophile is not derived from the enzyme, but instead is from the acetamido group at the C2 position of the substrate. The *N*-acetyl carbonyl group of the substrate acts as a nucleophile to attack the anomeric carbon to create a covalent oxazoline intermediate. The breakdown of this intermediate is achieved by the attack by a water molecule, which is activated by a general base residue. A second carboxylate-containing residue mostly orients and polarizes the *N*-acetyl carbonyl group to increase its nucleophilicity.

In GH33 and GH34, some sialidases and neuraminidases hydrolyze sialic acid-containing substrates in an *exo* fashion with retention of configuration, using a tyrosine residue to act as the catalytic nucleophile (Figure 2.6b) (Gloster and Davies, 2010). A Tyr/Glu couple is invoked to relay the charge from a close glutamate residue to provide a nucleophilic oxygen atom carrying some negative charge; it is proposed that not using a glutamate residue in this position avoids electrostatic repulsions with the sialic acid carboxylate group.

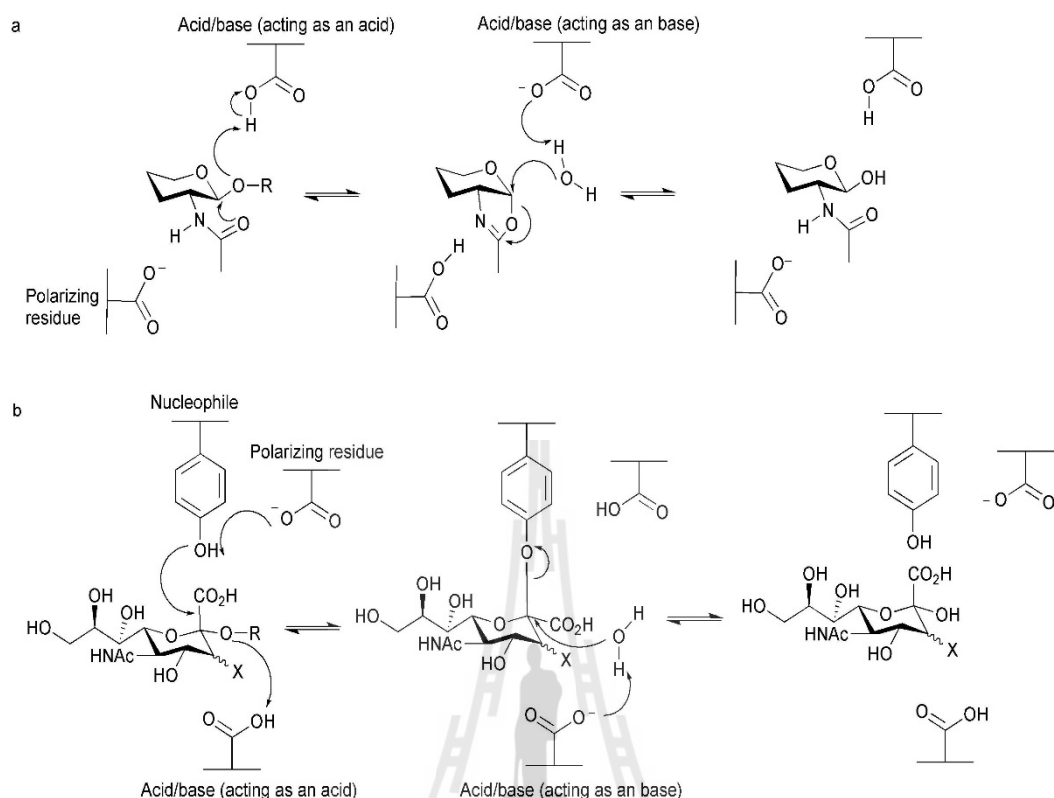


Figure 2.6 Unusual GH hydrolysis mechanisms (Gloster and Davies, 2010).

(a) Substrate-assisted mechanism. (b) Mechanism using a tyrosine residue as the nucleophile.

2.3 Catalytic nucleophile and acid/base mutants with rescued activity

2.3.1 Rescue of catalytic nucleophile mutants

In retaining glycoside hydrolases, rescue of the activity of mutants by azide and other small nucleophiles may be used to identify the catalytic acid/base and nucleophile residues. Mutation of the catalytic nucleophile of *Agrobacterium* sp. β -glucosidase to Ala, generated an enzyme that acted as an inverting transglycosidase, Abg Glu358Ala. This enzyme was nearly inactive, but could be rescued for cleavage of 2,4-dinitrophenyl β -glucoside by high concentrations of azide or formate, and the

product of the azide reaction was shown by NMR to be α -glucosyl azide. The Abg Glu358Ala mutant also cleaved α -glucosyl fluoride rapidly, transferring the glucose to a second substrate molecule to make α -cellobiosyl fluoride (Wang *et al.*, 1994). It was later shown that the nucleophile to glycine mutant of a *Sulfolobus solfataricus* β -glucosidase acts as a *retaining* glycosidase in the presence of formate, with the formate taking the place of the missing nucleophile residue to form an unstable intermediate (Figure 2.7) (Morraci *et al.*, 1998; Zechel and Withers, 2000).

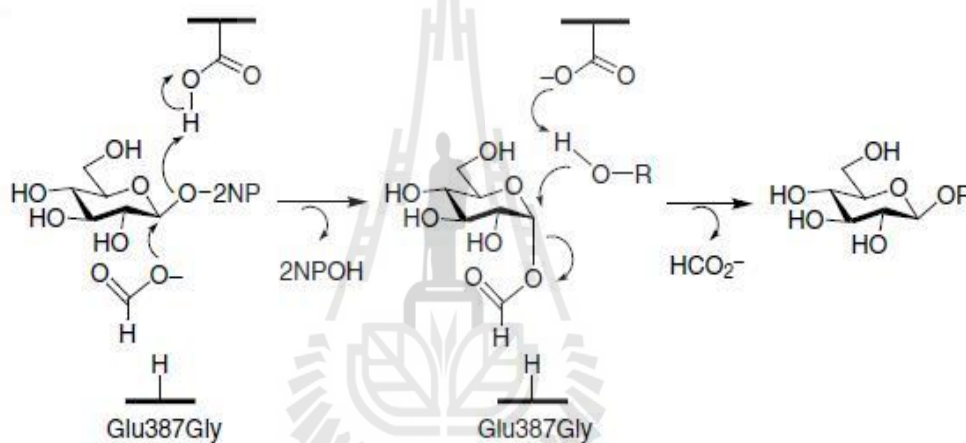


Figure 2.7 Rescue of catalytic activity in the nucleophile mutant *Sulfolobus solfataricus* β -glucosidase by formate (Zechel and Withers, 2001).

Moreover, these nucleophile mutants of retaining glycosidases that can be used for synthesis of specific oligosaccharides in appropriate quantities for many desired applications (Shaikh and Withers, 2008). These mutants cannot form a reactive α -glycosyl-enzyme intermediate for transglycosylation. However, when an α -glycosyl fluoride is present as a glycosyl donor, the mutant enzymes can transfer the glycosyl moiety to acceptor alcohols without hydrolysis of the products, as shown in Figure 2.8.

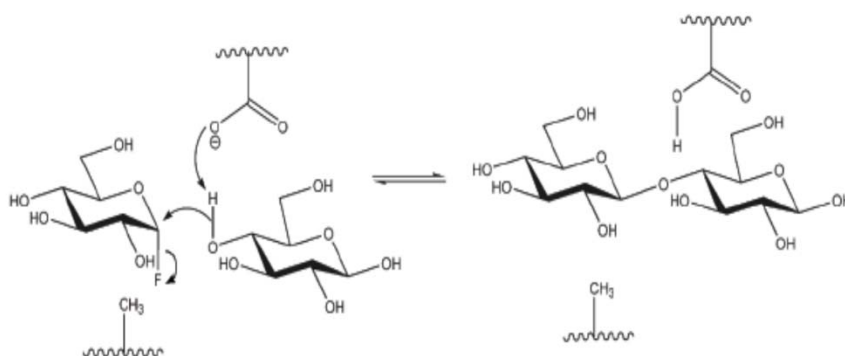


Figure 2.8 Mechanism of transglycosylation with a glycosynthase (Shaikh and Withers, 2008).

2.3.2 Rescue of catalytic acid/base mutants

The Ala mutant of the catalytic acid/base of the *Agrobacterium* β -glucosidase (Abg) enzyme (Figure 2.9), which completely lacks activity, can be reactivated for hydrolysis of 2,4-dinitrophenyl glycoside by azide, formate, or acetate, which results in the formation of glycoside with the same anomeric configuration as the substrate. For instance, β -glucosyl azide is obtained from azide rescue of the activity of the Abg acid/base mutant. In this case, the good leaving group has a low pK_a and therefore does not require protonation, which eliminates the requirement for the acid catalyst in the glycosylation step (Wang *et al.*, 1995).

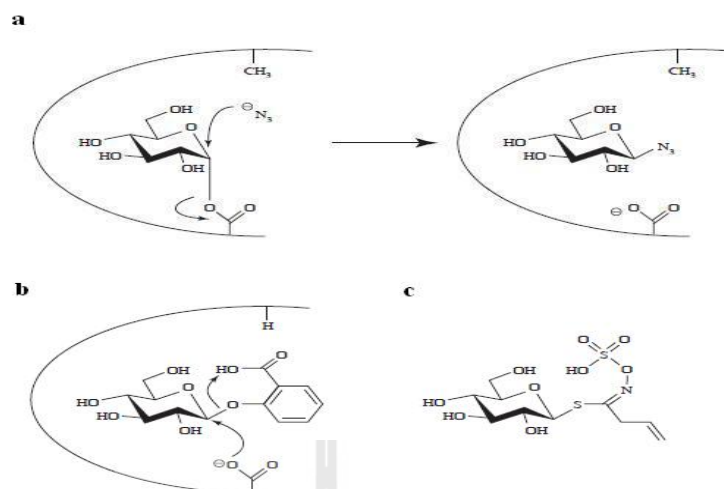


Figure 2.9 Rescue of catalytic activity in the acid/base mutant by azide (a), substrate assisted protonation (b) and the structure of sinigrin (c) (Ly and Withers, 1999).

An *ortho*-carboxyl group on an aryl substrate may also function as the general acid catalyst when bound to the mutant enzyme, but cannot be accommodated in the active site of the wild-type (WT) enzyme (Figure 2.9b). Such “substrate-assisted catalysis” was suggested to be important for the thioglycosidases of family GH1, such as *Sinapis alba* myrosinase, which has a Gln residue at the conserved catalytic acid/base position. This enzyme can hydrolyze its highly reactive substrate sinigrin (Figure 2.10) and other glucosinolate substrates to perform the glycosylation step without an acid catalyst, while ascorbate acts as a base catalyst in the deglycosylation step after departure of the aglycon (Burmeister *et al.*, 2000) (Figure 2.10).

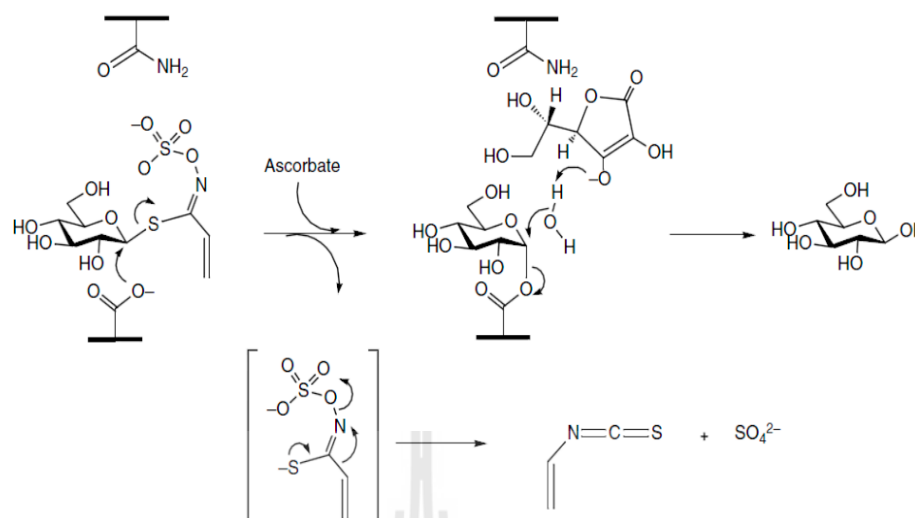


Figure 2.10 A natural version of chemical rescue with *Sinapis alba* myrosinase utilizes ascorbate as a general base catalyst (Burmeister *et al.*, 2000).

2.4 β -Glucosidases and GH family 1

β -Glucosidases (3.2.1.21) are GHs that hydrolyze the β -*O*-glycosidic bond at the anomeric carbon of a glucose moiety at the nonreducing end of a carbohydrate or glycoside molecule. β -Glucosidases are found in nearly all living organisms and have been implicated in a many roles, such as biomass conversion in microorganisms, and cell wall remodeling, activation of defense compounds, phytohormones, lignin precursors, aromatic volatiles, and metabolic intermediates by releasing glucose blocking groups from the inactive glucosides in plants (Esen, 1993; Seshadri *et al.*, 2009). To achieve specificity for these various functions, β -glucosidases must bind to a wide variety of aglycones, in addition to the glucose of the substrate.

In the system of Henrissat, β -glucosidases are found in at least 6 families of GH and show different structures depending on of which GH family they are a member as shown in Figure 2.11 (Henrissat, 1991; Cantarel *et al.*, 2009; Ketudat Cairns and Esen,

2010). The GH1, GH5 and GH30 families belong to Clan GH-A, the members of which have $(\beta/\alpha)_8$ barrel domains that contain their active sites. On the other hand, family GH 9 enzymes have $(\alpha/\alpha)_6$ structures, while GH3 β -glucosidases/exoglucanases have their active site in between two domains, one $(\beta/\alpha)_8$ barrel and one $(\beta/\alpha)_6$ sandwich domain (Figure 2.11). For the structure of GH116, none has yet determined, but GH116 protein sequences show weak similarity with proteins from GH families with $(\alpha/\alpha)_6$ structures.

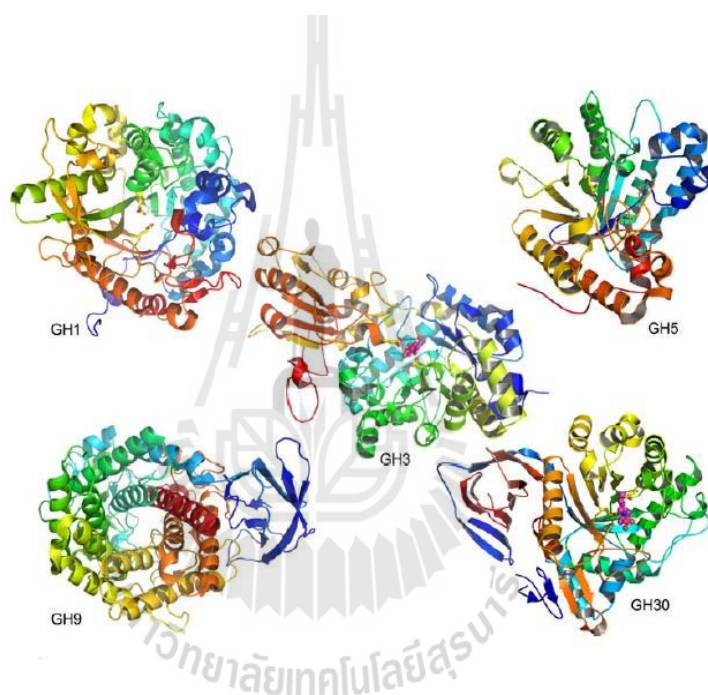


Figure 2.11 β -Glucosidase structures from various GH families (Ketudat Cairns and Esen, 2010).

In plants, β -glucosidases play essential roles in many biological processes, such as chemical defense against pathogens and herbivores (Morant *et al.*, 2008), lignification (Escamilla-Trevino *et al.*, 2006), cell wall modification (Hrmova and Fincher, 2001) and phytohormone activation (Schroeder and Nambara, 2006). Based on amino acid sequence similarities, plant β -glucosidase can be classified in GH families GH1, GH3 (Henrissat *et al.*, 1991) and GH5 (Opassiri *et al.*, 2007), while plants also have

uncharacterized GH116 genes that are likely to encode β -glucosidases (Ketudat Cairns *et al.*, 2012). The majority of plant β -glucosidases that have been identified and characterized fall in family GH1.

GH1 contains a wide range of β -glycosidases, including β -galactosidases, β -mannosidases, phospho- β -galactosidases, phospho- β -glucosidases, and thioglucosidases, in addition to β -glucosidases (Ketudat Cairns and Esen, 2010). The plant GH1 enzymes are mainly in a closely related subfamily, but, nevertheless, display a wide range of activities. Besides β -glucosidases with diverse specificities, plant GH1 enzymes include thio- β -glucosidases or myrosinases, β -mannosidases, disaccharidases, such as primeverosidase and furcatin hydrolase, and hydroxyisourate hydrolase, which hydrolyzes an internal bond in a purine ring, rather than a glycosidic linkage. In addition, many enzymes in this group are capable of releasing multiple kinds of sugars from aglycones, such as isoflavonoid β -glucosidases, which can release the disaccharide acuminose and malonyl glucose, in addition to glucose itself, from isoflavonoids. Other β -glucosidases in this subfamily may have high specificity for β -D-glucosides or β -D-glucosides and β -D-fucosides, or may hydrolyze other glycosides, such as β -D-galactosides, β -D-mannosides, and β -D-xylosides, as well. Primeverosidase has high specificity for primeverosides, with practically no hydrolysis of glucosides, while furcatin hydrolase can hydrolyze glucosides as well as disaccharide glycosides. Clearly, plant family 1 GHs have diverse glycone specificities.

2.5 GH1 transglycosidases

GH1 β -glycosidases typically use a retaining mechanism, in which catalysis usually proceeds in a two-step, double displacement mechanism. The enzymatic synthesis of

glycosidic bond using sugar substrate donor can be formed by transglycosidases. There are a large number of retaining GHs that catalyze both hydrolysis and transglycosylations, but not much is known regarding what determines the ratio between transglycosylation and hydrolysis (Teze *et al.*, 2013).

Transglucosidases (TGs) have been identified in GH1. Matsuba *et al.* (2010) reported two transglycosidases from carnation and delphinium that transfer glucose from phenolic glucosyl esters, such as feruloyl glucose and 1-*O*- β -D-vanillyl glucose, to the anthocyanin cyanidin 3-*O*-glucoside. The galactolipid:galactolipid galactosyltransferase was found to correspond to the GH1 enzyme SFR2 (sensitive to freezing 2), which is necessary for freezing tolerance in *Arabidopsis* (*Arabidopsis thaliana*). Galactolipid:galactolipid galactosyltransferase moves the galactosyl residues from one monogalactosyl diacyl glyceride to another to produce diacyl glycerol and β -linked oligogalactosyl diacyl glyceride (Moellering *et al.*, 2010).

2.6 Role of GH1 enzymes in rice

Rice (*Oryza sativa* L.) is the world's most important food crop and also a model plant for monocot species with a sequenced genome (International Rice Genome Project, 2005). As such, it serves as an excellent system to explore the functions of enzymes within gene families that have yet to be thoroughly explored, since the genomic resources are available and the knowledge gained is likely to be applicable to improve crop production over the long term. There are a wide range of polysaccharides, oligosaccharides, complex carbohydrates and glycoconjugates in plants, including rice, that play roles from structure to energy storage to signaling in development and response to stress.

Forty GH1 genes from rice were identified and 34 of these were noted to be likely to encode rice proteins that function as β -glucosidases (Opassiri *et al.*, 2006). Phylogenetic analysis identified 8 clusters of GH1 members that contain protein sequences from the dicot *Arabidopsis* and monocot rice that are more closely related to each other than to other proteins from the same plant outside their cluster (Opassiri *et al.*, 2006). The GH1 β -glucosidase BGlu1 (systematically named Os3BGlu7) is highly expressed in rice flower and germinating shoots (Opassiri *et al.*, 2003). Several rice GH1 enzymes have been expressed in *Escherichia coli* and characterized, and found to have rather broad glycone specificity, such as Os3BGlu7, Os4BGlu12 and Os3BGlu6 (Opassiri *et al.*, 2004, 2006; Seshadri *et al.*, 2009). Rice Os1BGlu4 is a glycoside hydrolase family 1 member in rice that is located in the cytoplasm and hydrolyzes β -linked gluco-oligosaccharides and certain glycosides, but its function remains unclear (Chen *et al.*, 2014). It does have transglycosylation activity on 4NP-oligosaccharides and alkyl glycosides, unlike Os9BGlu6, which showed no transglycosylation activity, unless its catalytic acid/base was mutated (Seshadri *et al.*, 2009; Hua *et al.*, 2013). Rice Os4BGlu16, and Os4BGlu18 were characterized to have monolignol β -glucosidase activities (Baiya *et al.*, 2014).

At/Os cluster 6 is the phylogenetic cluster that contains hydroxyisourate hydrolase (HIUH), which has the unusual sequence of HENG around the nucleophile instead of the usual TENG, and lacks the sugar binding residues (Raychaudhuri and Tipton, 2002; 2003). Os9BGlu31 was characterized from At/Os cluster 6 and found it to be a transglycosidase with little hydrolase activity and no HIUH activity (Luang *et al.*, 2013). The acyl-glucose-dependent anthocyanin glucosyltransferase TGs described by Matsuba *et al.* (2010), like Os9BGlu31, have the HENG sequence at the catalytic

nucleophile, but contain the conserved sugar-binding residues missing in the purine hydrolase HIUH. Ferulic acid and feruloyl glucose served as excellent substrates and other compounds serving as substrates included various cinaminic acids and their glucosyl esters, indole acetic acid (IAA), naphthalene acetic acid (NAA) and gibberellic acid GA₄ (Luang *et al.*, 2013). The transfer of glucosyl moieties between these substrates suggest that cross-talk between feruloyl glucose and phytohormone glucosyl conjugates is possible.

The rice enzymes in At/Os cluster 6 make up two subclusters, one comprising Os9BGlu31, Os9BGlu32, and Os9BGlu33, which is more divergent from other rice and Arabidopsis enzymes in At/Os cluster 6, and one comprising Os1BGlu2, Os1BGlu3, Os1BGlu5, Os5BGlu19, Os5BGlu20, Os5BGlu21, Os5BGlu22 and Os5BGlu23. The enzymes in the former subcluster all have the HENG sequence around the catalytic nucleophile, while the proteins in the larger subcluster have the equally unusual sequence of QENG around the catalytic nucleophile. The Arabidopsis enzymes in this cluster also have an unusual amino acid in front of the catalytic nucleophile, usually leucine (Leu, L). Whether this unusual sequence is involved in the unusual function of these enzymes, or simply reflects their evolution remains to be seen, since none of the Arabidopsis enzymes nor the rice enzymes in the larger subcluster have yet been characterized, but mutation of this site in Os9BGlu31 suggested it is not critical to transglucosidase activity (Luang *et al.*, 2013).

2.7 Site-directed mutagenesis and directed evolution

In 1975, when Smith sequenced the *Escherichia coli* phage ϕ X174, an important point of the sequencing process came from defining the position and reading frame of

the genes using nonsense mutants suppressible by amber or ochre suppressors (Smith, 1975). This highlighted the need for a specific mutagenic method that would target a specific base pair in the genome and introduce a desired change with sufficiently high efficiency (Kresge *et al.*, 2006).

Smith demonstrated that small oligonucleotides could form stable duplexes with the single-stranded DNA of phage ϕ X174 at low temperature even with a mismatch, which suggested that oligonucleotide-directed mutagenesis would be possible. Several years earlier, Clyde A. Hutchinson and Marshall H. Edgell had achieved mutagenesis with small fragments of ϕ X174 and restriction nucleases (Hutchinson and Edgell, 1971). They showed that the point mutants could be reverted by annealing mutant phage ϕ X174 DNA with fragments from the complementary strand of wild-type DNA prior to the transfection. Smith and colleagues eventually used the binding of the mismatched oligonucleotides to ϕ X174 DNA and extension by DNA polymerase to introduce specific mutations into the DNA (Hutchinson *et al.*, 1978; Zoller and Smith, 1982).

Site-directed mutagenesis is an *in vitro* procedure that use oligonucleotide primers to confer a desired mutation in a double-stranded DNA plasmid. One method that was developed by Kunkel (Kunkel, 1985), which takes advantage of a strain deficient in dUTPase and uracil deglycosylase so that the recipient *E. coli* degrades the uracil-containing wild-type DNA, was widely used. Later, polymerase chain reaction-based methods became more popular, due to the ability to produce the mutated sequence in great excess compared to the non-mutated template, which aided in isolation of mutant DNA clones (Urban *et al.*, 1997). Numerous studies have used site-directed mutagenesis to identify catalytically important residues and modify the activities of GH and TG functions, as outlined in Section 2.3, for instance.

Moreover, improvement of enzyme activity or identification of residues involved in catalysis can be done by mutational approaches that modify the mechanism, specificity or activity. The approach for converting enzyme activity from GH1 β -glycosidase into a β -transglycosidase has been attempted by the method called directed evolution, in which random mutations are introduced and the desired activity selected (Teze *et al.*, 2013). This work has been published on converting a glycoside hydrolase from *Thermus thermophilus* to a transglucosidase. Researchers have also set up the rational approach for the design of glycosidases into transglucosidases and to enhance the rate and substrate specificity of natural transglycosidases, such as amylosucrases and cyclodextrinases, by directed evolution (Kaur and Sharma, 2006).

2.8 Mass spectrometry

Mass spectrometry is a powerful sensitive technique to determine the mass of, detect, quantify, and identify known and unknown compounds of interest (Dettmer *et al.*, 2007). This method has been used in academic research, biotechnological development, pharmaceutical drug discovery, clinical testing, environmental analysis and geological testing. The complete process involves the conversion of the sample with or without fragmentation into ions in the gas phase, which are characterized by their mass to charge ratios (m/z) and relative abundances. The ions are separated in the mass spectrometer according to their mass-to-charge ratio and detected in proportion to their abundance. A mass spectrum of the molecule is produced. The mass spectrum shows the results in the form of a plot of ion abundance versus mass-to-charge ratio (m/z). The mass spectrometer consists of three major components. First, an ion source is the source for producing gaseous ions of the compounds. Second, the mass analyzer is for

resolving the ions into their characteristic mass components via their mass to charge ratio. Finally, the detector system detects ions and records the relative abundances of each m/z species.

The powerful use of the technique of mass spectrometry in metabolite research derives from its proven success in drug metabolite analysis and pharmacokinetic studies (Staack *et al.*, 2005). Mass spectrometry is already well established as a qualitative and quantitative tool for small molecules, which is different from its application to proteomics. Liquid chromatography electrospray ionization mass spectrometry (LC/ESI-MS) is the most common approach toward metabolite profiling studies. ESI offers many advantages over other ionization techniques, including the ability to analyze low and high mass compounds. It also has excellent quantitative capabilities, reproducibility, high sensitivity, simple sample preparation, soft ionization, and the absence of matrix (as required for matrix-assisted laser desorption/ionization mass spectrometry (MALDI)). The utility of ESI is in its ability to generate gaseous ions directly from the liquid phase, which makes this technique a convenient mass-analysis platform for both liquid chromatography and automated sample analysis. Atmospheric-pressure chemical ionization (APCI) mass spectrometry is not as widely used in metabolite-profiling studies. However, it can be a technique for the analysis of neutral molecules, such as lipids and phospholipids that are easier to ionize by APCI. APCI provides a higher dynamic range than ESI, which exhibits mass sensitive ionization. However, one of the drawbacks of APCI is that it does not exhibit any of the sensitivity gains with smaller columns or lower flow rates observed with ESI (Want *et al.*, 2005).

The mass analyzer is critical to the mass spectrometer resolution. The most commonly used are quadrupole, quadrupole ion trap, time-of-flight, and Fourier

transform ion cyclotron resonance (FTMS). Quadrupoles can be connected into triple quadrupole devices to perform tandem mass analysis. The first quadrupole (Q1) is used to scan across a preset m/z range of the parental ions. The second quadrupole (Q2) is also known as collision cell that focuses the ions while a collision gas is introduced into the proximity of the selected ion to allow collision-induced fragmentation to occur. The third quadrupole (Q3) separates the fragment ions from the collision cell (Q2). The time-of-flight (ToF) is a mass analyzer with unlimited mass range. It provides a higher resolution than quadrupole mass analyzers when combined with ESI, and can provide mass range up to m/z 10,000 with mass accuracy to less than 5 ppm. The ToF gained wide use due to its fast scanning capabilities (millisecond) and high resolution (Siudak, 2003).

2.9 Metabolite profiling of glycoconjugates

Profiling of secondary metabolites is a challenging task from an analytical technique standpoint. Mass spectrometry is the analytical technique most commonly used to identify unknown compounds within a sample and to elucidate the structure and chemical properties of different molecules, which are characterized by their mass to charge ratios (m/z) and relative abundances. This technique basically studies the effect of ionizing energy on molecules. One of the most powerful methods to analyze these compounds is the use of liquid chromatography together with mass spectrometry (LC/MS) (Moco *et al.*, 2006), but other methods are still useful. Profiling of glycoconjugates with mass spectrometry is a well-established analytical method and several papers have been published (Prasain *et al.*, 2004; Fossen and Andersen, 2006;

Stobiecki and Kachlicki, 2006; and March and Brodbelt, 2008). However, identification of the target compounds is still a difficult task.

To detect as many metabolites as possible, the physicochemical properties of the metabolites, i.e., their hydrophobicity, volatility, and acidity must be considered. Therefore, various separation and detection techniques, such as gas chromatography (GC-MS, Fiehn *et al.*, 2000; Liseč, *et al.*, 2006; Kusano *et al.*, 2007), liquid chromatography (LC-MS, Kristensen *et al.*, 2005; Moco *et al.*, 2006), capillary electrophoresis (CE-MS, Sato *et al.*, 2004; Takahashi *et al.*, 2006), Fourier transform ion cyclotron resonance (FT-ICR-MS, Aharoni *et al.*, 2002; Nakamura *et al.*, 2007; Oikawa *et al.*, 2006), and NMR (Krishnan *et al.*, 2005; Sekiyama *et al.*, 2007) have been applied to metabolomics.

Among these, GC-MS is one of the most popular methods in current metabolite profiling studies (Fiehn *et al.*, 2000). In addition to volatile compounds, GC-MS can detect hydrophilic metabolites, such as amino acids, organic acids, and sugars, by chemical derivatization of these metabolites. Moreover, in GC-MS analysis using the electron impact ionization method, it is possible to detect many fragment peaks derived from each compound, and these fragment peaks provide information of the structure of the metabolites and thereby help to identify the detected peaks as known metabolites. LC-MS is a powerful tool that has been used for profiling of secondary metabolites, including alkaloids, flavonoids, and phenyl propanoids. CE-MS can separate and detect ionic metabolites, including amino acids, organic acids, nucleotides, and sugar phosphates. Consequently, CE-MS analysis leads to the acquisition of a considerable amount of information on the metabolites of the central metabolic pathways. FT-ICR-MS has an ultra-high performance, particularly in terms of mass resolution and

sensitivity, leading to the detection of a huge number of peaks without the need for any steps for the separation of metabolites from a mixture by chromatography or electrophoresis. Additionally, FT-ICR MS needs only a few seconds for one scan; so, it enables high-throughput and high-resolution analysis. However, the necessary equipment is too large and expensive to be practical for most groups. NMR is also a useful technique for metabolite profiling, since it is able to determine the atomic state of compounds and enables the identification of metabolites that are otherwise unidentifiable by MS analysis (Oikawa *et al.*, 2008).

2.10 Flavonoids

Flavonoids are one of the important groups of plant secondary metabolites (Koes *et al.*, 1994). Flavonoids have been characterized in flag leaves and germinating seed of rice (Izawa and Shimamoto 1996; Gong *et al.*, 2013). Dong *et al.* (2014) reported the detection of various flavonoids in rice flag leaf, as shown in table 2.1.

Table 2.1 Accumulation of flavonoids in rice flag leaves (*Oryza sativa*).

Classification	Compounds
Flavone mono-C-glycosides	<i>O</i> -Methylapigenin C-hexoside <i>O</i> -Methychrysoeriol C-hexoside
Flavonone mono-C-glycosides	Naringenin C-hexoside
Flavone di-C,C-glycosides	Di-C,C-pentosyl apigenin C-hexosyl-C-pentosyl-apigenin di-C,C-hexosyl-apigenin di-C,C-pentosyl-luteolin di-C,C-hexoeryl-luteolin
C-glycosylflavone O-glycosides	C-rhamnosyl-apigenin <i>O</i> -hexoside C-hexosyl-luteolin <i>O</i> -pentoside C-pentosyl-apigenin <i>O</i> -hexoside C-pentosyl-chrysoeriol <i>O</i> -hexoside

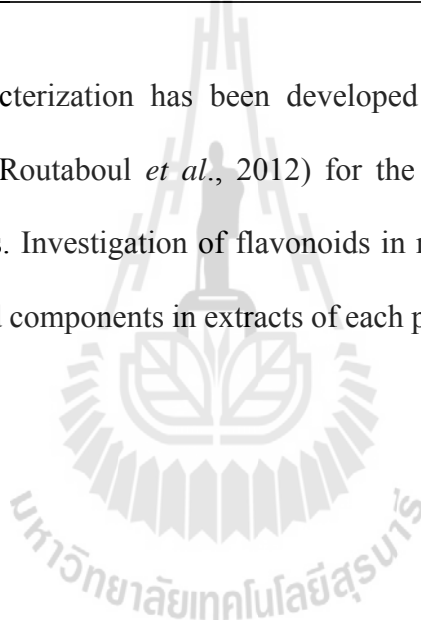
Table 2.1 Accumulation of flavonoids in rice flag leaves (*Oryza sativa*) (Cont.).

Classification	Compounds
Aromatic acylated C-pentosylflavone-O-hexosides	C-pentosyl-apigenin <i>O</i> -coumaloylhexoside C-pentosyl-apigenin <i>O</i> -caffeoylhexoside C-pentosyl-apigenin <i>O</i> -feruloylhexoside C-pentosyl-chrysoeriol <i>O</i> -feruloylhexoside
C-glycosylflavone O-glycosides	C-pentosyl-apigenin <i>O</i> -rhamnosyl-O-hexoside C-hexosyl-apigenin <i>O</i> -hexosyl-O-hexosyl-O-hexoside
Aromatic acrylated C-hexosylflavanone O-hexosides	C-hexosyl-naringenin <i>O</i> -coumaroylhexoside C-hexosyl-apigenin <i>O</i> -caffeoylhexoside
Flavone mono-O-glycosides	Chrysin <i>O</i> -hexoside Apigenin 7- <i>O</i> -glucoside Apigenin 7- <i>O</i> -rutinoside Luteolin 5- <i>O</i> -glucoside Chrysoeriol 7- <i>O</i> -hexoside Chrysoeriol 7- <i>O</i> -hexoside Selgin 5- <i>O</i> -hexoside Selgin 7- <i>O</i> -hexoside Tricetin <i>O</i> -hexoside 3',4',5'-tricetin <i>O</i> -hexoside Tricin 7- <i>O</i> -hexoside
Flavonol mono-O-glycosides	Kaempferol 3- <i>O</i> -glucoside Quercetin 3- <i>O</i> -hexoside Naringenin 5- <i>O</i> -glucoside Naringenin 7- <i>O</i> -glucoside Eriodictyol 7- <i>O</i> -glucoside Hesperetin 5- <i>O</i> -glucoside
Flavone O-malonylhexosides	Apigenin <i>O</i> -malonylhexoside Luteolin <i>O</i> -malonylhexoside Tricetin <i>O</i> -malonylhexoside Selgin <i>O</i> -malonylhexoside 3,4,5-tricetonoylhexoside Tricin <i>O</i> -rhamnol <i>O</i> -malonylhexoside
Flavones	Apigenin Luteolin Chrysoeriol Tricin
Flavonones	Naringenin

Table 2.1 Accumulation of flavonoids in rice flag leaves (*Oryza sativa*) (Cont.).

Classification	Compounds
Lignans	Tricin 4'- <i>O</i> -(erythro β -guaiacylglyceryl)ether Tricin 4'- <i>O</i> -(threo β -guaiacylglyceryl)ether Tricin 4'- <i>O</i> -(erythro β -guaiacylglyceryl)ether <i>O</i> -hexoside Tricin 4'- <i>O</i> -(threo β -guaiacylglyceryl)ether <i>O</i> -hexoside
Anthocyanins	Cyanidine 3- <i>O</i> -glucoside Malvedine 3- <i>O</i> -hexoside Cyanidine 3- <i>O</i> -rutioside Peonidine 3- <i>O</i> -hexoside

Structural characterization has been developed using LC-MS/MS or nuclear magnetic resonance (Routaboul *et al.*, 2012) for the identification of flavonoids in different plant species. Investigation of flavonoids in rice leaf has revealed that there are different flavonoid components in extracts of each part and subspecies (Dong *et al.*, 2014).



CHAPTER III

MATERIALS AND METHODS

3.1 General materials

3.1.1 Plasmid and bacterial strain

The *Os9bglu31* cDNA was previously cloned into the pET32a(+)/DEST expression vector to produce an N-terminally thioredoxin-, His₆- and S-tagged Os9BGlu31 fusion protein with an enterokinase cleavage site (EK site) between the fusion tags and Os9BGlu31, as shown in Figure 3.1 (Luang *et al.*, 2013). The *Escherichia coli* strains DH5 α and Origami (DE3) were used as bacterial host cells for molecular cloning and recombinant protein expression, respectively.

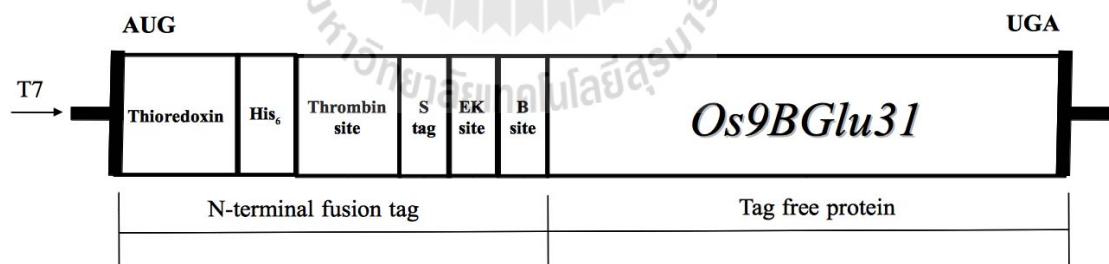


Figure 3.1 Diagram of the protein-coding sequence of recombinant pET32a(+)/DEST with the *Os9bglu31* cDNA inserted after the enterokinase cleavage site by directional Gateway recombination cloning (Luang *et al.*, 2013). Note that the components of the fusion protein are not diagrammed to scale.

3.1.2 Oligonucleotide and mutagenesis primers

All primers used for site-directed mutagenesis are shown in Table 3.1 and were ordered from Invitrogen Inc. (USA), except those for I172T, L183Q, L241D, and W243N mutant primers were ordered from Pacific Science Co., Ltd. (Bangkok, Thailand).

Table 3.1 Oligonucleotide primers for site-directed mutagenesis.

Mutant	Primer name	Nucleotide sequence (5'-3')	Length (bp)	T_m (°C)
Os9BGlu31	I172T_f	GCACTGTCAATGAGCCTAACACC GAGCCGATTGGCGGATACG	42	84.77
I172T	I172T_r	CGTATCCGCCAATCGGCTCGGTGT TAGGCTCATTGACAGTGC	42	84.77
Os9BGlu31	Y134W_f	CGGATACGATCAAGGAATCCAAC CGCCACGGCGATGCTCATTCC	44	87.38
L183Q	Y134W_r	GGAATGAGCATCGCCGTGGCGGT TGGATTCCTTGATCGTATCCG	44	87.38
Os9BGlu31	L134D_f	GGACAAATTGGGCTCACATTGGA CGGTTGGTGGTACGAGCCCG	43	86.61
L241D	L241D_r	CGGGCTCGTACCACCAACCGTCC AATGTGAGCCCAATTTGTCC	43	86.61
Os9BGlu31	W243A_f	GGGCTCACATTGCTCGGTGCGTG GTACGAGCCCGGGACG	39	89.5
W243A	W243A_r	CGTCCCGGGCTCGTACCACGCAC CGAGCAATGTGAGCCC	39	89.5
Os9BGlu31	W243D_f	GGGCTCACATTGCTCGGTGATTG GTACGAGCCCGGGACG	39	86.95

Table 3.1 Oligonucleotide primers for site-directed mutagenesis (Cont.).

Mutant	Primer name	Sequence	Length (bp)	T_m (°C)
W243D	W243D_r	CGTCCCGGGCTCGTACCAATCAC CGAGCAATGTGAGCCC	39	86.9
Os9BGlu31	W243F_f	GGGCTCACATTGCTCGGTTTCTGG TACGAGCCCGGGACG	39	86.3
W243F	W243F_r	CGTCCCGGGCTCGTACCAGAAAC CGAGCAATGTGAGCCC	39	86.3
Os9BGlu31	W243M_f	GGGCTCACATTGCTCGGTATGTG GTACGAGCCCGGGACG	39	85.83
W243M	W243M_r	CGTCCCGGGCTCGTACCACATAC CGAGCAATGTGAGCCC	39	85.83
Os9BGlu31	W243N_f	GGGCTCACATTGCTCGGTAATTG GTACGAGCCCGGGACG	39	84.81
W243N	W243N_r	CGTCCCGGGCTCGTACCAATTACC GAGCAATGTGAGCCC	39	84.81
Os9BGlu31	W243Y_f	GGGCTCACATTGCTCGGTTACTGG TACGAGCCCGGGACG	39	85.19
W243Y	W243Y_r	CGTCCCGGGCTCGTACCAGTAAC CGAGCAATGTGAGCCC	39	85.19

3.1.3 Phenolic compounds and flavonoids

To characterize Os9BGlu31 mutants in terms of their activity, we used the previously described method (Luang *et al.*, 2013). All phenolic compounds, such as ferulic acid, 4-hydroxybenzoic acid, 4-coumaric acid, vanillic acid, 1-naphthalene acetic acid, caffeic acid, syringic acid, *trans*-cinnamic acid, 1-naphthol, salicylic acid, 1-indole acetic acid, kaempferol 7-*O*-glucoside, and kaempferol were purchased from Sigma-Aldrich (St. Louis, MO, USA). Kaempferol 3-*O*-glucoside was kindly provided

by Prof. Dr. Toscahi Amahura, Matsuyama University, Japan. These flavonol compounds contain multiple hydroxyl groups that may serve as acceptors, while 4NPGlc (Sigma-Aldrich) was used as the donor substrate in the reaction.

3.1.4 Freeze-dried rice flag leaves

We have collaborated with Prof. Dr. Jong-Seong Jeon and Bancha Mahong of the Department of Plant Molecular Systems Biotechnology, Kyung Hee University, Yongin, Korea, who provided us with knockout Os9BGlu31 rice flag leaves. The *japonica* cultivars Dongjin and Nipponbare were the background genotypes of *osbglu31-1* and *osbglu31-4*, and *osbglu31-2* and *osbglu31-3*, respectively. Homozygous mutants for the insertions were identified by PCR analysis of genomic DNA isolated from mature rice leaves (Murray and Thompson, 1980).

3.2 General methods

3.2.1 Competent cell preparation

The bacteria (*E. coli* strains DH5 α and Origami(DE3)) were grown in 5 ml Lennox broth (LB, 10 g/l peptone, 5 g/l yeast extract, 5 g/l sodium chloride) at 37 °C, 200 rpm for 16 - 18 h as starter, then 1 ml starter was inoculated to 100 ml LB and cultured at 37 °C, 200 rpm until the OD₆₀₀ reached 0.4 - 0.6. The cell pellets were collected by centrifugation at 4000 rpm, 10 min, 4 °C. The pellets were resuspended in 10 ml of cold 0.1 M CaCl₂, gently mixed and stored on ice for 20 min. The cell suspension was centrifuged at 4000 rpm, 10 min, 4 °C, the supernatant discarded, and 2 ml of cold 0.1 M CaCl₂ added, after which the cells were kept on ice for 1 h. Then, 300 μ l glycerol was added, and the cell suspension was mixed very well and aliquoted

into microcentrifuge tubes with 50 μ l per tube. The tubes of competent cells were used immediately or kept at -80 °C.

3.2.2 Bacterial transformation

Fifty nanograms plasmid DNA was added into 50 μ l competent *E. coli* cells then gently mixed. The competent cells were incubated on ice for 10 min. The cells were heat shocked at 42 °C, 45 s, then immediately incubated on ice for 2 -3 min. Then, 500 μ l LB was added to the cells and they were incubated at 37 °C for 1 h. The mixture (100 μ l cell) was spread on an LB agar plate containing appropriate antibiotics, depending on the bacterial host and plasmid, and incubated at 37 °C overnight.

3.2.3 Site-Directed Mutagenesis

The mutations causing the amino acid substitution I172T, L183Q, L243D, W243N, W243A, W243D, W243F, W243M, and W243Y were introduced into the Os9BGlu31 coding sequence. The QuikChange® Site-Directed Mutagenesis Kit (Agilent-Stratagene, La Jolla, CA, USA) was used to generate the Os9BGlu31 mutations. The pET32a/*Os9bglu31* plasmid was used as a template for a full-length plasmid strand amplification from two complementary oligonucleotide primers containing the desired point mutation (Table 3.1). *Pfu* DNA polymerase (with proofreading activity) was used to synthesize the mutated plasmid DNA during the temperature cycling, which included step 1, 95 °C 30 s; step 2, 95 °C 30 s; step 3, 55 °C 1 min and step 4, 68 °C 15 min, with steps 2 to 4 repeated for 17 cycles. The products were treated with *DpnI* endonuclease for 3 h at 37 °C to eliminate methylated and hemimethylated DNA of the parental DNA template. Repair of the nicked circular dsDNA products was accomplished by transforming the DNA into competent DH5 α cells. The transformants were selected on agar plates containing 50 μ g/ml carbanicillin.

All mutations were confirmed by DNA sequencing (Invitrogen). The mutagenic oligonucleotide primers used for the kit were specifically designed according to the criteria of the QuikChange® manual (Stratagene, LaJolla, CA, USA) to have lengths of 25-45 bases with $T_m \geq 78$ °C. The T_m was calculated from following formula: $T_m = 81.5 + 0.41 (\%GC) - 675/N - \%mismatch$, where N is the primer length in bases, and %GC and % mismatch are whole numbers. The plasmids were extracted with plasmid extraction kits from Promega (Madison, WI, USA), according to the manufacturer's instructions.

3.2.4 SDS-PAGE

Polyacrylamide gel electrophoresis in the presence of sodium dodecyl sulfate (SDS-PAGE) was performed as described by Laemmli (1970) with 13% T polyacrylamide separating gels. The separating gel was prepared by mixing 3.3 ml distilled water, 2.5 ml 1.5 M Tris-HCl, pH 8.8, 4 ml 30% acrylamide /bisacrylamide solution, 100 µl 10% (w/v) SDS, 100 µl 10% (w/v) ammonium persulfate, and 4 µl TEMED. The 5% stacking gel was prepared by mixing 3.4 ml distilled water, 0.63 ml 0.5 M Tris-HCl, pH 6.8, 0.83 ml 30% acrylamide /bisacrylamide solution, 50 µl 10% (w/v) SDS, 50 µl 10% (w/v) ammonium persulfate, and 5 µl of TEMED. The protein sample was mixed with loading dye (2.5 M Tris-HCl, pH 6.8, 10% (w/v) SDS, 50% (v/v) glycerol, 0.5% (w/v) bromophenol blue, 4% (v/v) 2-mercaptoethanol) at 1:5 ratio and boiled at 100 °C for 5 min. The protein was loaded onto the gel under running buffer (25 mM Tris-HCl, 192 mM glycine, 0.1% SDS, pH 7.5) and placed in an electric field that was held at a potential of 150 volts until the dye front neared the bottom of the gel.

The protein bands were detected by the silver staining, the proteins were fixed in the gel by incubating in at least 5 gel volumes of ethanol:glacial acetic acid:milli-Q

water (30:10:60) 30 min at room temperature (approx. 25 °C) with gentle shaking. The fixing solution was discarded and 5 gel volumes of 30% ethanol was added, and incubated 30 min at room temperature. The gel was washed 3 times with milli-Q water, 5 volumes 0.1% AgNO₃ in milli-Q water (freshly prepared) was added, and the gel was incubated 30 min at room temperature. The solution was discarded and rinsed with milli-Q water 3 times 15 s each, the gel was developed in 100 ml developing solution (6 g sodium carbonate, in milli-Q water with 50 µl 37% formaldehyde), and stopped with stopping solution (10% methanol and 5% acetic acid) for 20 min. Then, the gel was transferred to nitrocellulose 2-3 h for drying.

3.2.5 Extraction of wild type and Os9BGlu31 knockout rice flag leaves

The wild type and knockout Os9BGlu31 rice flag leaves provided by Mr. Banha Mahong and Prof. Jong-Seong Jeon, from the Graduate School of Biotechnology and Crop Biotech Institute, Kyung Hee University, Korea, were freeze dried. Freeze-dried rice flag leaves were milled with a mortar and pestle at room temperature. The milled samples were kept in -30 °C before extraction, 100 mg was weighed and extracted with 1 mL 5% (v/v) or 70% (v/v) methanol in water with vortexing for 5 min and sonication for 15 min on ice. The extracts were centrifuged at 12,000 rpm for 10 min and the supernatants collected. The supernatants were analyzed on an ACQUITY UPLC system (Waters, USA) connected to a WATERS Xevo G2 Q-ToF mass spectrometer, as described in Section 3.6, and analyzed on an Agilent 1290 LC system (Agilent, USA) connected to an Agilent 6490 triple quadrupole mass spectrometer, as described in Section 3.7.

3.3 Protein expression and purification

The pET32a(DEST)/Os9BGlu31 plasmid, which includes the *Os9BGlu31* cDNA in frame to produce an N-terminally thioredoxin and His-tagged Os9BGlu31 fusion protein (Luang *et al.*, 2013), was transformed into *E. coli* strain Origami B(DE3) cells. The cells were cultured in LB media containing 50 µg/ml carbanicillin, 15 µg/ml kanamycin, and 12.5 µg/ml tetracyclin at 37 °C. When the culture reached an optical density at 600 nm of around 0.4-0.5, protein expression was induced by addition of IPTG to 0.4 mM. The induction temperature was set at 20 °C for 18 h. The cell pellets were collected by centrifugation and suspended in the extraction buffer (50 mM Tris-HCl, pH 8.0, 150 mM sodium chloride, 200 µg/ml lysozyme, 1% (v/v) Triton-X, 0.1 mg/ml trypsin inhibitor from soybean, 1 mM PMSF, 4 µg/ml DNase I) at approximately 25 °C, 30 min. Centrifugation removed insoluble debris, and the protein was purified from the soluble extract by Immobilized Metal-Affinity Chromatography (IMAC) on cobalt-equilibrated TALON resin (Clontech, Mountain View, CA, USA). The resin was washed with the equilibration buffer (150 mM NaCl, 50 mM Tris-HCl, pH 8.0), followed by 20 mM imidazole in the equilibration buffer, and eluted with 250 mM imidazole in the equilibration buffer. The fractions containing β-glucosidase activity, as judged by 4NPGlc hydrolysis, were pooled and imidazole removed by dialysis in 150 mM NaCl, 20 mM Tris-HCl buffer, pH 8.0. The dialyzed preparation was concentrated in a 30 kDa molecular mass cut off (MWCO) Centricon centrifugal filter (Millipore, Billerica, MA, USA). The N-terminal fusion tag was removed from the Os9BGlu31 fusion protein by cleavage with 6.4 ng enterokinase (New England Biolabs, Cambridge, MA, USA) per 1 mg of fusion protein at 23 °C for 18 h, followed by a second round of IMAC. The flow-through fractions containing β-glucosidase activity were pooled and

the protein purity was analyzed by SDS-PAGE. The Os9BGlu31 was dialyzed and concentrated with a 30 kDa MWCO Centricon filter to obtain approximately 5 mg/ml Os9BGlu31 protein in 150 mM NaCl, 20 mM Tris-HCl buffer, pH 8.0. All Os9BGlu31 mutants were expressed and purified in the same manner as the wild type protein.

3.4 Relative activities of Os9BGlu31 wild type and mutants

The activities with various glucose acceptor substrates were assayed with 0.25 mM acceptor, 5 mM 4-nitrophenyl β -D-glucopyranoside (4NPGlc) as glucose donor, and 3 μ g of Os9BGlu31 variant in 50 mM citrate buffer, pH 4.5. The reactions were incubated at 30 °C for 1 h and then stopped by adding formic acid to 1%. The reactions were centrifuged at 12,000 x g for 10 min, then supernatants were collected and analyzed by detection of 4NP and glucoconjugate products on an Acquity Ultra Performance LC (Waters, USA) with an Acquity UPLC BEH C18 (1.7 μ m, 2.1x50 mm) column (Waters). The mobile phase consisted of 0.1% formic acid in water (solvent A) and 0.1% formic acid in acetonitrile (solvent B) (Fisher Scientific, USA). The compounds were eluted with a linear gradient from 5 to 30% B (v/v) in 12.20 min, 30 to 100% B (v/v) in 1.40 min with flow rate of 0.3 mL/min. The diode array detector (DAD) was set to scan the range from 190-500 nm and the results were monitored and quantified at 340 nm. The 4NP released was quantified by comparison to a 4NP standard curve.

The protein absorbance was measured with a Nanodrop 2000c spectrophotometer (Thermo Scientific) at 280 nm and the protein concentration calculated from this absorbance with the extinction coefficient for each specific variant, which was calculated with the PROTEIN PARAMETERS program on the EXPASY website

(www.expasy.org). The extinction coefficient used for wild type, I172T, and L183Q is 1.72, that for W243Y is 1.65, and that for other W243 mutants is 1.63.

3.5 Evaluation of transglucosylation of kaempferol with 4NPGlc and kaempferol 3-*O*-glucoside

The products of transglycosylation by Os9BGlu31 and its W243 mutants were determined in reactions with 0.25 mM kaempferol as glucose acceptor, 5 mM 4NPGlc as substrate donor, and 5 μ g of wild type or mutant Os9BGlu31 in 50 mM citrate buffer, pH 4.5.

In another set of reactions, kaempferol 3-*O*-glucoside (m/z 447), was used as the sole substrate of the enzyme. The products were detected and relative levels quantified with an ACQUITY UPLC system (Waters, USA) equipped with a DAD detector and a WATERS Xevo G2 Q-ToF mass spectrometer. The mass spectrometer was run in the negative ion mode, and a capillary voltage of 2 kV, a source temperature of 100 °C and desolvation temperature of 200 °C were used. Desolvation gas flow was set as 600 l/h with the lock spray infusion flow rate at 20 μ L/min and lock spray capillary voltage at 2.50 kV. The collected data were analyzed with MassLynz Software in higher energy to describe the fragmentation behaviors. A reaction with Os9BGlu31 W243N was used for identification of the products from their mass spectra.

3.6 Rice flag leaf extracts as natural substrate for Os9BGlu31 enzyme assay

Wild type and Os9BGlu31 knockout mutant flag leaf extracts were produced as described in Section 3.2.5. For enzyme reactions with the leaf extracts, fifty milligrams of freeze-dried rice flag leaf powder were weighed and extracted with 500 μ l of 5% methanol or 70% methanol in water. Before assaying, 70% methanol extracts were evaporated by speed vacuum 3,000 rpm for 45 min to vaporize off the methanol. The reactions were set up with and without 0.25 mM naphthalene acetic acid as an artificial glucose acceptor and 5 μ g of Os9BGlu31 in 50 mM citrate buffer, pH 4.5. The reactions were incubated at 30 °C for 3 h and stopped with 1% formic acid. The reactions were centrifuged at 12,000 rpm for 10 min. The supernatants were quantified by ACQUITY UPLC system (Waters, USA) linked to a WATERS Xevo G2 Q-ToF mass spectrometer with a MassLynz Software.

3.6.1 UPLC G2 Q-ToF mass spectrometry analysis system

All rice flag leaf extracts and enzymatic assay samples were subjected to separation using an ACQUITY UPLC BEH C18 1.7 μ m, 2.1x100 mm column (Waters). The mobile phase consisted of 0.1% formic acid in water (solvent A) and 0.1% formic acid in acetonitrile (solvent B). The gradient varied linearly from 5 to 30% B (v/v) in 12.20 min, then 30 to 100% B (v/v) in 1.40 min at a flow rate of 0.3 mL/min. The UPLC effluent was delivered into the WATERS Xevo G2 Q-ToF mass spectrometer. The WATERS Xevo G2 Q-ToF mass spectrometry was equipped with an electrospray ionization (ESI) source and separately run in negative ion mode and positive ion mode. For the negative ion mode, the capillary voltage was 2 kV, source temperature was 100 °C and desolvation temperature was 200 °C. The desolvation flow gas flow was set

as 600 liters/h with the lock spray infusion flow rate and lock spray capillary at 20 $\mu\text{L}/\text{min}$ and 2.50 kV, respectively. On the other hand, positive ion mode was set up with a capillary voltage of 3 kV, a source temperature of 100 $^{\circ}\text{C}$ and desolvation temperature of 280 $^{\circ}\text{C}$. The desolvation gas flow was set at 600 liters/h with the lock spray infusion flow rate and lock spray capillary at 20 $\mu\text{l}/\text{min}$ and 3 kV, respectively.

3.6.2 UPLC triple quadrupole mass spectrometry analysis

Quantification of feruloyl glucose was done on an Agilent 1290 UPLC system (Agilent, USA) and a Agilent 6490 triple quadrupole mass spectrometer with MassHunter Software. All extract and enzymatic assay samples were subjected to separation over an Agilent SB-C18 RRHD 1.8 μm , 2.1 \times 150 mm column (Agilent, USA). The mobile phase consisted of 0.2% formic acid in water (solvent A) and 0.2% formic acid in acetonitrile (solvent B). The gradient varied linearly from 5 to 50% B (v/v) in 13 min, 50 to 70% B (v/v) in 1 min, and 70 to 10% B (v/v) in 2 min with flow rate 0.3 ml/min. The Agilent UPLC effluent was delivered into an Agilent 6490 triple quadrupole mass spectrometer equipped with an ESI source in negative ion mode. For the negative ion mode, a capillary voltage of 3 kV, and a gas temperature of 300 $^{\circ}\text{C}$ were used. The gas flow was set as 16 liters/min, nebulizer at 45 psi with the sheath gas heater at 300 $^{\circ}\text{C}$ and sheath gas flow at 11 l/min. The targeted parental ion was 1-*O*-feruloyl- β -D-glucose at m/z of 355 and its fragment was at m/z of 175 in negative ion mode.

A control reaction containing 0.25 mM ferulic acid with 5 mM 4NPGlc in 50 mM citrate buffer, pH 4.5, was used to calibrate the ferulic acid response by measuring the response of the m/z 355 fragment of product ion at m/z 134 with an elution time of 9.2 min. A set of 10-fold serial dilutions from 1/10 to 10^{-4} were set-up to check the

linearity of the response. The 1-*O*-feruloyl- β -D-glucose standard was produced by a reaction of 5 μ g wild type Os9BGlu31, which only produces 1-*O*-feruloyl β -D-glucose as a transglycosylation product, with 4NPGlc in identical conditions to the control. Both reactions were incubated at 30 °C for 1 h, and stopped with 1% formic acid. The ferulic acid response in 10-fold serial dilutions from concentration at 0.00025-0.25 mM of the enzymatic reaction was used to set-up a standard curve for ferulic acid. This standard curve was used to calibrate the response for ferulic acid in the enzymatic reaction. The determined amount of ferulic acid in the enzymatic reaction was subtracted from that in the control reaction to determine the amount of 1-*O*-feruloyl- β -D-glucose present in the reaction. The selected product ions were at *m/z* 193, 178, 175, and 134. The response of the *m/z* 175 product ion, which gave the highest abundance in Multiple Reaction Monitoring (MRM) of the feruloyl glucose peak that eluted in 7.2 min, was used for quantification. The relative levels of feruloyl glucose in rice extracts were calculated based on this response.

CHAPTER IV

RESULTS AND DISCUSSION

4.1 Os9BGlu31 expression and purification

The *Os9bglu31* cDNA was previously cloned into the pET32a(+)/DEST expression vector to produce an N-terminally thioredoxin-, His₆- and S-tagged Os9BGlu31 fusion protein with an enterokinase cleavage site before the start of the Os9BGlu31 sequence, as shown in Figure 3.1 (Luang *et al.*, 2013). The expression of Os9BGlu31 His-tagged fusion protein in *E. coli* strain Origami B (DE3) was induced with 0.4 mM IPTG concentration and induction time at 18 h. (Luang *et al.*, 2013).

In initial experiments, the Os9BGlu31 fusion protein was purified by immobilized metal affinity chromatography (IMAC). The 70 kDa thioredoxin- and His-tagged Os9BGlu31 fusion protein fractions contained many contaminant protein bands after 1st IMAC column. In later experiments, including those comparing the mutant enzymes and wild type, the protein was first purified by IMAC on TALON resin. It was then cleaved by enterokinase, and the 50 kDa tag-free protein was further purified by a 2nd round of IMAC. The purity of the protein increased to greater than 90% (Figure 4.1).

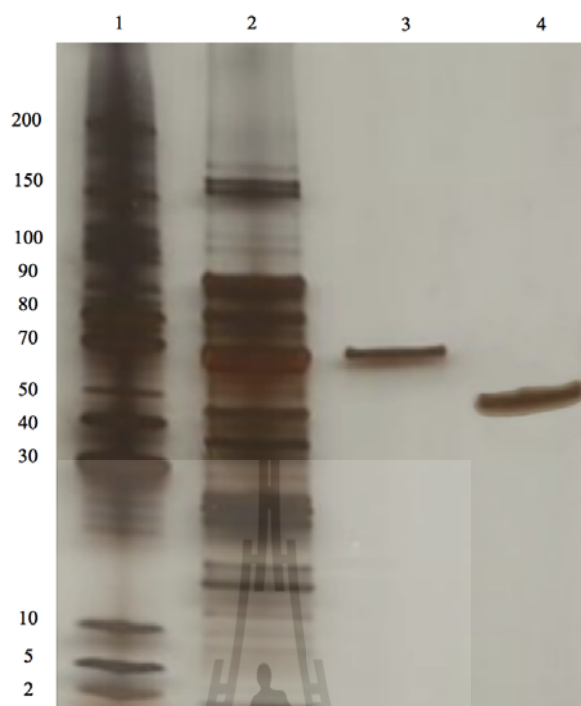


Figure 4.1 Silver-stained SDS PAGE gel of Os9BGlu31 W243N throughout purification. Lane 1, Invitrogen low molecular-mass markers (masses shown at left in kDa); Lane 2, crude extract of soluble proteins from *E. coli* strain Origami B(DE3) containing pET32a(+)/DEST-*Os9BGlu31* plasmid after induction with 0.4 mM IPTG 18 h; Lane 3, the N-terminal thioredoxin/His₆-tagged Os9BGlu31 W243N fusion protein after the first IMAC step; Lane 4, the purified Os9BGlu31 W243N mutant protein after cleavage of the fusion protein with enterokinase and removal of the tag with a 2nd IMAC step.

4.2 Effect of mutations of W243, L183, and I172 on Os9BGlu31 activity

We hypothesized that the high transglycosylation versus hydrolysis activity of Os9BGlu31 transglucosidase might be due to poor binding of water as an acceptor substrate, relative to other acceptors. Comparison of the active site of a homology model of Os9BGlu31 with the X-ray crystal structure of the 2-deoxy-2-fluoroglucoside complex of Os3BGlu6, a GH1 β -glucosidase with no significant transglycosylation activity (Seshadri *et al.*, 2009), identified several residues differing around the acceptor substrate (water) binding site, as shown in Figure 4.2. We changed I172, L183, and L241 to the corresponding residues in Os3BGlu6 (I172T, L183Q and L241D) and W243 to the N found in Os3BGlu7 β -glucosidase (W243N) in order to make acceptor binding site more hydrophilic.

The activities of the mutant enzymes were similar or higher than wild type, except for the L241D mutant, which gave little soluble protein, so that it could not be characterized. Compared to wild type Os9BGlu31, all three characterized mutants have higher ratios of transfer of glucose to the 1-naphthol hydroxyl group to that to the 1-naphthalene acetic acid carboxylic group, but only the W243N mutant had a higher rate of hydrolysis (34%) relative to transglycosylation of ferulic acid compared to wild type (9%). We had hypothesized that mutant enzymes should have more hydrolysis activity than wild type, since the residues introduced by the mutations have more hydrophilic amino acid side chains for water binding, but all mutants still maintained higher rates of transglycosylation than the hydrolysis. However, the mutant enzymes transfer glucose to hydroxyl groups better than the wild type enzyme and showed differences in acceptor specificity, as shown by the relative activity in Figure 4.3.

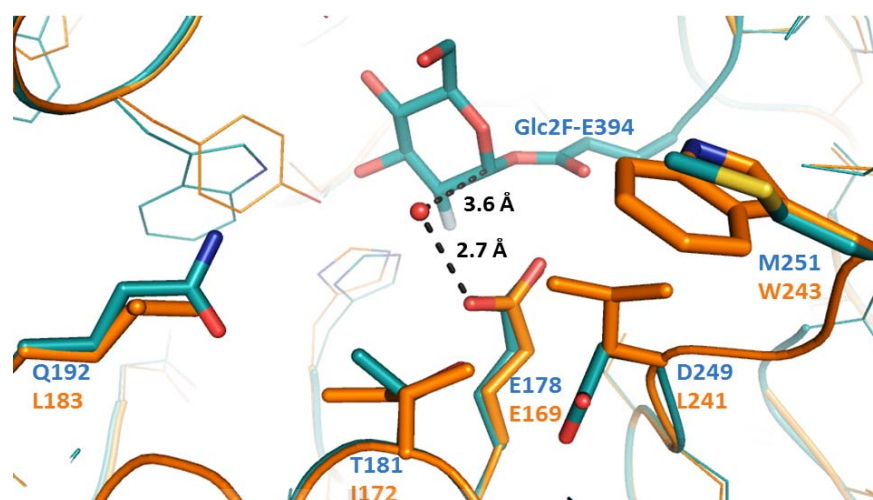


Figure 4.2 Superposition of a homology model of Os9BGlu31 transglucosidase on the X-ray crystal structure of the Os3BGlu6 β -glucosidase covalent intermediate with 2-fluoro- α -D-glucoside (PDB code 3GNR). Os9BGlu31 is shown with orange carbons, while the Os3BGlu6 structure carbons are green. The putative nucleophilic (acceptor) water in the Os3BGlu6 complex is shown as a red sphere and the distances between it and the anomeric carbon of 2-fluoroglucose and the catalytic acid base (E178) are indicated. The protein backbones are shown as ribbons. The side chains of residues surrounding the proposed water/acceptor/aglycone binding site that were significantly less polar in Os9BGlu31 compared to Os3BGlu6, the catalytic acid/ base residues, and the 2-fluoroglucose-bound nucleophile of Os3BGlu6 are shown in thick stick representation with labels for Os3BGlu6 on top and Os9BGlu31 on the bottom, while other side chains are shown as lines. Os9BGlu31 residues I172, L183, and L241 were within 5.5 Å of the acceptor water binding site in this superposition, while W243 (8.7 Å away) was also chosen for mutagenesis due to the importance of the corresponding residue in the substrate specificities of Os3BGlu6, Os3BGlu7 and Os4BGlu12.

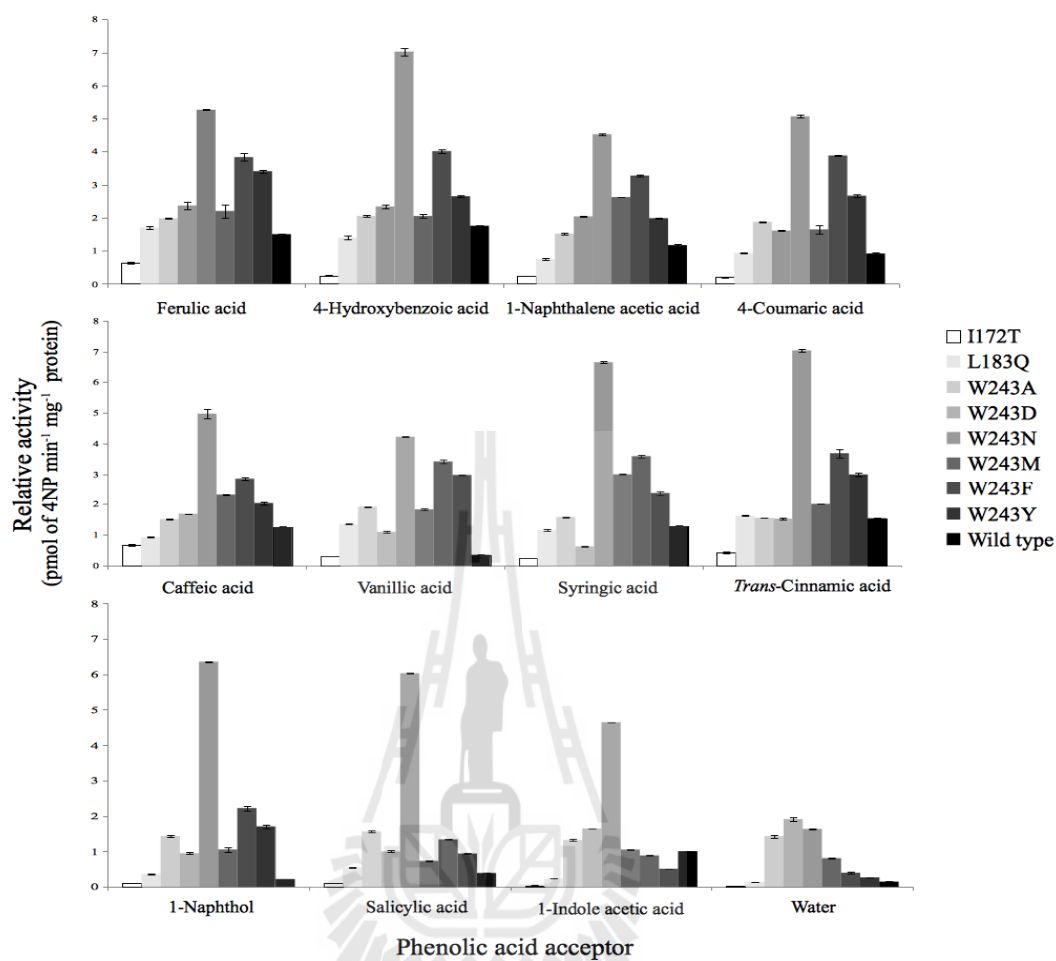


Figure 4.3 Relative activities of Os9BGlu31 and its active site cleft mutants with various acceptors. Activities were tested with 5 mM 4NPGlc donor and 0.25 mM acceptor substrate. 4NP released was detected by UPLC (Waters, USA).

4.3 Substrate specificity for transglucosylation of Os9BGlu31 W243 mutants

Both wild type Os9BGlu31 and W243N mutant enzymes transfer the glucosyl moiety from a donor substrate to an acceptor, but the Os9BGlu31 W243N enzyme has higher velocity and is more likely to transfer glucose to hydroxyl groups and water. We have substituted the W243 position with alanine (small), methionine (hydrophobic, non aromatic), phenylalanine (aromatic), tyrosine (aromatic hydroxyl), and aspartate (acidic) residues. Minor effects on the optimum pH were observed, as shown in Figure 4.4. The quantification of 4NP released from 4NPGlc in the presence of different acceptors by UPLC allowed the relative activities of these mutants for transglucosylation of various aromatic acceptors to be determined. Each of the W243 mutant enzymes showed higher rates of transfer to ferulic acid, naphthol and water and higher ratios of transfer to naphthol compared to naphthalene acetic acid than wild type Os9BGlu31. However, they showed different relative rates with different acceptors, depending on the amino acid substituted for W243.

Moreover, some of the W243 mutant enzymes show multiple products in reactions with phenolic acceptors that have both carboxyl and hydroxyl groups that can act as acceptors, such as ferulic acid (Figure 4.5A), 4-hydroxybenzoic acid (Figure 4.5B), 4-coumaric acid (Figure 4.5C), caffeic acid (Figure 4.5D), sinapic acid (Figure 4.5E), and vanillic acid (Figure 4.5F) as shown below. The W243N mutant could produce two products for each of these substrates, while the W243A mutant could only produce detectable amounts of the earlier eluting product for ferulic acid and caffeic acid, as seen for ferulic acid in Figure 4.5A. Other mutants were intermediate in their abilities to produce the two products. These products were found to have the same m/z but

different retention times. Since these acceptors have only one hydroxyl and one carboxylic group to which to add glucose, the extra products not seen in the reactions with wild type Os9BGlu31 were surmised to be glucoside products, most of which eluted from the C18 column before the glucose ester products, due to their higher polarity. Therefore, the W243 mutants have ability to transfer glucose to both hydroxyl groups to produce glucoside linkages and carboxylic group to produce ester linkages, while wild type enzyme can produce only ester linkages in detectable amounts.

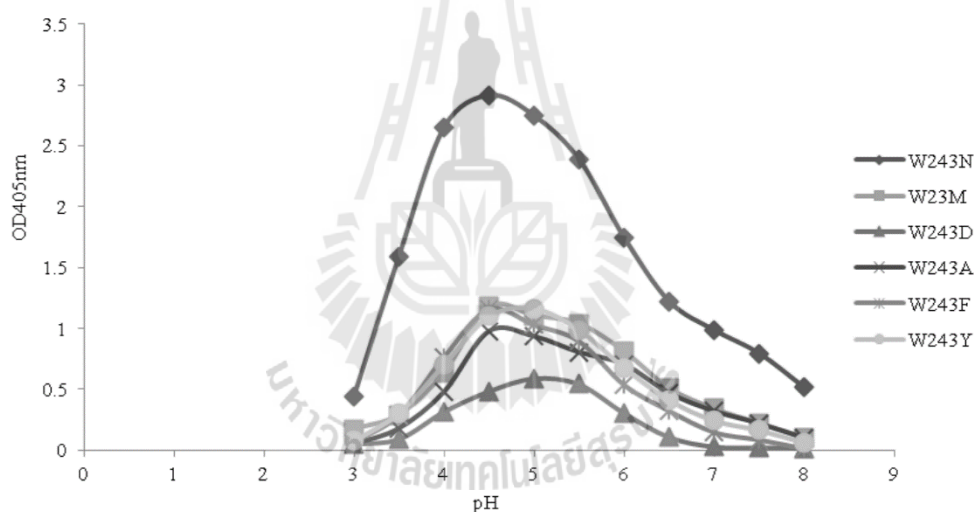


Figure 4.4 Activity versus pH curves of Os9BGlu31W243 mutants. The optimal pH is 4.5-5.0 for all mutants in buffers of 100 mM citric acid and 200 mM Na₂HPO₄ from pH 3-8.

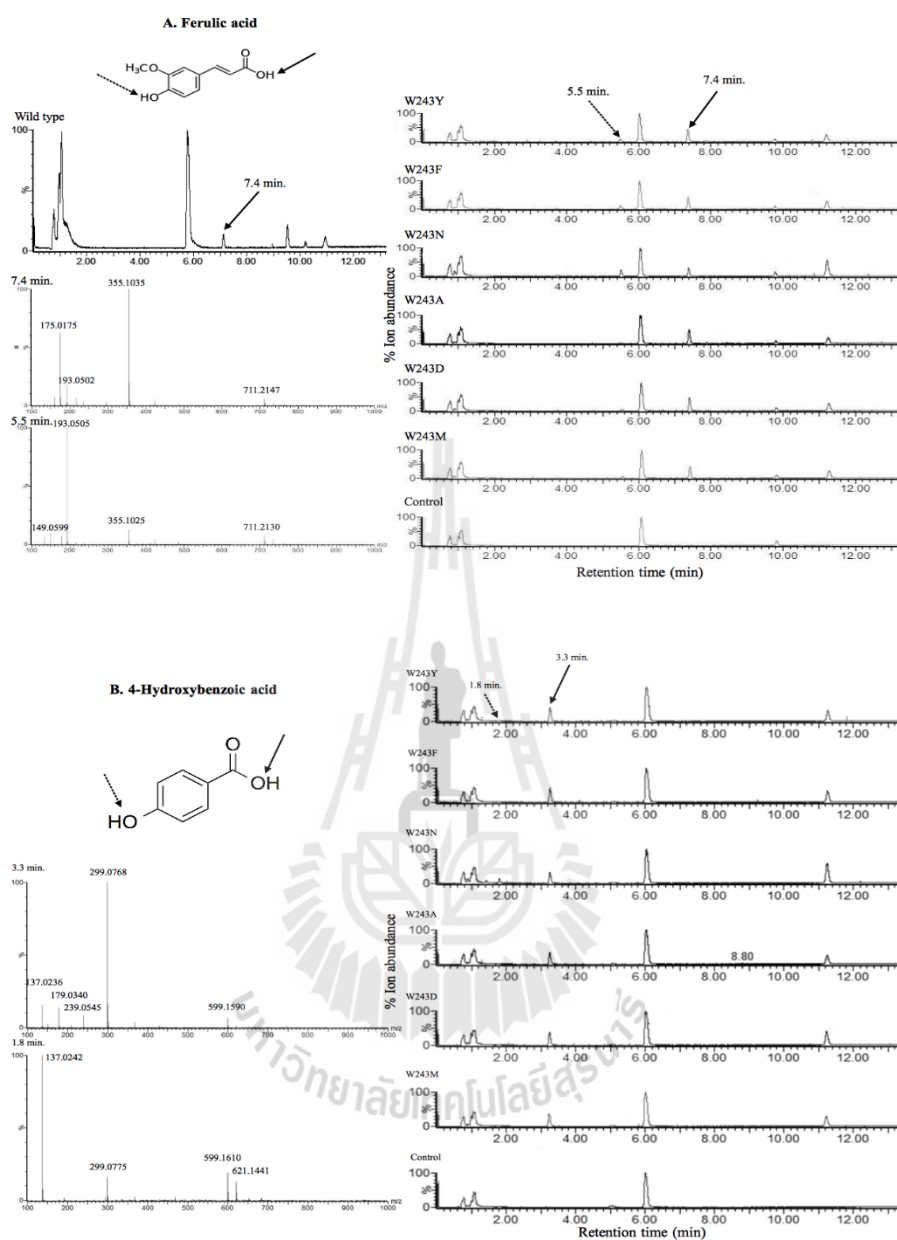


Figure 4.5 Chromatograms of reaction mixtures of Os9BGluc31 W243 variants' transfer of glucose to phenolic acid acceptors. Most W243 mutants, but not wild type Os9BGluc31 can transfer to both hydroxyl and carboxylic acid groups. A, Transfer to ferulic acid; and B, Transfer to 4-hydroxybenzoic acid.

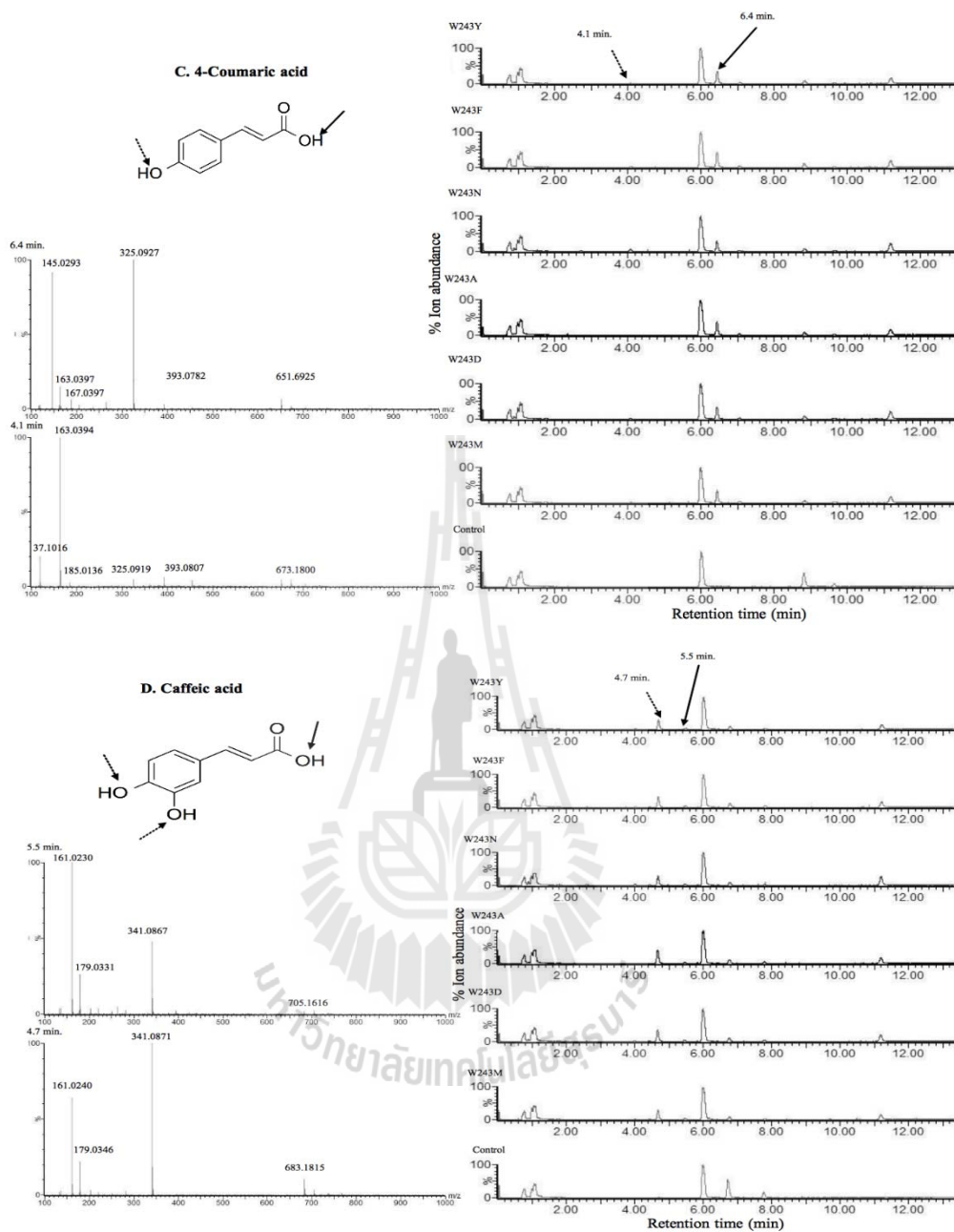


Figure 4.5 Chromatograms of reaction mixtures of Os9BGlu31 W243 variants' transfer of glucose to phenolic acid acceptors. Most W243 mutants, but not wild type Os9BGlu31 can transfer to both hydroxyl and carboxylic acid groups. C, Transfer to 4-coumaric acid; and D, Transfer to caffeic acid.

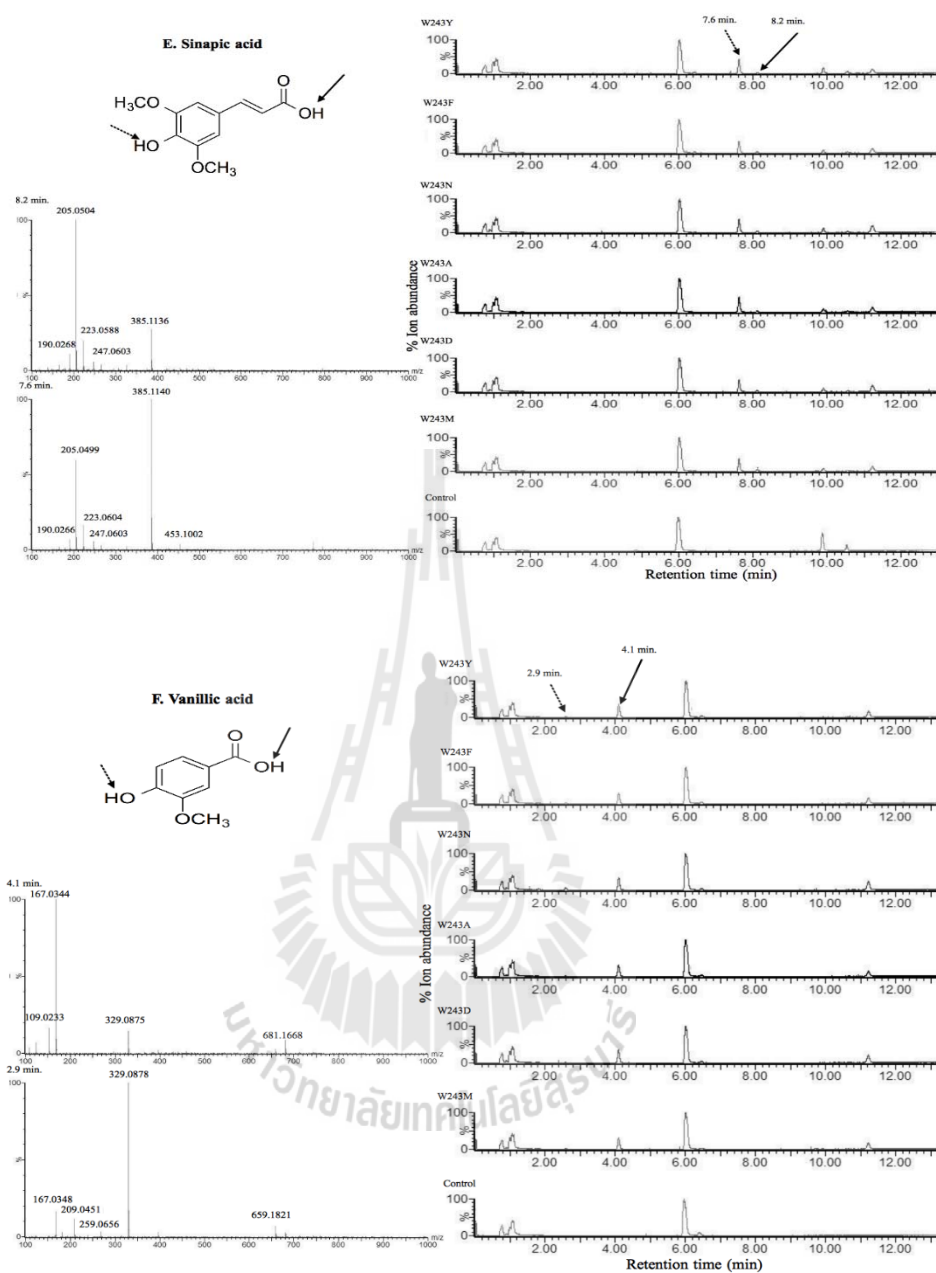


Figure 4.5 Chromatograms of reaction mixtures of Os9BGlu31 W243 variants' transfer of glucose to phenolic acid acceptors. Most W243 mutants, but not wild type Os9BGlu31 can transfer to both hydroxyl and carboxylic acid groups. E, Transfer to sinapic acid; and F, Transfer to vanillic acid.

4.4 Determination of the fragmentation patterns and glucosylation position of kaempferol mono-*O*-glucosides

To further explore the regioselectivity of the Os9BGlu31 W243N mutant in glucosylation of hydroxyl groups compared to the Os9BGlu31 wild type enzyme, we analyzed the glucosylation positions on the kaempferol molecule, which is a flavonol that has four hydroxyl groups to which glucosyl groups can be attached. The W243N mutant transferred glucose to kaempferol acceptor at multiple positions to provide 3 monoglucosides and 3 diglucosides, while wild type Os9BGlu31 produced only one kaempferol monoglucoside under the same conditions, as shown the chromatograms in Figure 4.6. Injection of kaempferol 3-*O*- β -D-glucoside standard showed that it coeluted with 4NP, and the extracted single ion mass chromatogram showed it is present as a product in the reaction with the Os9BGlu31 W243N, but not the wild type. Analysis of the UV-visible spectra and mass spectra helped us to identify three kaempferol monoglucosides, three kaempferol diglucosides, and one kaempferol acceptor substrate, as shown in Table 4.1. However, all the peaks have very similar UV spectra with maximum absorbance peaks around 264-265 nm for the first peak and 362-365 nm at the second peak, which is typical for kaempferol glycosides (Gaynor *et al.*, 1988; Riggi *et al.*, 2013). In contrast, the glycosylation position has a significant influence on the fragmentation behavior of kaempferol-*O*-glucosides. The fragmentation behavior of kaempferol glucosides and the relative abundance of their radical aglycone ions correlate with glucosylation position. The probable [M-H]⁻ product ion fragmentation positions of kaempferol 3-*O*, 7-*O*, and 4'-*O*-glucosylated isomers of kaempferol are shown in Figure 4.7 and supported by the mass spectra in Figure 4.8. These fragmentation patterns are expected from the resonance structures for the radicals

created by homolytic cleavage shown in Figure 4.9. As shown, homolytic cleavage of the 3-*O*- and 4'-*O*-glucosides will result in radical delocalization over the whole structure, thereby stabilizing these structures and resulting in a greater abundance of the immediate products shown in Figure 4.7. In contrast, the 5-*O*- and 7-*O*- glucosides do not have as extensive delocalization, so homolytic cleavage is not favored. Therefore, the $[M-H]^-$ product ion spectra of 3-*O*, 7-*O*, and 4'-*O* glucosylated isomers of kaempferol show differences in the relative abundances of aglycon $[Y_0]^-$ and radical aglycon $[Y_0-H]^-$ ions. Since compound 4 (Figure 4.8A) co-eluted with the kaempferol 3-*O*-glucoside standard and showed the expected fragmentation pattern, it was concluded to be kaempferol 3-*O*-glucoside, while compound 6 (Figure 4.8C), which showed a similar homolytic cleavage was concluded to be kaempferol 4'-*O*-glucoside. Although the fragmentation pattern of compound 5 (Figure 4.8B) is consistent with either kaempferol 5-*O*-glucoside or kaempferol 7-*O*-glucoside, kaempferol 7-*O*-glucoside is less sterically hindered and is found in nature (Nijveldt *et al.*, 2001; Calderón-Montaña *et al.*, 2011). The wild type enzyme has also been observed to use apigenin 7-*O*-glucoside, which has a similar structure, as a donor, and compound 5 was produced by both the wild type and mutant enzymes. Thus, the kaempferol *O*-glucoside of compound 5 was deduced to be kaempferol 7-*O*-glucoside.

The fragmentation behavior of these isomers was investigated based on the production of $[M-H]^-$, which correlated to an abundance of $[Y_0-H-CO-H]^-$ ion at m/z 255 for compound 4 (Figure 4.8A) and $[Y_0-CO]^-$ ion at m/z 257 for compound 5 (Figure 4.8B) (Ablajan *et al.*, 2006), but a corresponding ion was not found in the spectrum of compound 6 (Figure 4.8C), which is glycosylated on the other aromatic ring, suggesting that the $[Y_0-H]^-$ ion at m/z 284 is the precursor of $[Y_0-H-CO-H]^-$, while the Y_0^- ion at m/z 285 is the precursor of $[Y_0-CO]^-$.

Table 4.1 Parameters of kaempferol glucosides observed in UPLC G2-Q-ToF-MS^E. The chromatographic retention time, mass spectrum peaks, and UV-vis absorbance peak values shown were obtained from the reaction catalyzed by the Os9BGlu31 W243N mutant.

Peak no.	Peak name	RT (min)	MW	MS ^E data (m/z)	UV (nm)
1	Kaempferol 3,7-di- <i>O</i> -glucoside	7.9	610	609(M-H) ⁻ , 447(M-Glc-H) ⁻ , 285(M-2Glc-H) ⁻ , 255(M-2Glc-CO-3H) ⁻	265, 345
2	Kaempferol 4',7-di- <i>O</i> -glucoside	8.6	610	609(M-H) ⁻ , 447(M-Glc-H) ⁻ , 285(M-2Glc-H) ⁻ , 257(M-2Glc-CO-H) ⁻	265, 361
3	Kaempferol 3,4'-di- <i>O</i> -glucoside	8.8	610	609(M-H) ⁻ , 446(M-Glc-H-H) ⁻ , 283(M-2Glc-2H) ⁻ , 255(M-2Glc-CO-3H) ⁻	265, 336
4	Kaempferol 3- <i>O</i> -glucoside	10.9	448	447(M-H) ⁻ , 284(M-Glc-H) ⁻ , 255(M-Glc-CO-H) ⁻	264, 365
5	Kaempferol 7- <i>O</i> -glucoside	11.2	448	447(M-H) ⁻ , 285(M-Glc-H) ⁻ , 257(M-Glc-CO-2H) ⁻	265, 362
6	Kaempferol 4'- <i>O</i> -glucoside	11.4	448	447(M-H) ⁻ , 284(M-Glc-H) ⁻	265, 346
7	Kaempferol	13.7	286	285(M-H) ⁻ , 239(M-H ₂ CO ₂ -H) ⁻	265, 366

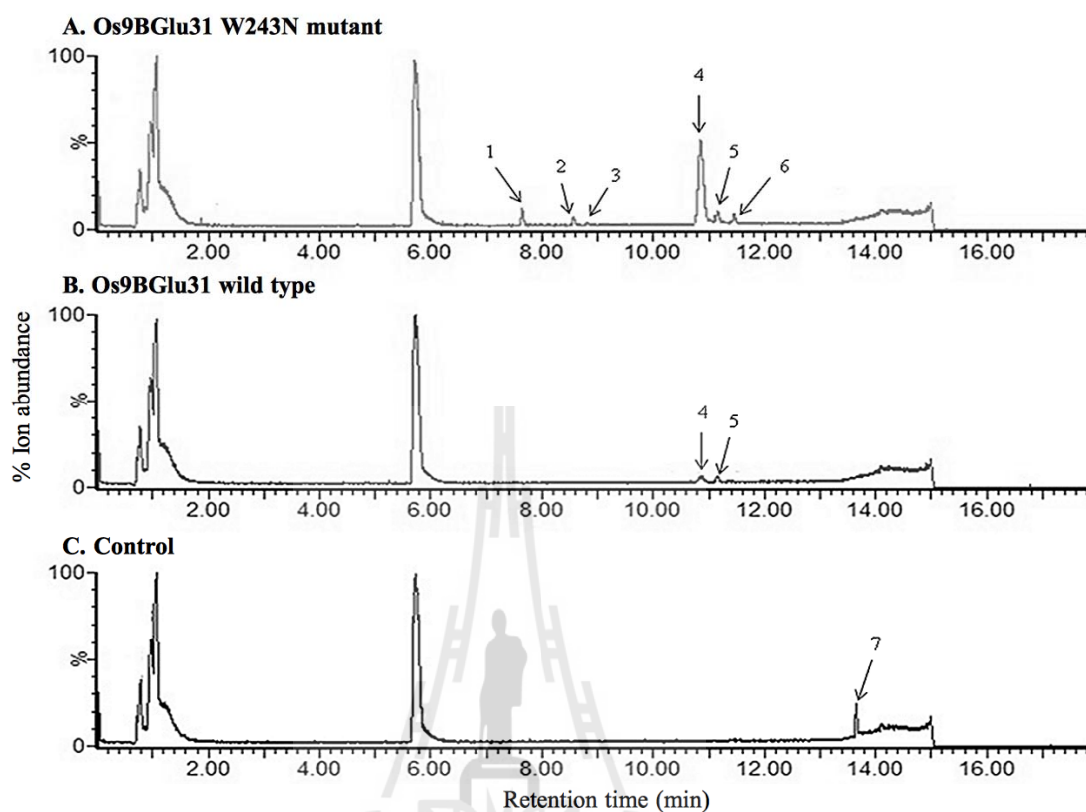


Figure 4.6 Chromatograms of products from kaempferol transglycosylation by wild type and W243N variants of Os9BGlu31 using 4NPGlc as a glucosyl donor. The UPLC G2 Q-ToF-MSMS chromatograms of the products in negative ion mode are shown with the products labeled with numbers as follows: kaempferol 3,7-di-*O*-glucoside (1); kaempferol 4',7-di-*O*-glucoside (2); kaempferol 3,4'-di-*O*-glucoside (3); kaempferol 3-*O*-glucoside and 4NP (4); kaempferol 7-*O*-glucoside (5); kaempferol 4'-*O*-glucoside (6); and kaempferol (7).

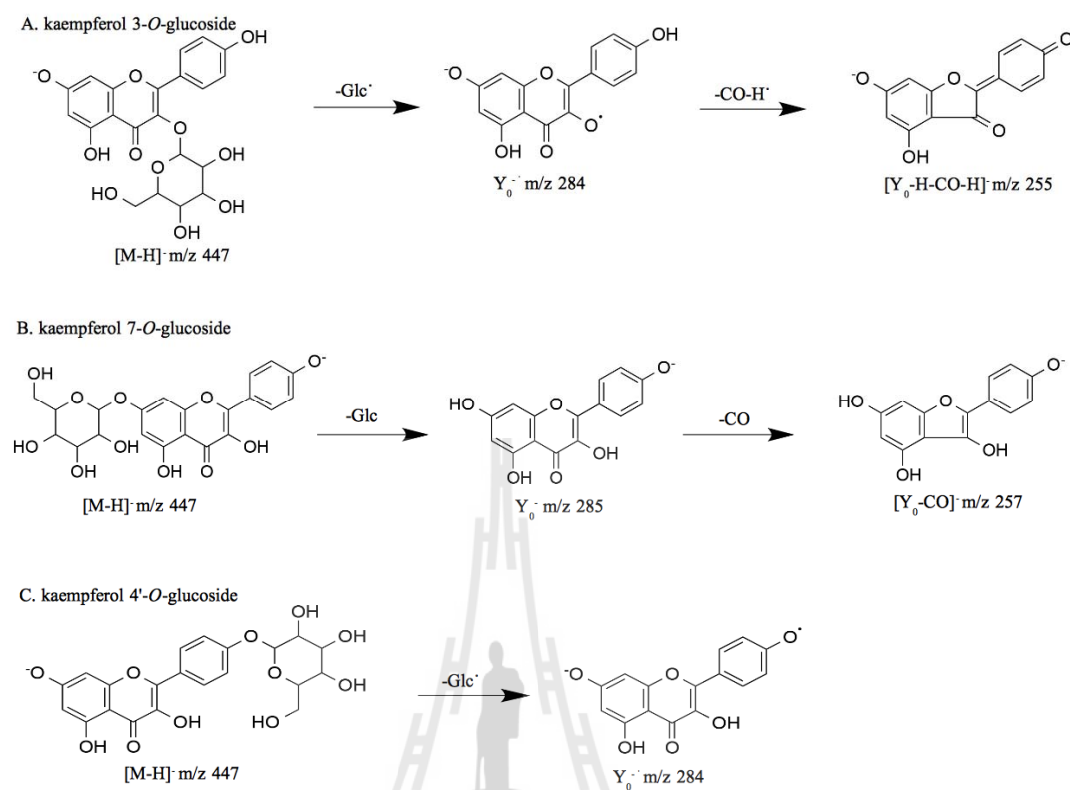


Figure 4.7 The fragmentation pathways of kaempferol mono-*O*-glucosides. (A) 3-*O*-glucoside; (B) kaempferol 7-*O*-glucoside; and (C) kaempferol 4'-*O*-glucoside and the possible mechanisms for the formation of radical ions based on MS/MS spectra.

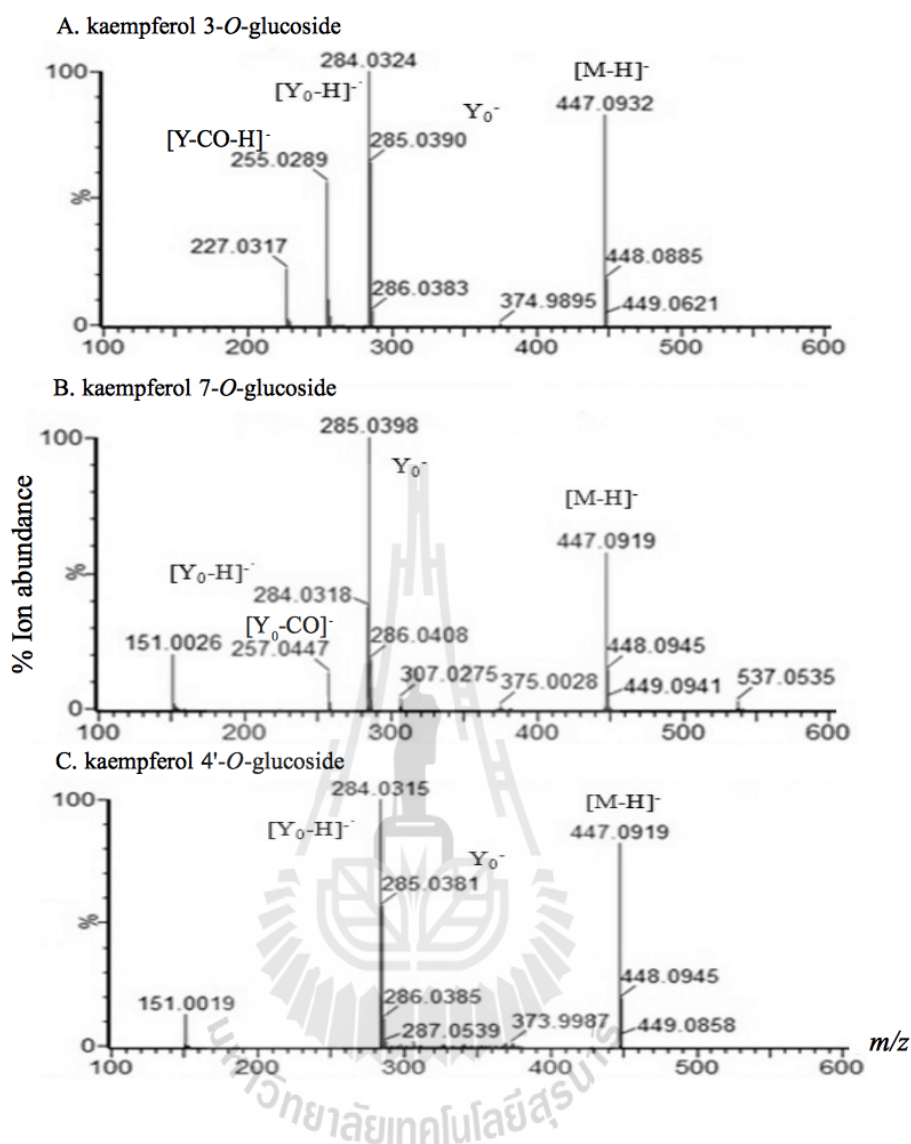


Figure 4.8 [M-H]⁻ product ion spectra of compounds 4, 5, and 6 in negative ion mode.

(A) Compound 4: kaempferol 3-*O*-glucoside (m/z 447); (B) compound 5: kaempferol 7-*O*-glucoside (m/z 447); (C) compound 6: kaempferol 4'-*O*-glucoside (m/z 447).

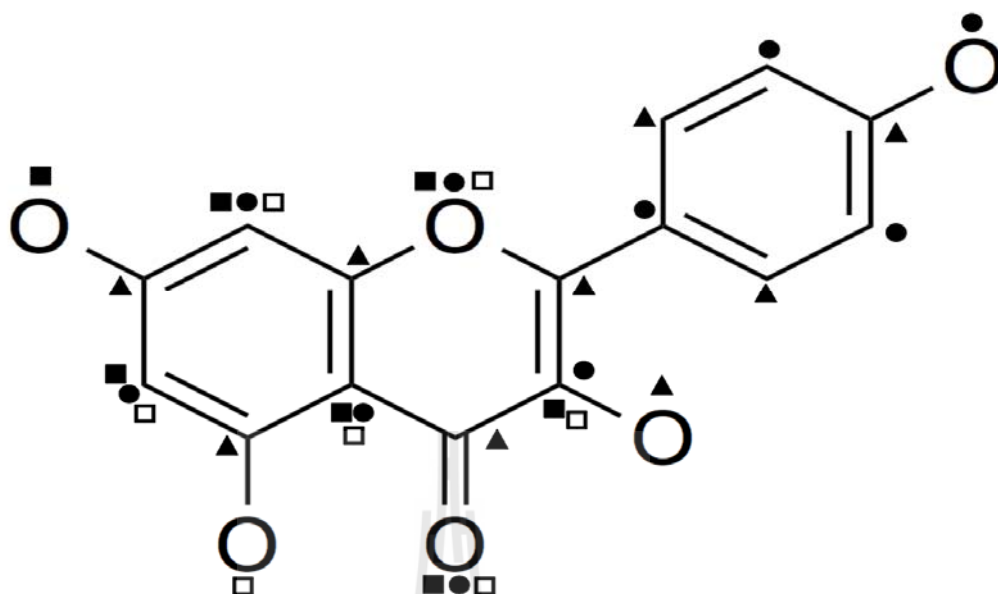


Figure 4.9 Kaempferol structural diagram representing radical delocalization positions from homolytic cleavage ions of glucose from position 3 (dark triangles), 5 (white squares), 7 (dark squares), and 4' (dark circles). Notice: fewer resonance structures are possible for homolytic cleavage at positions 5 and 7.

4.5 Fragmentation behavior of kaempferol di-*O*-glucosides

As shown in Figure 4.10 A-C, kaempferol di-*O*-glucosides with different glucose positions have different fragmentation patterns that can be used to identify these compounds. The fragmentation of the $[M-H]^-$ m/z 609 parent ion resulted in an abundant $[Y_0-H-CO-H]^-$ ion at m/z 255 for compound 1 (Figure 4.9A) and compound 3 (Figure 4.10C), but this fragment was not observed in the spectrum of compound 2 (Figure 4.10B). Since the m/z 255 ion was identified as a fragment of kaempferol 3-*O*-glucoside, compound 2 (Figure 4.10B) must not contain a glucosyl moiety at position 3, and could be tentatively identified as kaempferol 7,4'-di-*O*-glucoside. The product glycosides were identified based on these spectra and the results of radical elimination at the 3, 7, and 4' positions of kaempferol di-*O*-glucosides resulting in the homolytic cleavage diagrammed in Figure 4.9. When glucose forms a glycosidic bond at the 3-*O* and 7-*O* positions, it is likely to produce Y_0^- m/z 285, as depicted in Figure 4.10, due to the relatively high stability of the fragment generated by loss of a glucosyl residue, compared to that resulting from glucose radical loss. These results suggest that the glucose at position 3 might be eliminated as a glucosyl radical ion to form $[Y_0^3-H]^+$ m/z 446 and a second radical ion elimination at position 7 or 4' would form a $[Y_0-2H]^-$ m/z 283 ion from kaempferol 3,7-di-*O*-glucoside and kaempferol-3,4'-di-*O*-glucoside. As noted earlier, kaempferol 4',7-di-*O*-glucoside has a unique fragmentation behavior without $[Y_0-CO-2H]^-$ m/z 255 ion formation. As discussed for kaempferol 7-*O*-glucoside, glucose at the 7-*O* position is more likely to be eliminated as a glucosyl moiety than as a radical $[Y_0^7-H]^-$, so peaks at m/z 447 and Y_0^- m/z 285 are expected. The possibility to eliminate a second glucose from the 4' position of the $[Y_0^7-H]^-$ m/z 447 ion could result in the $[Y_0-H]^-$ m/z 284 ion as shown in Figure 4.12. The homolytic

cleavage at positions 3 and 4' of kaempferol 3,4'-di-*O*-glucoside results in a fairly stable fragment due to radical neutralization to form $[Y_0-2H]^-$ m/z 283 with the highest relative abundance, as shown in Figure 4.13.

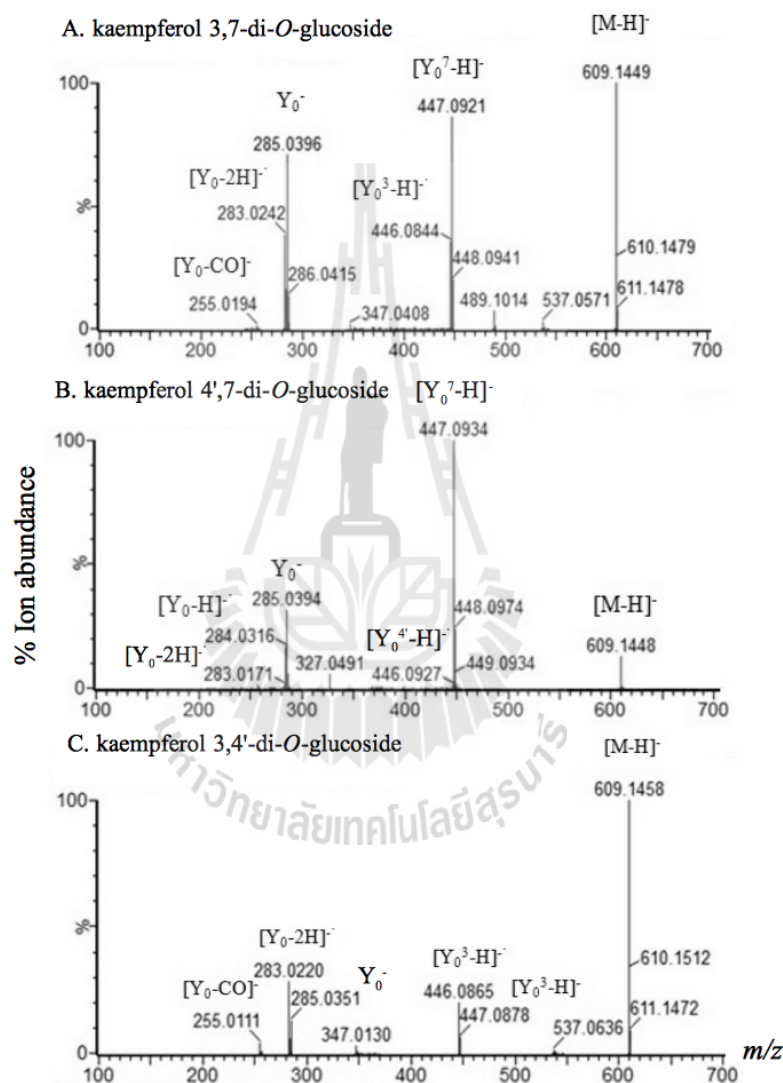


Figure 4.10 $[M-H]^-$ product ion mass spectra of compounds 1, 2, and 3 in negative ion mode. (A) compound 1: kaempferol 3,7-di-*O*-glucoside (m/z 609); (B) compound 2: kaempferol 4',7-di-*O*-glucoside (m/z 609); (C) compound 3: kaempferol 3,4'-di-*O*-glucoside (m/z 609).

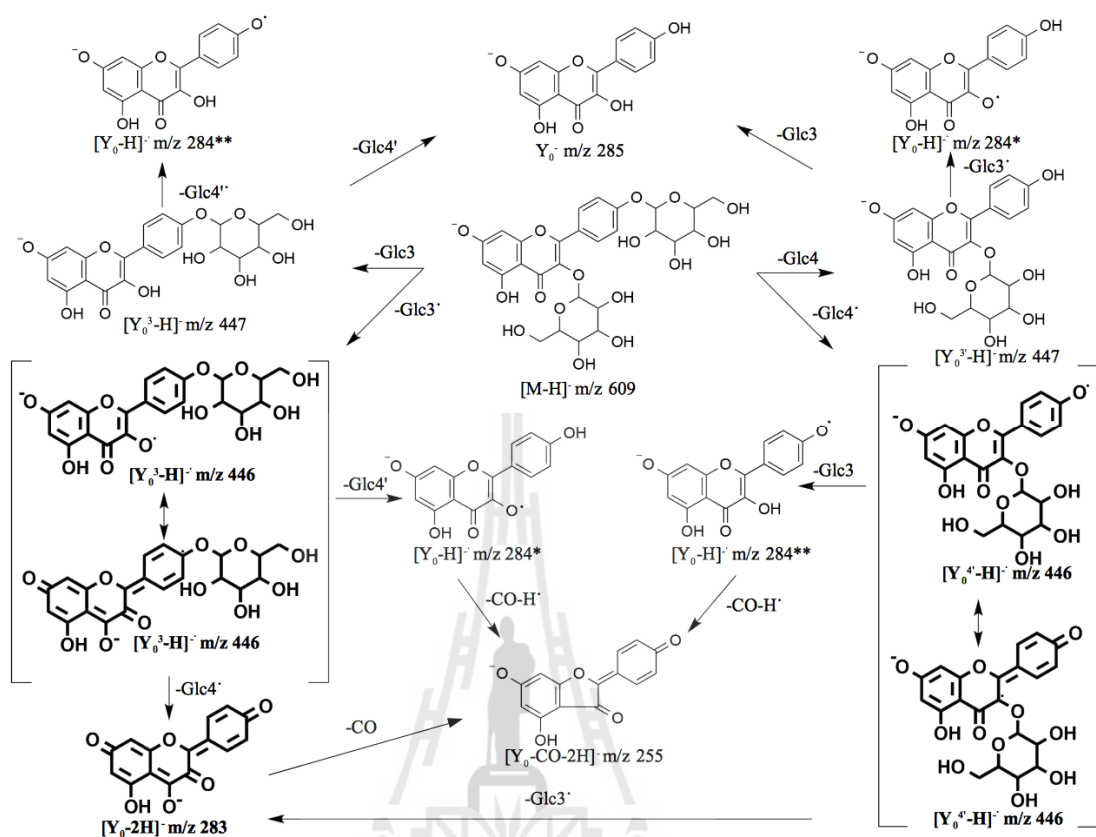


Figure 4.13 The fragmentation pathways of kaempferol 3,4'-di-*O*-glucoside and the possible mechanisms for the formation of radical ions observed in the MS/MS spectra (Notice: * and ** = the same structure; Black=stable; Black and bold=stable and high relative abundance).

4.6 Kaempferol 3-*O*-glucoside as acceptor and donor for Os9BGlu31

W243 mutants

The identification of kaempferol glycosides allowed us to compare the different W243 mutants for kaempferol glucoside production. Figure 4.14 shows the chromatograms for the W243N, wild type Os9BGlu31 and boiled enzyme control reactions, which indicate that the W243N mutant can transfer glucose from kaempferol 3-*O*- β -D-glucoside to the 7-*O* and 4'-*O* positions, while the wild type recombinant enzyme cannot effectively do so. The W243N mutant can transfer the glucosyl moiety from kaempferol 3-*O*- β -D-glucoside to the 7- and 4'-hydroxyl positions of kaempferol aglycone to produce diglucosides and monoglucosides as shown from the chromatogram in Figure 4.14. Thus, mutation of the W243 to a smaller, more polar residue (N) relaxed the donor and acceptor substrate specificity of Os9BGlu31.

Furthermore, all of the W243 mutant enzymes can also produce kaempferol-di-*O*-glucosides from kaempferol 3-*O*- β -D-glucoside, as shown in Figure 4.15. Production of compound 5 from compound 4 by the W243A mutant (Figure 4.15E) indicates that this mutant has the highest activity to deglycosylate kaempferol 3-glucoside and prefers to transfer to the 7-*O*-position, whereas the highest activities to transfer to the 4'-*O* position were from the W243M and W243N mutants (Figure 4.15F). Kaempferol di-*O*-glucosides were produced from kaempferol 3-*O*- β -D-glucoside (compound 4), with the highest amount of kaempferol 3,7-di-*O*-glucoside (compound 1) in the reaction with the W243F mutant (Figure 4.15A), which along with W243Y showed the highest production of kaempferol 7-*O*- β -D-glucoside from 4NPGlc and kaempferol. Kaempferol 4',7-di-*O*-glucoside (compound 2) was only produced from 3-*O*-glucoside by W243N, although it was barely detectable even with this variant, while W243M

could produce similar amounts to W243N when 4NPGlc was used as the donor (Figure 4.15B). The W243N mutant also produced the largest amount of kaempferol 3,4'-di-*O*-glucoside (Figure 4.15C). Thus, Os9BGlu31 variants with different amino acids at residue 243 show different donor and acceptor position specificities, which could be used for differential production of 6 types of kaempferol glycosides.

In wild type and each variant, the 7-*O*-position was the most often glucosylated, but the variants with smaller residues at residue 243 were able to glucosylate other positions more effectively. As might be expected, the W243F and W243Y mutants that maintained the aromatic side chains, but with less bulk, were most similar to wild type, while smaller residues had greater abilities to glycosylate the 3-*O* and 4'-*O* hydroxyls. In fact, the W243A mutant, where the whole indole ring was removed to leave a methyl side chain, had the highest activity toward the 3-*O* position as an acceptor or donor. Nonetheless, bulk was not the only factor, since the hydrophilic asparagine and aspartate side chains and hydrophobic methionine side chain gave higher activity than alanine for glycosylation at the 4' hydroxyl.

In common with Os9BGlu31 transglucosidase, the residue corresponding to W243 is an important determinant of substrate specificity in GH1 β -glucosidases (Chuenchor *et al.*, 2008; Sansenya *et al.*, 2012). The corresponding N245 in Os3BGlu7 (rice BGlu1) β -glucosidase is critical to efficient oligosaccharide hydrolysis. Mutation of this residue to V decreased the k_{cat}/K_m for cellotriose 15 fold (Chuenchor *et al.*, 2008), while conversion to M decreased k_{cat}/K_m 18 fold and conversion of the corresponding H252 in Os4BGlu14 caused a 2.5-fold drop in this value (Sansenya *et al.*, 2012). In contrast, changing Os3BGlu6 M251 to N resulted in a 24-fold increase in the k_{cat}/K_m for cellotriose and smaller increases for other gluco-oligosaccharides. Here, we have

verified that this position is also important for acceptor specificity in transglycosylation by Os9BGlu31 transglucosidase, in which W243 appears to restrict acceptor and donor aglycone usage and the regio-specificity of glucosyl transfer.

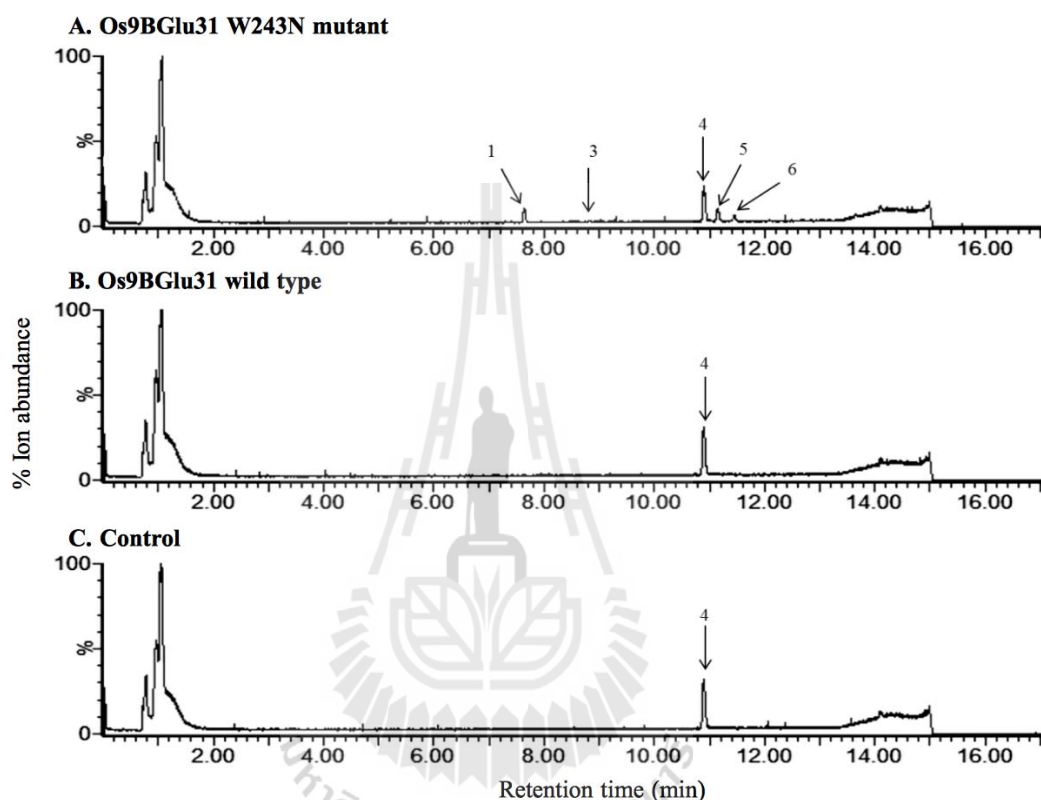


Figure 4.14 Chromatograms of reaction solutions of Os9BGlu31 wild type and W243N mutant using kaempferol 3-*O*- β -D-glucoside alone as substrate. For W243N the visible products are 1, kaempferol 3,7-di-*O*-glucoside, at retention time of 7.6 min (*m/z* 609); 3, kaempferol 3,4'-di-*O*-glucoside, 8.8 min (*m/z* 609); 4, kaempferol 3-*O*-glucoside (substrate), 10.9 min (*m/z* 447); 5, kaempferol 7-*O*-glucoside, 11.2 min (*m/z* 447); and 6, kaempferol 4'-*O*-glucoside, 11.4 min is (*m/z* 447).

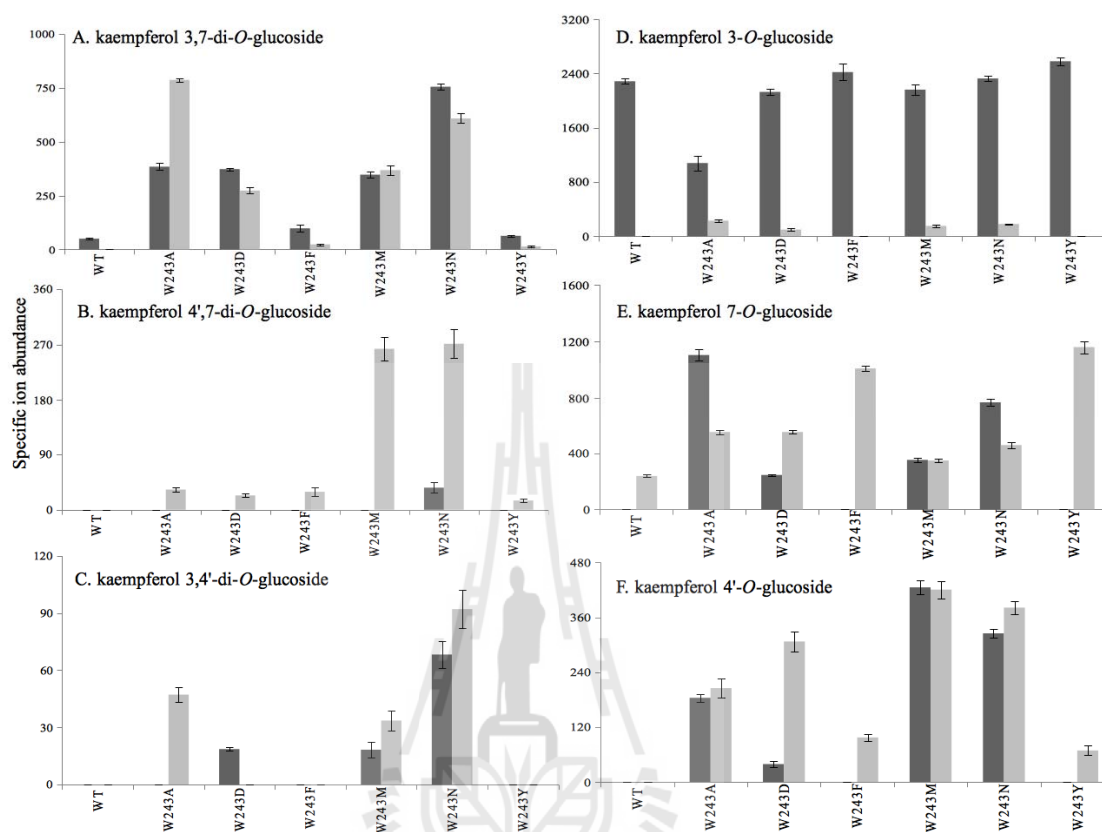


Figure 4.15 Comparison of reaction products for glycosylation of kaempferol by Os9BGlu31 WT and W243 variants. The dark bars indicate the measured abundances of ions for the product or remaining substrate in reactions with kaempferol 3-*O*-glucoside as the lone substrate and the light gray bars indicate the amount of products produced in reactions with kaempferol as acceptor and 4NPGlc as the donor substrate showing the production of kaempferol 3,7-di-*O*-glucoside (A); kaempferol 4',7-di-*O*-glucoside (B); kaempferol 3,4'-di-*O*-glucoside (C); kaempferol 3-*O*-glucoside (D); kaempferol 7-*O*-glucoside (E); and kaempferol 4'-*O*-glucoside (F).

4.7 UPLC G2 Q-ToF-MS-based rice flag leaf metabolite profiling

We carried out metabolite profiling of wild type rice flag leaf extracts in two different percentages of methanol (5% and 70%), due to the ability of metabolites to dissolve in different polarity solvents. The metabolites identified included both aglycons and glycosides. LC-MS is regarded as a powerful tool for metabolite profiling of secondary metabolites. The 5% (Table 4.3) and 70% (Table 4.4) methanol in water used to extract glycon and aglycon compounds were the solvent systems from previous studies on glucoconjugates (Matsuba *et al.*, 2010; Chen *et al.*, 2013). We characterized compounds with high throughput UPLC-ESI-MSMS in positive and negative ion modes of 70% methanol in water and 5% methanol in water, as shown in the chromatograms in Figures 4.16 and 4.17, respectively. With the two different solvents, different extracted compounds were detected. Moreover, the mode of mass spectrometry (positive and negative ion mode) detected different compounds in the chromatogram. Compounds with m/z corresponding to naringin, kaempferol 3-*O*-rutinoside, peonidine 3-*O*- β -D-galactoside, and oenin were detected only in positive ion mode. On the other hand, compounds with masses corresponding to sinapoyl glucose, kaempferol 3-*O*- β -D-glucopyranosyl 7-*O*-rhamnoside, kaempferol 3-*O*-glucoside, tricetin 4'-*O*-(guaiacylglyceryl)ether 7-*O*-glucoside, and gibberellin A5 were only observed in negative ion mode. Therefore, the mode of ionization is important for detection of unknowns and needs to be adjusted to that which is the most suitable for each compound.

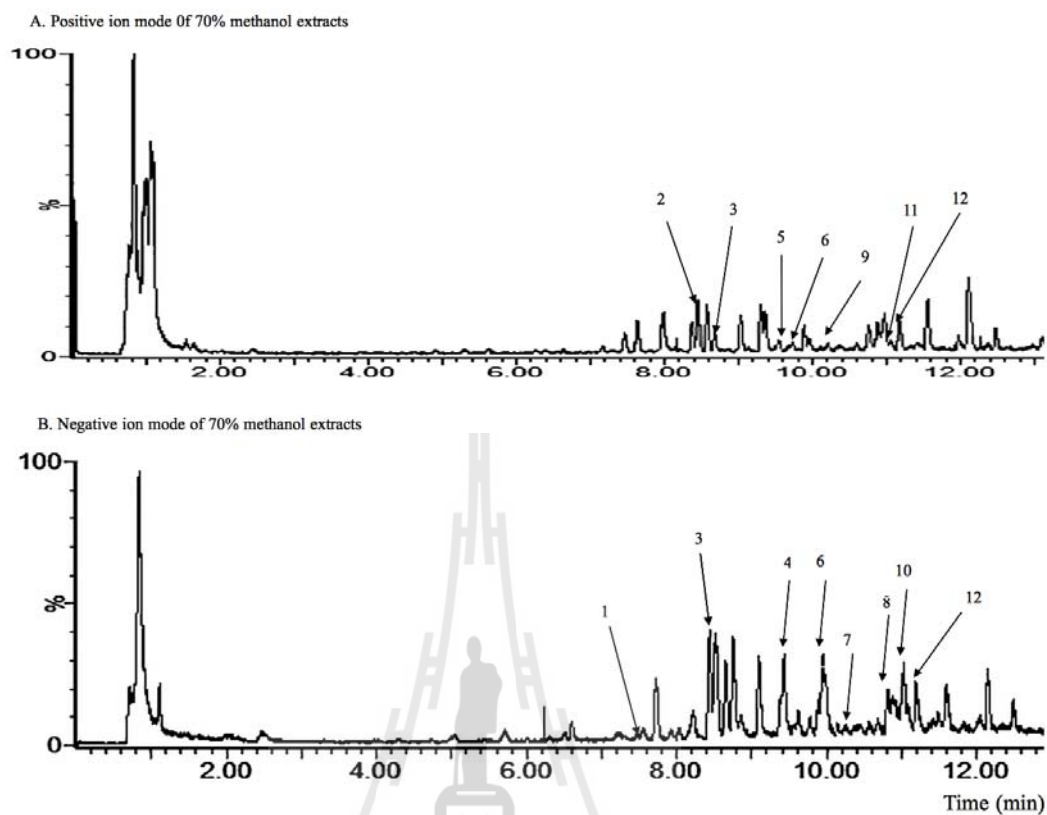


Figure 4.16 The chromatogram of rice flag leaf extracts in positive (A) and negative (B) ion modes from extraction with 70% methanol in water. The putative compounds were identified based on the calculated m/z of the compounds in the database falling within 5 ppm of the measured m/z . The compounds that had acceptable matches to the peaks based on this criteria are catalogued in Table 4.3.

Table 4.2 Putative identification of compounds from wild type rice flag leaves extracted in 70% methanol in water. The compounds were found in each single peak from the chromatogram and the differences from the expected masses of the matching compounds ($\Delta m/z$) calculated in ppm.

Putative compound	Negative ion mode						Positive ion mode					
	Formula	RT	UV peaks (nm)	Calc. Mass	Ext. Mass	$\Delta m/z$ ppm	Formula	RT	UV peaks (nm)	Calc. Mass	Ext. Mass	$\Delta m/z$ ppm
1. Sinapoyl glucoside	C ₁₇ H ₂₁ O ₁₀	7.5	325	385.1140	385.1140	0	NA	NA	NA	NA	NA	NA
2. Naringin	NA	NA	NA	NA	NA	NA	C ₂₆ H ₂₉ O ₁₅	8.5	270,350	581.1508	581.1506	-0.3
3. Rutin	C ₂₇ H ₂₉ O ₁₆	8.7	270,348	609.1456	609.1461	0.8	C ₂₇ H ₃₀ O ₁₆	8.7	270,350	611.1603	611.1607	0.7
4. Kaempferol-3- <i>O</i> - β -D-glucoparanosyl-7- <i>O</i> -rhamnoside	C ₂₇ H ₂₉ O ₁₅	9.5	270, 340	593.1506	593.1512	1.0	NA	NA	NA	NA	NA	NA
5. Kaempferol-3- <i>O</i> -rutinoside, Kaempferol-3-glucoside-3"-rhamnoside, Kaempferol-3- <i>O</i> -neohesperiside	NA	NA	NA	NA	NA	NA	C ₂₇ H ₃₁ O ₁₅	9.7	270,350	595.1679	595.1657	-3.7
6. Isorhamnetin-3-galactosyl-Isorhamnetin-3- <i>O</i> -rutinoside	C ₂₈ H ₃₂ O ₁₆	9.9	269, 319	623.1618	623.1618	0	C ₁₈ H ₃₂ O ₁₆	9.9	270,320	625.1752	625.1763	1.8
7. Kaempferol-3- <i>O</i> -glucoside	C ₂₁ H ₁₉ O ₄	10.4	270, 348	447.0933	447.0933	-1.1	NA	NA	NA	NA	NA	NA
8. Tricin4'(guaiacylglyceryl)ether 7- <i>O</i> -glucoside	C ₂₃ H ₂₃ O ₁₂	10.8	348	687.1925	687.1931	2.8	NA	NA	NA	NA	NA	NA
9. Peonidine-3- <i>O</i> - β -galactopyranoside	NA	NA	NA	NA	NA	NA	C ₂₂ H ₂₃ O ₁₁	10.9	268,334	463.1230	463.1235	1.1
10. Gibberalin A5	C ₁₉ H ₂₁ O ₅	11.0	270, 345	329.1386	329.1394	2.4	NA	NA	NA	NA	NA	NA
11. Oenin	NA	NA	NA	NA	NA	NA	C ₂₃ H ₂₅ O ₁₂	11.1	270,350	493.1338	493.1341	0.6
12. Cirsiliol	C ₁₇ H ₁₃ O ₇	11.2	270, 348	329.0659	329.0667	2.4	C ₁₇ H ₁₅ O ₇	11.2	270, 350	331.0819	331.0812	-2.1

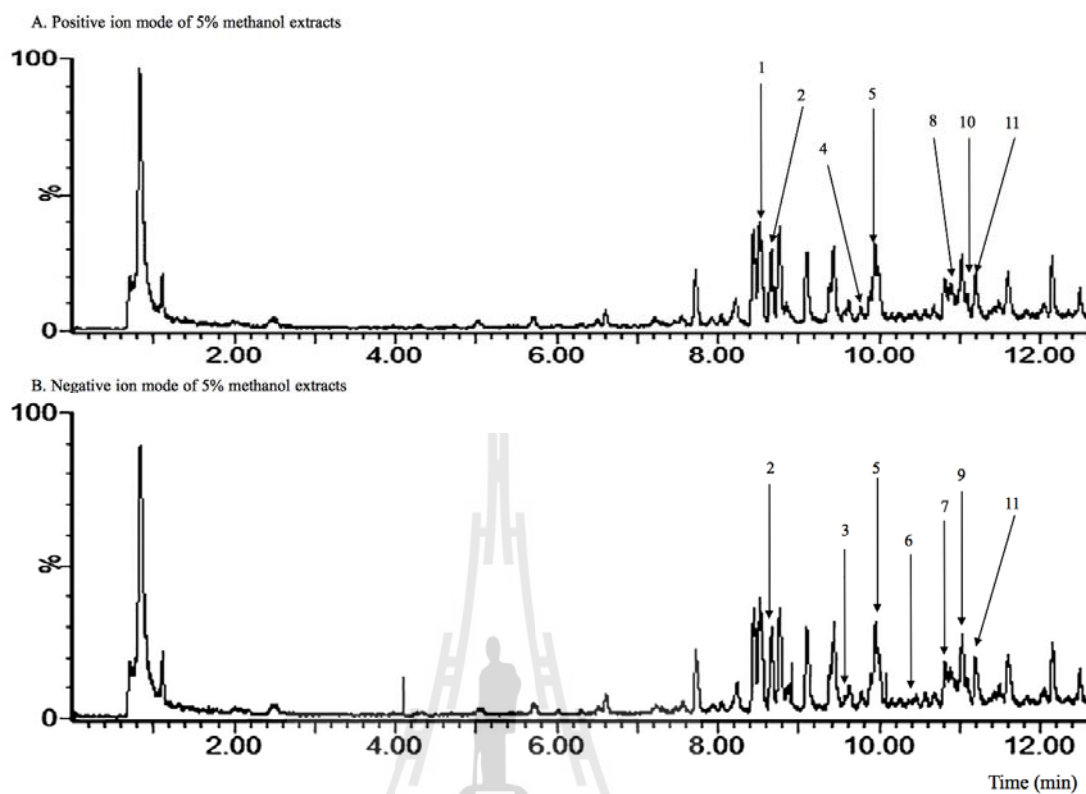


Figure 4.17 The chromatogram of rice flag leaf extracts in positive (A) and negative ion mode (B) from extraction with 5% (v/v) methanol in water. The putative compounds were identified from their m/z , with database compounds with calculated masses within 5 ppm of the measured mass considered an acceptable match. The matched compounds are catalogued in Table 4.4.

Table 4.3 Putative compounds extracted from wild type rice flag leaves in 5% methanol in water. The compounds found in the database with calculated masses matching each single peak from the chromatogram are listed and the differences between the measured mass and the expected masses of the matching compounds ($\Delta m/z$) calculated in ppm.

Putative compound	Negative ion mode						Positive ion mode					
	Formula	RT	UV	Calc. Mass	Ext. Mass	$\Delta m/z$ ppm	Formula	RT	UV	Calc. Mass	Ext. Mass	$\Delta m/z$ ppm
1. Naringin	NA	NA	NA	NA	NA	NA	C ₂₆ H ₂₉ O ₁₅	8.5	270,350	581.1508	581.1506	-0.3
2. Rutin	C ₂₇ H ₂₉ O ₁₆	8.7	270,348	609.1456	609.1461	0.8	C ₂₇ H ₃₀ O ₁₆	8.7	270,350	611.1603	611.1607	0.7
3. Kaempferol-3- <i>O</i> - β -D-glucoparanosyl-7- <i>O</i> -rhamnoside	C ₂₇ H ₂₉ O ₁₅	9.5	270, 340	593.1506	593.1512	1.0	NA	NA	NA	NA	NA	NA
4. Kaempferol-3- <i>O</i> -rutinoside, Kaempferol-3-glucoside-3''-rhamnoside, Kaempferol-3- <i>O</i> -neohesperiside	NA	NA	NA	NA	NA	NA	C ₂₇ H ₃₁ O ₁₅	9.7	270,350	595.1679	595.1657	-3.7
5. Isorhamnetin-3-galactosyl-Isorhamnetin-3- <i>O</i> -rutinoside	C ₂₈ H ₃₂ O ₁₆	9.9	269, 319	623.1618	623.1618	0	C ₁₈ H ₃₂ O ₁₆	9.9	270,320	625.1752	625.1763	1.8
6. Kaempferol-3- <i>O</i> -glucoside	C ₂₁ H ₁₉ O ₄	10.4	270, 348	447.0933	447.0933	-1.1	NA	NA	NA	NA	NA	NA
7. Tricin 4'-(guaiacylglyceryl)ether 7- <i>O</i> -glucoside	C ₂₃ H ₂₃ O ₁₂	10.8	348	687.1925	687.1931	2.8	NA	NA	NA	NA	NA	NA
8. Peonidine-3- <i>O</i> - β -galactopyranoside	NA	NA	NA	NA	NA	NA	C ₂₂ H ₂₃ O ₁₁	10.9	268,334	463.1230	463.1235	1.1
9. Gibberellin A5	C ₁₉ H ₂₁ O ₅	11.0	270, 345	329.1386	329.1394	2.4	NA	NA	NA	NA	NA	NA
10. Oenin	NA	NA	NA	NA	NA	NA	C ₂₃ H ₂₅ O ₁₂	11.1	270,350	493.1338	493.1341	0.6
11. Cirsiliol	C ₁₇ H ₁₃ O ₇	11.2	270, 348	329.0659	329.0667	2.4	C ₁₇ H ₁₅ O ₇	11.2	270, 350	331.0819	331.0812	-2.1

4.8 Effect of Os9BGlu31 gene knockout on metabolite profile

The UPLC G2 Q-ToF-MS results showed that wild type and knockout Os9BGlu31 rice flag leaf 70% methanol extracts could be distinguished. One observed difference between the wild type and homologous knockout rice flag leaves was the amount of feruloyl glucose ester (FAG), as shown the chromatogram in Figure 4.18. The knockout Os9BGlu31 rice lines could accumulate FAG in flag leaves, which appears to be related to the ability of the Os9BGlu31 enzyme to use FAG as a glucosyl donor substrate. Removal of Os9BGlu31 might lead to the build-up of FAG, which is the substrate of this enzyme. We tested four different homologous knockout Os9BGlu31 rice lines to confirm that for each line in which Os9BGlu31 gene expression was undetectable, there was an increase in the FAG peak, which was measured as the selected specific negative ion at m/z 355.1035 in Figure 4.19. The accumulation of FAG by knockout Os9BGlu31 was significantly increased FAG when compare with wild type controls by calculation of area under the ion abundance curve peak of the selected m/z 355.1035, as shown in Table 4.5.

We also characterized the amount of FAG in wild type and knockout Os9BGlu31 rice flag leaf 70% methanol extracts by selecting a specific fragment ion on a triple quadruple mass spectrometer. The FAG peak was measured using Multiple Reaction Monitoring (MRM) from UPLC triple quadrupole mass spectrometry for its specific fragmentation product ions. Product ions are at m/z 193, 178, 175, and 134, which are from precursor ion at m/z 355 and retention of 7.2 min with the product ion at m/z 175 having the highest abundance in negative ion mode, as shown the standard curve for FAG in Figure 4.21. The calculation of FAG amount using this method was done by selecting the specific parent ion at m/z 355 and its fragment ion at m/z 175.

In order to calculate the amount of feruloyl glucose represented by the peaks, a standard curve was set-up based on the reaction of recombinant Os9BGlu31 enzyme with ferulic acid and 4NPGlc. The response for the ferulic acid was determined from the control reaction, which was used to determine the amount of ferulic acid in the reaction containing Os9BGlu31 enzyme. Since the wild type recombinant Os9BGlu31 enzyme only produces feruloyl glucose from ferulic acid, the difference between the concentrations of ferulic acid in the control and Os9BGlu31 reactions was taken as the concentration of FAG. The amount of ferulic acid and FAG in 10-fold serial dilutions showed good linearity in the response from 0.000025-0.25 mM, as shown in Figures 4.21 and 4.22. The final concentrations calculated in the flag leaf extracts are shown in Table 4.6. Although no internal standard was included to calculate the absolute levels, the linearity of the standard curve suggests that they should indicate the relative levels in the extracts. The highest amount of FAG accumulated in knockout Os9BGlu31 rice lines when compare with wild type by measuring selected ion abundance from the chromatogram of rice flag leaf extract in Figure 22. Interestingly, *os9bglu31-4* samples were shown to have lower selective ion abundance indicating lower FAG concentrations, which might be explained by the rice flag leaves samples' age. The *osbglu31-4* samples were constructed, harvested, and stored a longer time than the other knockout Os9BGlu31 rice lines. Thus, FAG might be degraded during the storage time between their preparation and the harvesting of the other knockout lines. However, each knockout Os9BGlu31 rice line and its segregated wild type control was grown in parallel and analyzed at the same time, so the data show that all wild type controls had lower FAG when compared with knockout lines.

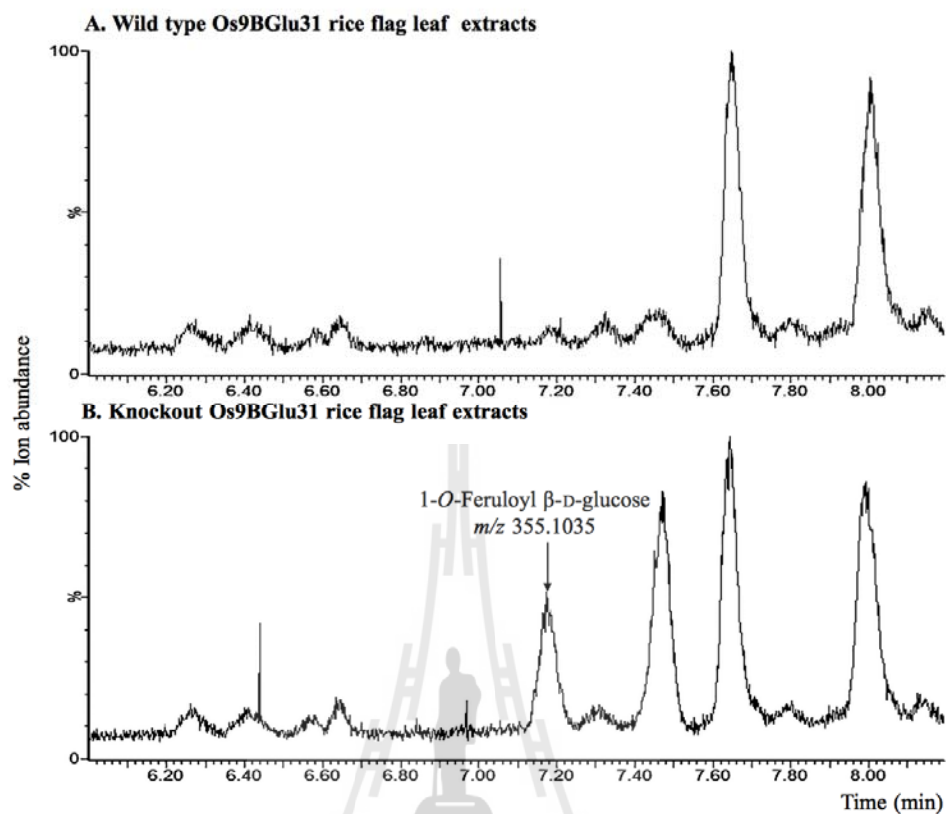


Figure 4.18 The UPLC G2 Q-ToF-MS total ion chromatogram of 70% methanol extracts of wild type (A) and the homozygous Os9BGlu31 knockout line *osbglu31-2* (B) rice flag leaves. 1-O-Feruloyl-β-D-glucose (FAG) was detected with m/z 355.1035 in the knockout Os9BGlu31. FAG is accumulated in the knockout Os9BGlu31 line leaves, but not in wild type.

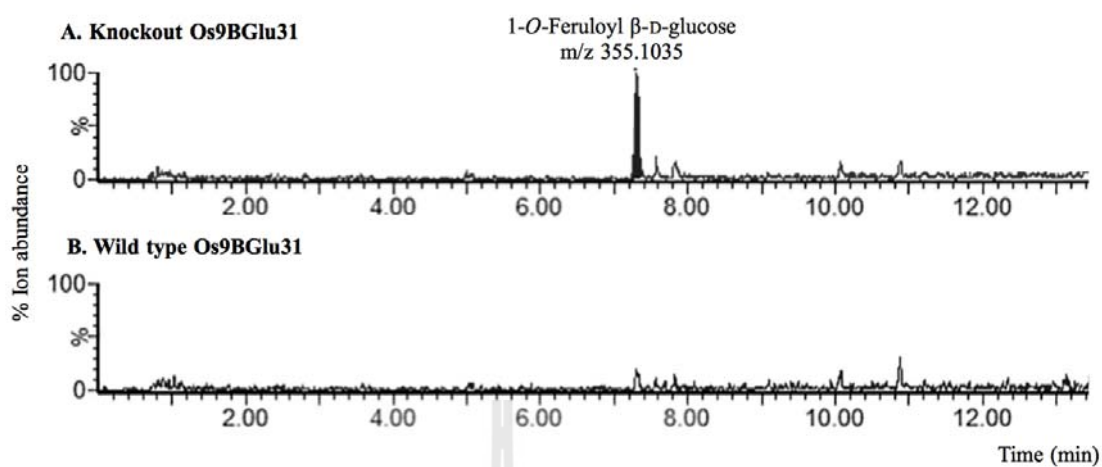


Figure 4.19 The specific selected ion (m/z 355.1035) UPLC G2 Q-ToF-MS chromatogram showing the accumulation of 1-*O*-feruloyl- β -D-glucose (m/z 355.1035) in homozygous knockout line *bglu31-3* (A). A lower amount of FAG was detected in the wild type segregated line (B).



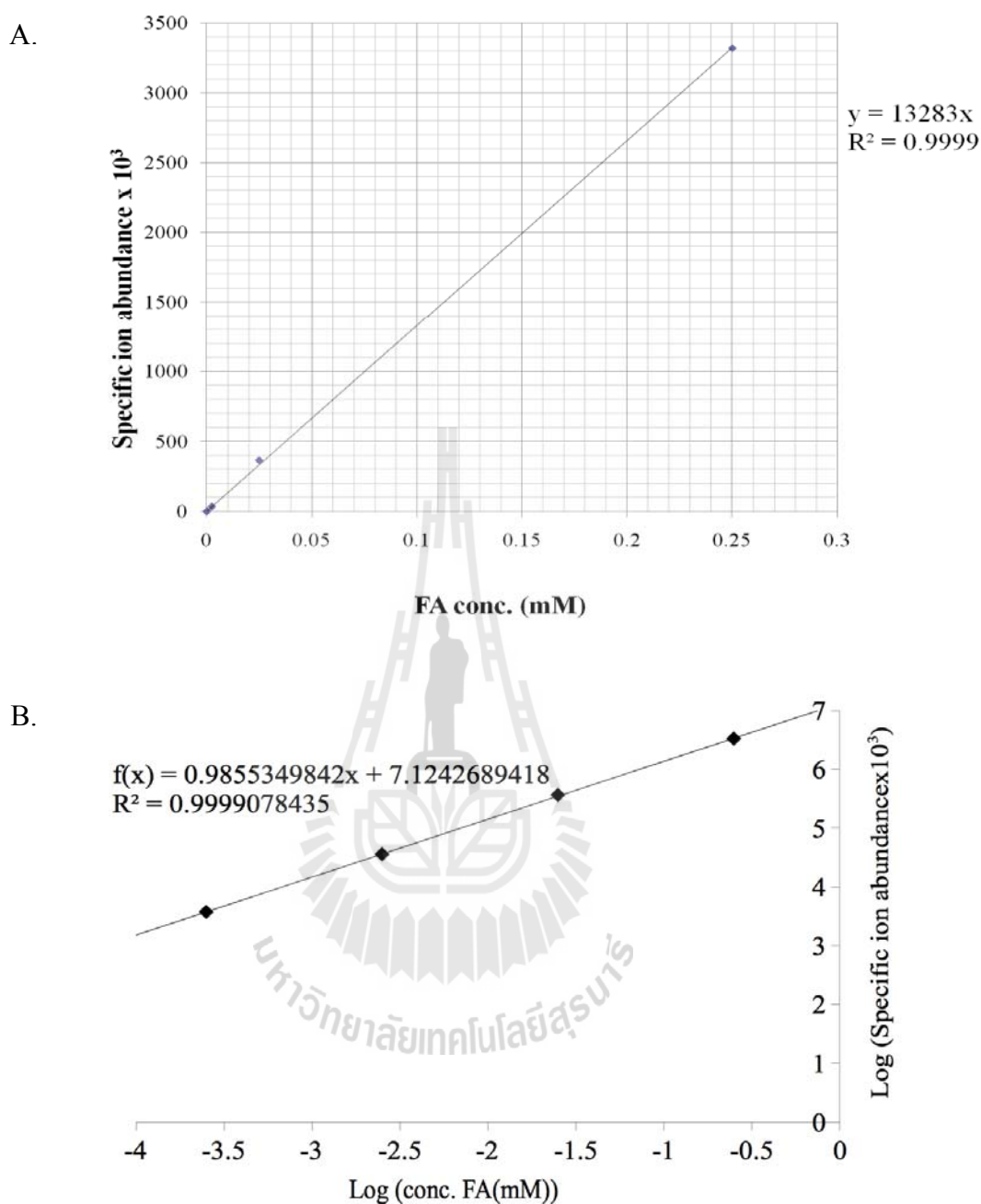


Figure 4.20 The standard curve of specific fragment ion response for ferulic acid concentration at m/z 134 of the normal scale (A) and the log-log scale (B). The curve was made by 10-fold serial dilution of a control reaction containing 0.25 mM ferulic acid with 5 mM 4NPGlc. This curve was used to calculate the amount of ferulic acid in the associated enzymatic reaction in 10-fold dilution.

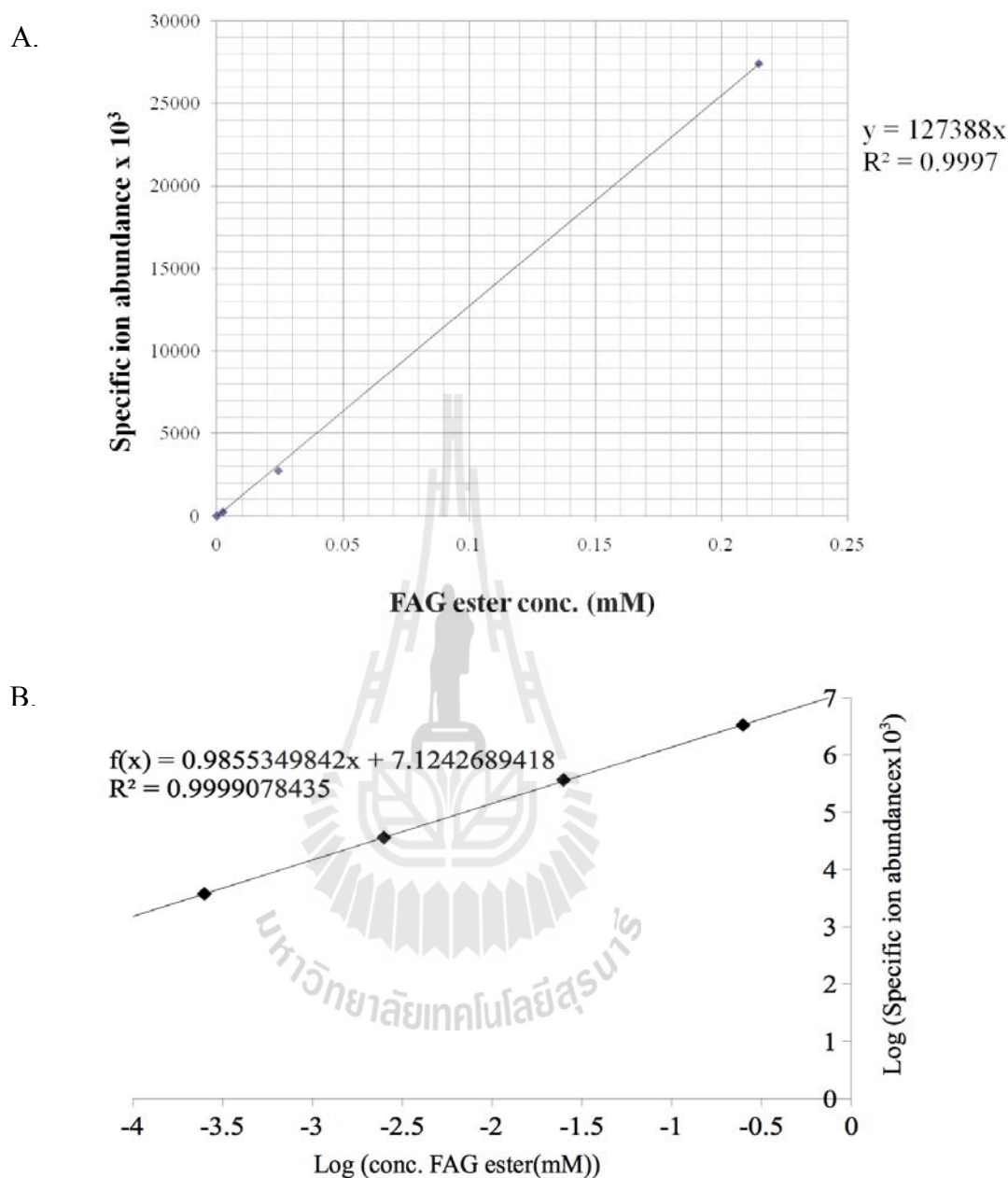


Figure 4.21 The standard curve of specific fragment ion response for 1-*O*-feruloyl β -D-glucoside concentration at *m/z* 175 of the normal scale (A) and the log-log scale (B). The curve was made by 10-fold serial dilution of Os9BGlu31 enzymatic reaction containing 0.25 mM ferulic acid with 5 mM 4NPGlc. This curve was used to calculate the amount of 1-*O*-feruloyl β -D-glucoside in rice flag leaf extracts.

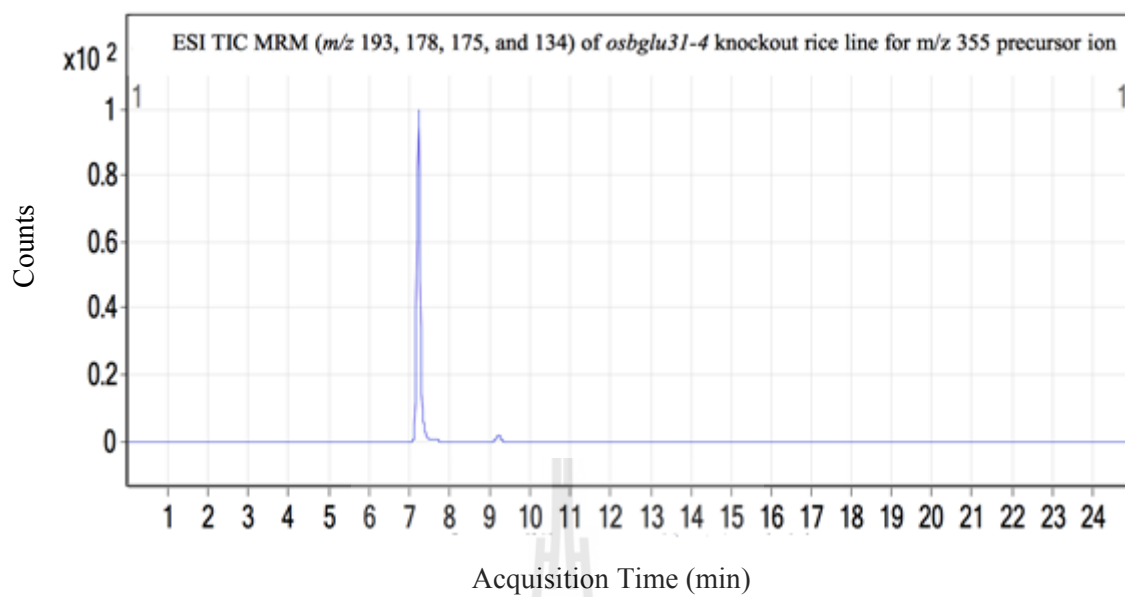


Figure 4.22 The chromatogram from ESI from UPLC MRM triple quadrupole mass spectrometer show in the selected precursor ion at m/z 355 in MRM mode.

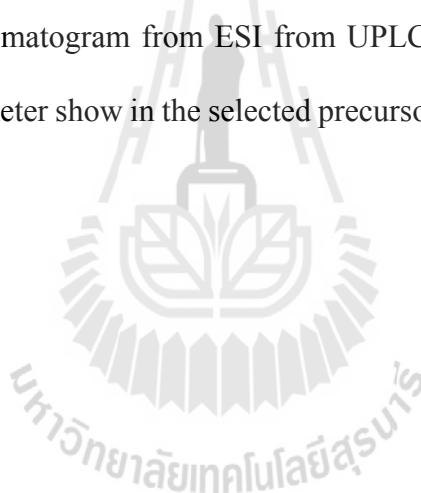


Table 4.4 The 1-*O*-feruoyl- β -D-glucoside (FAG ester) peak areas in UPLC G2-Q-ToF MS for homozygous knockout Os9BGlu31 lines *bglu31-4*, *bglu31-1*, *bglu31-2*, and *bglu31-3* and corresponding wild type segregation lines. Knockouts lacking Os9BGlu31 accumulated FAG ester, which acts as a donor substrate for transglucosylation by Os9BGlu31.

Line	Knockout Os9BGlu31 FAG area (Total ion abundance)	Wild type Os9BGlu31 FAG area (Total ion abundance)
<i>osbglu31-1</i>	69.63	14.25
<i>osbglu31-2</i>	80.09	N.D.
<i>osbglu31-3</i>	483.5	N.D.
<i>osbglu31-4</i>	734.21	N.D.
<i>osbglu31-4(1)</i>	24.89	N.D.
<i>osbglu31-4(2)</i>	22.71	N.D.
<i>osbglu31-4(3)</i>	26.45	N.D.

N.D. means not detectable.



Table 4.5 1-*O*-Feruloyl β -D-glucopyranoside concentration in 70% methanol in water extracts of rice flag leaves determined by UPLC triple quadrupole-MSMS. Each different homozygous knockout Os9BGlu31 gene line is compared to parallel wild type line that segregated from the knockout line in self crossing. All extracts were detected by UPLC triple quadrupole mass spectrometer with the selected parental ion of m/z 355 and product ion at m/z 175 for their relative abundance and specific ion peak areas, and compared to a standard curve of FAG generated by reaction of FA with 4NPGlc to calculate the concentrations in the extracts.

Line	Knockout Os9Bglu31 FAG (μM)	Wild type Os9BGlu31 FAG (μM)
<i>osbglu31-1</i>	11.1	0.875
<i>osbglu31-2</i>	6.94	1.46
<i>osbglu31-3</i>	9.39	1.21
<i>osbglu31-4(1)</i>	6.14	0.393
<i>osbglu31-4(2)</i>	4.18	0.487
<i>osbglu31-4(3)</i>	5.62	0.359

4.9 Rice flag leaf extract as a natural glucose donor substrate for

Os9BGlu31

Rice flag leaf extracts from both wild type and knockout Os9BGlu31 lines can act as glucose donor substrates for recombinant Os9BGlu31 enzyme. To identify potential donor substrates in the extracts, we have characterized the enzymatic transfer of glucose to the synthetic auxin, naphthalene acetic acid (NAA), which is not naturally found in rice. When NAA was added in the reaction for testing the transglucosidase activity, a peak with the mass of triclin 4'-*O*-(guaiacylglyceryl)ether 7-*O*-glucoside was found to decrease in the reaction with active enzyme and NAA acceptor, while the peak for NAA-Glc appeared, as shown in Figure 4.23. This result suggests that triclin 4'-*O*-(guaiacylglyceryl)ether 7-*O*-glucoside acted as a glucose donor substrate of Os9BGlu31. Triclin 4'-*O*-(guaiacylglyceryl)ether 7-*O*-glucoside is a glucoside that matches the m/z 687.1931 (accurate mass) peak that was observed in negative ion mode. The mass spectra of the NAA-glucosyl ester product and the putative triclin 4'-*O*-(guaiacylglyceryl)ether 7-*O*-glucoside substrate donor are shown in Figure 4.24.

Both wild type and knockout Os9BGlu31 rice flag leaf extracts were used as the natural glucose donor substrates. The amounts of NAA-glucosyl ester produced from the wild type and knockout lines were similar, the build-up of FAG in the mutant lines did not appear to contribute as much as other natural glucose donors in the extracts. The results show that Os9BGlu31 enzyme can transfer glucose to NAA acceptor to produce NAA-glucosyl ester by using natural glucose donor substrates other than FAG.

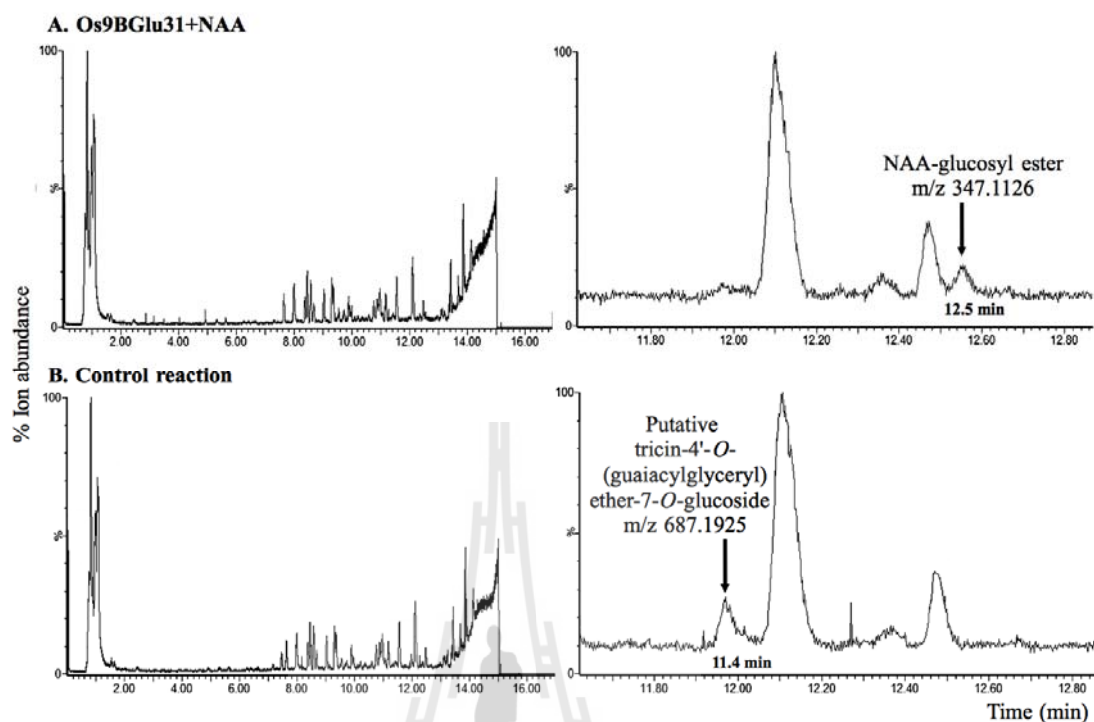


Figure 4.23 The chromatogram of 1-*O*-naphthalene acetic acid β -D-glucose (NAA-glucosyl ester) production from Os9BGlu31 reaction using rice flag leaf extracts as the glucose donor source. The peak of NAA-glucose ester eluted at 12.4 min (A) and a peak with the *m/z* of 687.1925, which corresponds to that of tricetin 4'-*O*-(guaiacylglyceryl)ether 7-*O*-glucoside, eluted at 11.4 min (B).

Table 4.6 1-*O*-NAA-glucosyl (NAA-Glc) ester produced by Os9BGlu31 in *in vitro* enzymatic reactions with rice flag leaf extracts. Fifteen micrograms of wild type Os9BGlu31 recombinant, 5 mg of dried-rice flag leaf 70% methanol extracts, and 0.25 mM 1-naphthalene acetic acid enzyme was incubated at 30 °C, for 3 h and the reaction stopped with 1% formic acid and analyzed by UPLC G2-Q-ToF-MS.

Line	NAA-Glc in knockout (Total ion abundance)	NAA-Glc in WT (Total ion abundance)	NAA-Glc in Control Rxn (Total ion abundance)
<i>osbglu31-1</i>	22.83	24.01	N.D.
<i>osbglu31-2</i>	18.28	16.25	N.D.
<i>osbglu31-3</i>	18.8	20.21	N.D.
<i>osbglu31-4</i>	32.26	29.32	N.D.
<i>osbglu31-4(1)</i>	28.25	25.49	N.D.
<i>osbglu31-4(2)</i>	21.33	19.98	N.D.
<i>osbglu31-4(3)</i>	19.4	21.17	N.D.

N.D. means not detectable.

CHAPTER V

CONCLUSION

The rice (*Oryza sativa*) vacuolar Os9BGlu31 transglucosidase acts to transfer glucosyl moieties between a broad range of phenolic acids, flavonols, and their 1-*O*-acyl- β -D-glucose esters. To investigate the basis for high transglycosylation activity and low hydrolase activity of this enzyme, recombinant Os9BGlu31 and its active-site mutants were expressed and characterized. The W243N mutant has ability to transglucosylate both carboxylic and hydroxyl groups of phenolic acid acceptors, unlike wild type that transglucosylates only the carboxylic group to produce phenolic acid ester. Thus, the W243N mutant was selected to test its activity on multiple hydroxyl groups, including those of kaempferol, from which it can produce monoglucosides and diglucosides with glucosyl substituents at the 3-, 7- and 4' hydroxyls. The residues of the active site cleft, especially W243, play an important role in the specificity of the transglucosidase activity of Os9BGlu31, so the mutation of W243 to other amino acids allowed the enzyme to transfer glucose to multiple hydroxyl groups on the kaempferol aglycone to produce kaempferol glucosides. These results suggest that increasing the polarity of amino acid side chains around the active site could produce higher transglucosidase activity on hydroxyl groups than the wild type enzyme. Due to the limited amounts of these compounds, the fragmentation behavior from ESI-MS/MS mass spectrometry in negative ion mode was used to differentiate the monoglucosides. The strategy and information generated by this analysis allowed the further

identification of kaempferol 3,7-di-*O*-glucoside, kaempferol 4',7-di-*O*-glucoside, and kaempferol 3,4'-di-*O*-glucoside, which allows assessment of these components in reaction mixtures, and may be applied to plant extracts in the future. The identification of Os9BGlu31 W243 as a key residue restricting transglycosylation specificity from this analysis will allow engineering the enzyme for production of products of interest, as well as assessment of the likelihood of substrate specificity in related transglucosidases.

Os9BGlu31 transglucosidase acts to transfer glucosyl moieties between phenolic acids, phytohormones, and flavonoids *in vitro*. This enzyme may act in rice to transfer glucose from donors to acceptors for rice growth, but no evidence for this was previously found in rice. Four homologous T-DNA and Tos17/2 insertions functioned to inactivate the *os9bglu31* gene. All *os9bglu31* knockout lines were used to confirm that rice lacking this enzyme could accumulate enzyme substrates. 1-*O*-Feruloyl- β -D-glucoside (FAG), which has been reported to be a substrate *in vitro* by Luang *et al.* (2013), was found to accumulate in the homozygous knockout lines, which suggests that FAG is the substrate for Os9BGlu31 *in vivo*. Moreover, compounds with masses matching flavonoid glycosides, such as kaempferol glycoside, naringin, rutin, tricetin *O*-glycoside, and peonidine glycoside were found in the extracts and these could be natural substrate donors, acceptors or products. NAA, a synthetic phytohormone that is not naturally found in rice, was added into the reaction to accept glucose transferred from glucose donors by Os9BGlu31. In these reactions, a compound with the mass of tricetin 4'-*O*-(guaiacylglyceryl)ether 7-*O*-glucoside was seen to decrease, suggesting it can serve as a donor substrate, at least *in vitro*. Interestingly, no significant difference was seen in NAA glycosylation between wild type and *os9bglu31* knockout line extracts,

despite much higher levels of FAG in the knockout lines. This suggests that other natural substrate donors, like flavonoids could donate their glucose, although an increase in their aglycone residues were not detected by the mass spectrometry technique. Further work would be facilitated if all compounds in rice were published in the database and their unique standards run on LC-MS, since in this study the identities of some peaks with changing abundance in knockout lines or after enzyme treatment could not be determined.





REFERENCES

REFERENCES

- Ablajan, K., Abliz, Z., Shang, X. Y., He, J. M., Zhang, R. P., and Shi, J. G. (2006). Structural characterization of flavonol 3,7-di-*O*-glycosides and determination of the glycosylation position by using negative ion electrospray ionization tandem mass spectrometry. **J. Mass Spectrom.** 41: 352-360.
- Agard, N. J., and Bertozzi, C. R. (2009). Chemical approaches to perturb, profile, and perceive glycans. **Acc. Chem. Res.** 42: 788-797.
- Aharoni, A., Ric de Vos, C., H, Verhoeven, H. A., Maliepaard, C. A., Kruppa, G., and Bino, R. (2002). Nontargeted metabolome analysis by use of Fourier transform ion cyclotron mass spectrometry. **OMICS.** 6: 217-234.
- Airley, R. E., and Mobasheri, A. (2007). Hypoxic regulation of glucose transport, anaerobic metabolism and angiogenesis in cancer: novel pathways and targets for anticancer therapeutics. **Chemotherapy.** 53: 233-256.
- Baiya, S., Hua, Y. L., Ekkhara, W., and Ketudat Cairns, J. (2014). Expression and enzymatic properties of rice (*Oryza sativa L.*) monolignol β -glucosidase. **Plant Sci.** 227: 101-109.
- Baumann, M. M., Eklöf, J. M., Michel, G., Kalla, Åsa.M. Teeli, T. T., Czjzek, M., and Brumer III, H. (2007). Structural evidence for the evolution of xyloglucanase activity from xyloglucan endo-transglycosylases: biological implications for cell wall metabolism. **Plant Cell.** 19: 1947-1963.
- Boltje, T. J., Buskas, T., and Boons, G. J. (2009). Opportunities and challenges in synthetic oligosaccharide and glycoconjugate research. **Nat. Chem.** 1: 611-622.

- Bowles, D., Lim, E. K., Poppenberger, B., and Vaistij, F. F. (2006). Glycosyltransferases of lipophilic small molecules. **Annu. Rev. Plant Biol.** 57: 567-597.
- Burmeister, W. P., Cottaz, S., Driguez, H., Palmieri, S., and Henrissat, B. (1997). The crystal structures of *Sinapis alba* myrosinase and of a covalent glycosyl-enzyme intermediate provide insights into the substrate recognition and active-site machinery of an S glycosidase. **Structure.** 5: 663-675.
- Butler, M. S. (2008). Natural products to drugs: natural product-derived compounds in clinical trials. **Nat. Prod. Rep.** 25: 475-516.
- Calderón-Montaño, J. M., Burgos-Morón, E., Pérez-Guerrero, E., and López-Lázaro, M. (2011). A Review on the dietary flavonoid kaempferol. **Mini-Rev. Med. Chem.** 11: 298-344.
- Campbell, J. A., Davies, G. J., Bulone, V., and Henrissat, B. (1997). A classification of nucleotide-diphospho-sugar glycosyltransferases based on amino acid sequence similarities. **Biochem. J.** 326: 929-939.
- Cantarel, B. L., Coutinho, P. M., Rancurel, C., Bernard, T., Lombard, V., and Henrissat, B. (2009). The Carbohydrate-Active EnZymes database (CAZy): an expert resource for glycogenomics. **Nucleic Acids Res.** 37: D233-D238.
- Chen, R., Baiya, S., Lee, S., Mahong, B., Jeon, J. S., Ketudat-Cairns, J., and Ketudat-Cairns, M. (2014). Recombinant expression and characterization of the cytoplasmic rice β -glucosidase Os1BGlu4. **PLOS ONE.** 9(5): e96712.
- Chen, W., Gong, L., Guo, Z., Wang, W., Zhang, H., Liu, X., Yu, S., Xiong, L., and Luo, J. (2013). A novel integrated method for large-scale detection, identification,

- and quantification of widely targeted metabolites: application in the study of rice metabolomics. **Mol. Plant.** 6(6): 1769-1780.
- Chuenchor, W., Pengthaisong, S., Robinson, R. C., Yuvaniyama, J., Oonanant, W., Bevan, D. R., Esen, A., Chen, C. J., Opassiri, R., Svasti, J., and Ketudat Cairns, J. R. (2008). Structural insights into rice BGlu1 β -glucosidase oligosaccharide hydrolysis and transglycosylation. **J. Mol. Biol.** 377(4): 1200-1215.
- Chuenchor, W., Pengthaisong, S., Robinson, R. C., Yuvaniyama, J., Svasti, J., and Ketudat Cairns, J. R. (2011). The structural basis of oligosaccharide binding by rice BGlu1 β -glucosidase. **J. Struct. Biol.** 173: 169-179.
- Cipolla, L., and Peri, F. (2011). Carbohydrate-based bioactive compounds for medicinal chemistry applications. **Mini-Rev. Med. Chem.** 11: 39-54.
- Cuyckens, F., and Claeys, M. (2004). Mass spectrometry in the structural analysis of flavonoids. **J. Mass Spectrom.** 39: 1-15.
- Cipolla, L., Araújo, A. C., Bini, D., Gabrielli, L., Russo, L., and Shaikh, N. (2010). Discovery and design of carbohydrate-based therapeutics. **Expert Opin. Drug Discovery.** 5: 721-737.
- Davies, G. J., Ducros, V. M. A., Varrot, A., and Zechel, D. L. (2003). Mapping the conformational itinerary of β -glycosidases by X-ray crystallography. **Biochem. Soc. Trans.** 31: 523-527.
- Dettmer, K., Aronov, P. V., and Hammock, B. D. (2007). Mass spectrometry-based metabolomics. **Mass Spectrom Rev.** 26: 51-57.
- Dong, X., Chen, W., Wang, W., Zhang, H., Liu, X., and Luo, J. (2014). Comprehensive profiling and natural variation of flavonoids in rice. **JIPB.** 56(9): 876-886.

- Eklöf, J. M. and Brumer, H. (2010). The XTH gene family: an update on enzyme structure, function, and phylogeny in xyloglucan remodeling. **Plant Physiol.** 153: 456-466.
- Enzyme Nomenclature Committee. (1992). **Recommendation of the nomenclature committee of the international union of biochemistry and molecular biology (IUBMB)**, Academic Press, New York, NY.
- Eom, J. S., Cho, J. I., Reinders, A., Lee, S. W., Yoo, Y., Tuan, P. Q., Choi, S. B., Bang, G., Park, Y. I., and Cho, M. H. (2011). Impaired function of the tonoplast-localized sucrose transporter in rice, OsSUT2, limits the transport of vacuolar reserve sucrose and affects plant growth. **Plant Physiol.** 157: 109-119.
- Fabre, N., Rustan, I., de Hoffmann, E., and Quetin-Leclerc, J. (2001). Determination of flavone, flavonol, and flavonone aglycones by negative ion liquid chromatography electrospray ion trap mass spectrometry. **J. Am. Soc. Mass Spectrom.** 12: 707-715.
- Fernie, A. R., Trethewey, R. N., Krotzky, A. J., and Willmitzer, L. (2004). Metabolite profiling: from diagnostics to systems biology. **Nat. Rev. Mol. Cell Biol.** 5: 763-769.
- Fettke, J., Chia, T., Eckermann, N., Smith, A., and Steup, M. (2006). A transglucosidase necessary for starch degradation and maltose metabolism in leaves at night acts on cytosolic heteroglycans (SHG). **J. Plant Physiol.** 46(4): 668-684.
- Fiehn, O., Kopka, J., Dormann, P., Altmann, T., Trethewey, R. N., and Willmitzer, L. (2000). Metabolite profiling for plant functional genomics. **Nat. Biotechnol.** 18: 1157-1161.

- Fossen, T. and Andersen, O. M. (2006). **Spectroscopic techniques applied to flavonoids. Flavonoids: Chemistry, Biochemistry and Applications.** Boca Raton; CRC Press. 37-142.
- Franceschi, P., Dong, Y., Strupat, K., Vrhovsek, U., and Mattivi, F. (2012). Combining intensity correlation analysis and MALDI imaging to study the distribution of flavonols and dihydrochalcones in golden delicious apples. **J. Exp. Bot.** 63: 1123-1133.
- Gantt, R. W., Peltier-Pain, P., and Thorson, J. S. (2011). Enzymatic methods for glycol (diversification/randomization) of drugs and small molecules. **Nat. Prod. Rep.** 28: 1811-1853.
- Gaynor, J. D., Buttery, B. R., Buzzell, R. I., and Mac Tavish, D. C. (1988). HPLC separation and relative of kaempferol glycosides in soybean. **Chromatographia.** 25: 1049-1053.
- Gong, L., Chen, W., Gao, Y., Liu, X., Zhang, H., Xu, C., Yu, S., Zhang, Q., and Luo, J. (2013). Genetic analysis of the metabolome exemplified using a rice population. **Proc. Natl. Acad. Sci. USA.** 110: 20320-20325.
- Grata, E., Guillarme, D., Gleuser, G., Broccard, J., Carrupt, P., Veuthey, J., Rudaz, S., and Walfender, J. (2009). Metabolite profiling of plant extracts by ultra-high-pressure liquid chromatography at elevated temperature coupled to time-of-flight mass spectrometry. **J. Chromatogr. A.** 1216: 5660-5668.
- Hart, G. W., Slawson, C., Ramirez-Correa, G., and Lagerlof, O. (2011). Cross talk between O GlcNAcylation and phosphorylation: roles in signaling, transcription, and chronic disease. **Annu. Rev. Biochem.** 80: 825-858.

- Henrissat, B. (1991). A classification of glycosyl hydrolases based on amino acid sequence similarities. **Biochem. J.** 280: 309-316.
- Henrissat, B., Callebaut, I., Fabrega, S., Lehn, P., Mornon J. P, Davies G. (1995). Conserved catalytic machinery and the prediction of a common fold for several families of glycosyl hydrolases. **Proc. Natl. Acad. Sci. U.S.A.** 92: 7090-7094.
- Henrissat, B., and Davies, G. J. (1997). Structural and sequence-based classification of glycosyl hydrolases. **Curr. Opin. Struct. Biol.** 7: 637-644.
- Henrissat, B., and Davies, G. J. (2000). Glycoside hydrolases and glycosyltransferases. Families, modules, and implications for genomics. **Plant Physiol.** 124: 1515-1519.
- Hutchison, C. A., and Edgell, M. H. (1971). Genetic assay for small fragments of bacteriophage ϕ X174 deoxyribonucleic acid. **J. Virol.** 8: 181-189.
- Hvattum, E., and Ekeberg, D. (2003). Studying of the collision-induced radical cleavage of flavonoid glycosides using negative electrospray ionization tandem quadrupole mass spectrometry. **J. Mass Spectrom.** 38: 43-49.
- Irakli, M. N., Samanidou, V. F., Biliaderis, C. G., and Papadoyannis, I. N. (2012). Simultaneous determination of phenolic acids and flavonoids in rice using solid-phase extraction and RP-HPLC with photodiode array detection. **J. Sep. Sci.** 35: 1603-1611.
- Izawa, T., and Shimamoto, K. (1996) Becoming a model plant: The importance of rice to plant science. **Trends Plant Sci.** 1: 95-99.
- Jung, E. S., Lee, S., Lim, S., Ha, S., and Lee, C. (2013). Metabolite profiling of the short term responses of rice leaves (*Oryza sativa* cv. Ilmi) cultivated under different

- LED lights and its correlations with antioxidant activities. **Plant Sci.** 210: 61-69.
- Jeon, J. S., Lee, S., Jung, K. H., Jun, S. H., Jeong, D. H., Lee, J., Kim, C., Jang, S., Yang, K., and Nam, J. (2000). T-DNA insertional mutagenesis for functional genomics in rice. **Plant J.** 22:561-570.
- Jeong, D. H., An, S. Y., Kang, H. G., Moon, S., Han, J. J., Park, S., Lee, H. S., An, K. S., An, G. H. (2002). T-DNA insertional mutagenesis for activation tagging in rice. **Plant Physiol.** 130: 1636-1644.
- Ketudat-Cairns, J. R., and Esen, A. (2010). β -Glucosidases. **Cell. Mol. Life Sci.** 67: 3389-3405.
- Ketudat Cairns, J. R., Pengthaisong, S., Luang, S., Sansenya, S., Tankrathok, A., and Svasti, J. (2012). Protein-carbohydrate interactions leading to hydrolysis and transglycosylation in plant glycoside hydrolase family 1 enzymes. **J. Appl. Glycosci.** 458: 2011-2022.
- Kiessling, L. L., and Splain, R. A. (2010). Chemical approaches to glycobiology. **Ann. Rev. Biochem.** 79, 619-653.
- Kim, J. W., and Dang, C. V. (2006). Cancer's molecular sweet tooth and the Warburg effect. **Cancer Res.** 66: 8927-8930.
- Koes, R. E., Quattrocchio, F., and Mol, J. N. M. (1994). The flavonoid biosynthetic pathway in plants: Function and evolution. **BioEssays.** 16: 123-132.
- Koshland, D. E., Jr. (1953). Stereochemistry and mechanism of enzymatic reaction. **Biol. Rev.** 28: 416-436.
- Krege, N., Simoni, R. D., and Hill, R. L. (2006). The development of site-directed mutagenesis by Micheal Smith. **J. Biol. Chem.** 281(39): e31.

- Krishnan, P., Kruger, N. J., and Ratcliffe, R. G. (2005). Metabolite fingerprinting and profiling in plants using NMR. **J. Exp. Bot.** 56: 255-265.
- Kristensen, C., Morant, M., Olsen, C. E., Ekstrom, C. T., Galbraith, D. W., and Moller, B. L. (2005). Metabolic engineering of dhurrin in transgenic Arabidopsis plants with marginal inadvertent effects on the metabolome and transcriptome. **Proc. Natl. Acad. Sci. U.S.A.** 102: 1779-1784.
- Kaur, J., and Sharma, R. (2006). Directed evolution an approach to engineer enzymes. **Crit. Rev. Biotechnol.** 26: 165-199.
- Kusano, M., Fukushima, A., Kobayashi, M., Hayashi, N., Jonsson, P., and Moritz, T. (2007). Application of a metabolomic method combining one-dimensional and two-dimensional gas chromatography time-of-flight/mass spectrometry to metabolic phenotyping of natural variants in rice. **J. Chromatogr. B Anal. Tech. Biomed. Life Sci.** 855: 71-79.
- Kunkel, T. A. (1985). **Proc. Natl. Acad. Sci. U.S.A.** 82(2):488-492. PMID: 3881765
- Lairson, L. L. and Withers, S. G. (2004). Mechanistic analogies amongst carbohydrate modifying enzymes. **Chem. Commu.** 20: 2243-2248.
- Lairson, L. L., Henrissat, B., Davies, G. J., and Withers, S. G. (2008). Glycosyltransferases: structures, functions, and mechanisms. **Ann. Rev. Biochem.** 77: 521-555.
- Lee, S. S, Hong, S. Y., Errey, J. C., Izumi, A., Davies, G. J., and Davis, B. G. (2011). Mechanistic evidence for a front-side, S_Ni-type reaction in a retaining glycosyltransferase. **Nat. Chem. Biol.** 7: 631-638.
- Lepenies, B., Yin, J., and Seeberger, P. H. (2010). Applications of synthetic carbohydrates to chemical biology. **Curr. Opin. Chem. Biol.** 14: 404-411.

- Lisec, J., Schauer, N., Kopka, J., Willmitzer, L., and Fernie, A. R. (2006). Gas chromatography mass spectrometry-based metabolite profiling in plants. **Nat. Protoc.** 1: 387-396.
- Luang, S., Cho, J. I., Mahong, B., Opassiri, R., Akiyama, T., Phasai, K., Komvongsa, J., Sasaki, N., Hua, Y. L., Matsuba, T., Ozeki, Y., Jeon, J. S., and Ketudat Cairns, J. R. (2013). Rice Os9BGlu31 is a transglucosidase with the capacity to equilibrate phenylpropanoid, flavonoid, and phytohormone glycoconjugates. **J. Biol. Chem.** 288: 10111-10123.
- Luang, S., Hrmova, M., and ketudat-cairns, J. R. (2010). High-level expression of barley beta D-glucan exohydrolase HvExoI from a codon-optimized cDNA in *Pichia pastoris*. **Protein Expr. Purif.** 73(1): 90-98.
- Luczkiewicz, M., Glod, D., and Bucinski, T. A. (2004). LC-DAD UV and LC-MS for the analysis of isoflavonoids and flavones from *in vitro* and *in vivo* biomass of *Genista tinctoria* L. **Chromatographia.** 60: 179-185.
- Ly, H. D. and Withers, S. G. (1999). Mutagenesis of glycosidases. **Ann. Rev. Biochem.** 68: 487-522.
- Macheda, M. L., Rogers, S., and Best, J. D. (2005). Molecular and cellular regulation of glucose transporter (GLUT) proteins in cancer. **J. Cell. Physiol.** 202: 654-662.
- Mackenzie, L. F., Wang, Q. P., Warren, R. A. J., and Withers, S. G. (1998). Chemical and biological approach. **J. Am. Chem. Soc.** 120: 5583-5584.
- March, R. and Brodbelt, J. (2008). Analysis of flavonoids: tandem mass spectrometry, computational methods, and NMR. **J. Mass. Spectrom. Ion Physics.** 43: 1581-1617.

- Matsuba, Y., Sasaki, N., Tera, M., Okamura, M., Abe, Y., Okamoto, E., Nakamura, H., Funabashi, H., Takatsu, M., Saito, M., Matsuoka, H., Nagasawa, K., and Ozeki, Y. (2010). A novel glucosylation reaction on anthocyanins catalyzed by acyl glucose-dependent glucosyltransferase in the petals of carnation and delphinium. **Plant Cell**. 22: 3374-3389.
- Matsuda, F., Hirai, M. Y., Sasaki, E., Ariyama, K., Yonekura-sakakibara, K., Provar, N. J., Sakurai, T., Shimada, Y., and Saito, K. (2010). AtMetExpress development: a phytochemical atlas of Arabidopsis development. **Plant Physiol**. 152: 566-578.
- Matsuda, F., Okazaki, Y., Oikawa, A., Kusano, M., Nakabayashi, R., Kikuchi, J., Yonemaru, J. I., Ebana, K., Yano, M., and Saito, K. (2012). Dissection of genotype-phenotype associations in rice grains using metabolome quantitative trait loci analysis. **Plant J**. 70: 624-636.
- Matsuda, F., Yonekura-Sakakibara, K., Niida, R., Kuromori, T., Shinozaki, K., and Saito, K. (2009). MS/MS Spectral tag-based annotation of non-targeted profile of plant secondary metabolites. **Plant J**. 57: 555-577.
- McCarter, J. and Withers, S. G. (1994). Mechanisms of enzymatic glycoside hydrolysis. **Curr. Opin. Struct. Biol**. 4: 885-892.
- Miyahara, T., Sakiyama, R., Ozeki, Y., and Sasaki, N. (2013). Acyl-glucose-dependent glucosyltransferase catalyzes the final step of anthocyanin formation in *Arabidopsis*. **J. Plant Physiol**. 170: 619-624.
- Miyao, A., Tanaka, K., Murata, K., Sawaki, H., Takeda, S., Abe, K., Shinozuka, Y., Onosato, K., and Hirochika, H. (2003). Target site specificity of the Tos17 retrotransposon shows a preference for insertion within genes and against

- insertion in retrotransposon-rich regions of the genome. **Plant Cell**. 15: 1771-1780.
- Moco, S., Bino, R. J., Vorst, O., Verhoeven, H. A., de Groot, J., and van Beek, T. A. (2006). A liquid chromatography-mass spectrometry-based metabolome database for tomato. **Plant Physiol**. 141: 1205-1218.
- Moellering, E. R., Muthan, B., and Benning, C. (2010). Freezing tolerance in plants requires lipid remodeling at the outer chloroplast membrane. **Science**. 330: 226-228.
- Moracci, M. Trincone, A., Perugino, G., Ciaramella, M., and Rossi M. (1998). Restoration of the activity of active-site mutants of the hyperthermophilic β -glycosidase from *Sulfolobus solfataricus*: dependence of the mechanism on the action of external nucleophiles. **Biochem**. 37: 17262-17270.
- Murray, M. G., and Thompson, W. F. (1980). Rapid isolation of high molecular-weight plant DNA. **Nucleic Acids Res**. 8: 4321-4325.
- Moellering, E. R., and Benning, C. (2010). Galactoglycerolipid metabolism under stress: a time for remodeling. **Trends Plant Sci**. 16 (2): 98-107.
- Nishizaki, Y., Yasunaga, M., Okamoto, E. Okamoto, M., Hirose, Y., Yamaguchi, M., Ozeki, Y., and Sasaki, N. (2013). p-Hydroxybenzoyl-glucose Is a zwitter donor for the biosynthesis of 7-polyacylated anthocyanin in delphinium. **Plant Cell**. 25: 4150-4165.
- Nijveldt, R. J., van Nood, E., van Hoorn, D. E. C., Boelens, P. G., van Norren, K., and van Leeuwen, P. A. M. (2001). Flavonoids: a review of probable mechanisms of actions and potential applications. **J. Clin. Nutr**. 74:397-418.

- Newman, D. J. and Cragg, G. M. (2007). Natural products as sources of new drugs over the last 25 years. **J. Nat. Prod.** 70: 461-477.
- Nakamura, Y., Kimura, A., Saga, H., Oikawa, A., Shinbo, Y., and Kai, K. (2007). Differential metabolomics unraveling light/dark regulation of metabolic activities in *Arabidopsis* cell culture. **Plant J.** 227: 57-66.
- Oikawa, A., Matsuda, F., Kusano, M., Okazaki, Y., and Saito, K. (2008). Rice Metabolomics. **Rice.** 1: 63-71.
- Oikawa, A., Nakamura, Y., Ogura, T., Kimura, A., Suzuki, H., and Sakurai, N. (2006). Clarification of pathway-specific inhibition by Fourier transform ion cyclotron resonance/mass spectrometry-based metabolic phenotyping studies. **Plant Physiol.** 142: 398-413.
- Opassiri, R., Hua, Y., Wara-Aswapati, O., Akiyama, T., Svasti, J., Esen, A., and Ketudat Cairns, J. R. (2004). β -Glucosidase, exo- β -glucanase and pyridoxine transglucosylase activities of rice BGlu1. **Biochem. J.** 379: 125-131.
- Opassiri, R., Ketudat Cairns, J. R., Akiyama, T., Wara-Aswapati, O., Svasti, J., and Esen, A. (2003). Characterization of a rice β -glucosidase highly expressed in flower and germinating shoot. **Plant Sci.** 165: 627-638.
- Opassiri, R., Pomthong, B., Onkoksoong, T., Akiyama, T., Esen, A., and Ketudat-Cairns, J. R. (2006). Analysis of rice glycosyl hydrolase family 1 and expression of Os4BGlu12 beta-glucosidase. **BMC Plant Biol.** 6: 33.
- Piens, K., Fauré, R., Sundqvist, G., Baumann, M. J., Saura-Valls, M., Teeri, T. T., Cottaz, S., Planas, A., Drigues, H., and Brumer, H. (2008). Mechanism-based labeling defines the free energy change for formation of the covalent

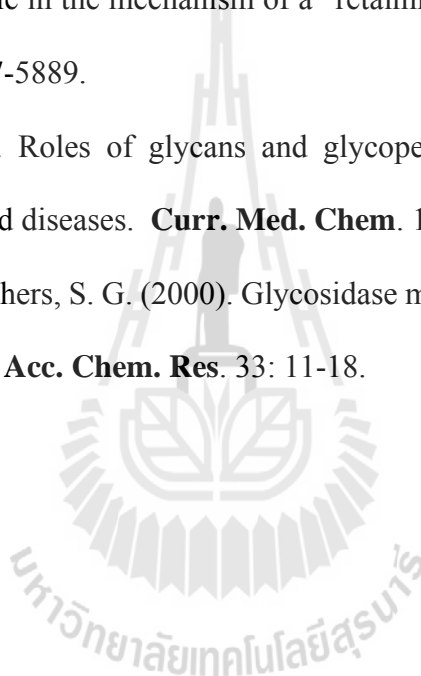
- glycosyl-enzyme intermediate in a xyloglucan endo-transglycosylase. **J. Biol. Chem.** 32: 21864-21872.
- Placic, M. M., and Sujino, K. (2009). Assays for glycosyltransferases. **Trends Glycosci. Glycotechnol.** 13: 361-370.
- Prasain, J. K., Wang, C. C., and Barnes, S. (2004). Mass spectrometric methods for the determination of flavonoids in biological samples. **Free Radical Biol. Med.** 37: 1324-1350.
- Raychaudhuri, A. and Tipton, P. A. (2002). Cloning and expression of the gene for soybean hydroxyisourate hydrolase. Localization and implications for function and mechanism. **Plant Physiol.** 130: 2061-2068.
- Riggi, E., Avola, G., Siracusa, L., and Ruberto, G. (2013). Flavonol content and biometrical traits as a tool for the characterization of “Cipolla di Giarratana”: A traditional Sicilian onion landrace. **Food Chem.** 140: 812-816.
- Rora, A., and Nair M. G. (1998). Structure-activity relationships for antioxidant activities of a series of flavonoids in a liposomal system. **Free Radical Biol. Med.** 24: 13-55.
- Routaboul, J. M., Dubos, C., Beck, G., Marquis, C., Bidzinski, P., Loudet, O., and Lepiniec, L. (2012). Metabolite profiling and quantitative genetics of natural variation for flavonoids in Arabidopsis. **J. Exp. Bot.** 63: 3749-3764.
- Rudd, P. M., Elliott, T., Cresswell, P., Wilson, I. A., and Dwek, R. A. (2001). Glycosylation and the immune system. **Science.** 291: 2370-2376.
- Sansenya, S., Maneesan, J., and Ketudat Cairns, J. R. (2012). Exchanging a single amino acid residue generates or weakens a +2 cello-oligosaccharide binding subsite in rice β -glucosidases. **Carbohydr. Res.** 351: 130-133.

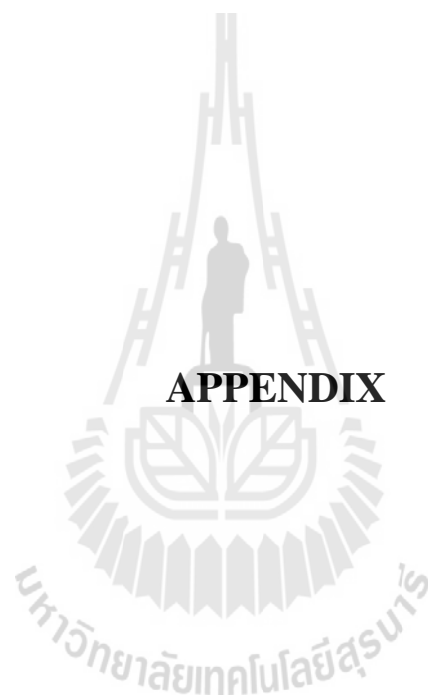
- Sato, S., Soga, T., Nishioka, T., and Tomita, M. (2004). Simultaneous determination of the main metabolites in rice leaves using capillary electrophoresis mass spectrometry and capillary electrophoresis diode array detection. **Plant J.** 40: 151-163.
- Schijlen, E. G. W., de Vos, C. H. R., van Tunen, A. J., and Bovy, A. G. (2004). Modification of flavonoid biosynthesis in crop plants. **Phytochem.** 65: 2631-2648.
- Sekiyama, Y. and Kikuchi, J. (2007). Towards dynamic metabolic network measurements by multidimensional NMR-based fluxomics. **Phytochem.** 68: 2320-2329.
- Seshadri, S., Akiyama, T., Opassiri, R., Kuaprsert, B., and Ketudat Cairns, J. R. (2009). Structural and enzymatic characterization of Os3BGlu6, a rice β -glucosidase hydrolyzing hydrophobic glycosides and (1 \rightarrow 3) and (1 \rightarrow 2)-linked disaccharides. **Plant Physiol.** 151: 47-58.
- Sharma, R., Cao, P., Jung, K. H., Sharma, M., Ranold, P. C. (2013). Construction of a rice glycoside hydrolase phylogenetic tree and identification of target for biofuel research. **Plant Sci.** 330(4): 1-15.
- Singh, S., Phillips, G. N. and Thorson, J. S. (2012). The structural biology of enzymes involved in natural product glycosylation. **Nat. Prod. Rep.** 29: 1201-1237.
- Sinseadka, T., Wongpornchai, S., and Rayanakorn, M. (2010). Quantification of flavonoids in black rice by liquid chromatography negative electrospray ionization tandem mass spectrometry. **J. Agri. Food Chem.** 60: 11723-11732.
- Siudak, G. (2003). **The expanding role in mass spectrometry in biotechnology.** MCC Press. San Diego. CA, USA. 67.

- Staack, R. F., Varesio, E., and Hopgarther, G. (2005). The combination of liquid chromatography/tandem mass spectrometry and chip-based infusion for improve screening and characterization of drug metabolite. **Mass Spectrom.** 19: 618-623.
- Staszko, A., Swarczewicz, B., Banasiak, J., Muth, D., asinski, M., and Stobiecki, M. (2011). LC/MS profiling of flavonoid glycoconjugates isolated from hairy roots, suspension root cell cultures and seedling roots of *Medicago truncatula*. **Metabolomics.** 7: 604-613.
- Stobiecki, M. and Kachlicki, P. (2006). Isolation and identification of flavonoids. In E. Grotewold (Ed.), **The Science of Flavonoids**. Springer, New York. 47-70.
- Takahashi, H., Hayashi, M., Goto, F., Sato, S., Soga, T., and Nishioka, T. (2006). Evaluation of metabolic alteration in transgenic rice over-expressing dihydroflavonol-4 -reductase. **Ann. Bot. (London).** 98: 819-825.
- Tanphanuch, W., Chantarangsee, M., Maneesan, J., and Ketudat-Cairns, J. R. (2008). Genomic and expression analysis of glycosyl hydrolase family 35 genes from rice (*Oryza sativa* L.). **BMC Plant Biology.** 8: 78-84.
- Teze, D., Hendrickx, J., Czjzek, M., Ropartz, D., Sanejouand, Y. H., Tran, V., Tellier, C., Dion, M. (2013). Semi rational approach for converting a GH1 β -glycosidase into a β -transglucosidase. **Protein Eng. Des. Sel.** 27(1): 13-19.
- Thibodeaux, C. J., Melançon III, C. E., and Li u, H. W. (2008). Natural-product sugar biosynthesis and enzymatic glycodiversification. **Angew. Chem. Int. Ed. Eng.** 47: 9814-9859.
- Toonkool, P., Metheenukul, P., Sujiwattanasat, P., Paiboon, P., Tongtubtim, N., Ketudat Cairns, M., Ketudat Cairns, J., and Svasti, J. (2006). Expression and

- purification of dalcocinase, a β -glucosidase from *Dalbergia cochinchinensis* Pierre, in yeast and bacterial hosts. **Protein Expr. Purif.** 48: 195-204.
- Urban, A., Neukirchen, S., and Jaegen, K. E. (1997). A rapid and efficient method for site-directed mutagenesis using one-step overlap extension PCR. **Nucleic Acids Res.** 25(11): 2227-2228.
- Varki, A., and Chrispeels, M. J. (1999). **Essentials of Glycobiology**. Cold Spring Harbor Laboratory Press, Cold Spring Harbor, N.Y. 253.
- Wang, L. X., and Huang, W. (2009). Enzymatic transglycosylation for glycoconjugate synthesis. **Curr. Opin. Chem. Biol.** 13: 592-600.
- Wang, Q., and Withers, S. G. (1995). Substrate-assisted catalysis in glycosidases. **J. Am. Chem. Soc.** 117: 10137-10138.
- Wang, Y., Tang, L., He, Y. Q., Wang, C. H., Welbeck, E. W., Bligh, S. W., Wang, Z. T. (2008). Characterization of fifty-one flavonoids in a Chinese herbal prescription longdan xiegon detetion by high-performance liquid chromatography coupled to electrospray ionization tandam mass spectrometry and photodiode array detection. **Rapid Commun. Mass Spectrom.** 22(12): 1767-1778.
- Want, E. J., Cravatt, B. F., and Suizdak, G. (2005). The expanding role of mass spectrometry in metabolite profiling and characterization. **Mini Rev.** 6: 1941-1951.
- Wei, C., Liang, G., Zilong, G., Wensheng, W., Hongyan, Z., Xianqing, L. Sijin., Y. Lizhong, X., Jie. L. (2013). A novel integrated method for large-scale detection, identification and quantification of widely-targeted metabolites: Application in study of rice metabolomics. **Mol. Plant.** 6(6): 1769-1780.

- Wei, J., Xun, L., Yang, L., Yang, G., Fu, L., Yang, L., Wang, J., Gao, J., Cheng, S., Duan, Q., and Li, H. (2013). Glycosynthase with broad substrate specificity – an efficient biocatalyst for the construction of oligosaccharide library. **Eur. J. Org. Chem.** 138: 2412-2419.
- Withers, S. G., Warren, R. A. J., Street, I. P., Rupitz, K., Kempton, J. B., and Aebersold, R. (1990). Unequivocal demonstration of the involvement of a glutamate residue as a nucleophile in the mechanism of a “retaining” glycosidase. **J. Am. Chem. Soc.** 112: 5887-5889.
- Zhang, X. L. (2006). Roles of glycans and glycopeptides in immune system and immune-related diseases. **Curr. Med. Chem.** 13: 1141-1161.
- Zechel, D. L., and Withers, S. G. (2000). Glycosidase mechanisms: anatomy of a finely tuned catalyst. **Acc. Chem. Res.** 33: 11-18.





APPENDIX

Luang, S., Cho, J. I., Mahong, B., Opassiri, R., Akiyama, T., Phasai, K., **Komvongsa, J.**, Sasaki, N., Hua, Y. L., Matsuba, T., Ozeki, Y., Jeon, J. S., and Ketudat Cairns, J. R. (2013). Rice Os9BGlu31 is a transglucosidase with the capacity to equilibrate phenylpropanoid, flavonoid, and phytohormone glycoconjugates. **J. Biol. Chem.** 288(11): 10111-10123.



CURRICULUM VITAE

NAME Ms. Juthamath Komvongsa

DATE OF BIRTH May 27, 1983

PLACE OF BIRTH Nakhon Phanom

EDUCATION

2009-2014 School of Biochemistry, Institute of Science, Suranaree
University of Technology, Nakhon Ratchasima,
Thailand.

Ph.D. in Biochemistry

2007 Faculty of Pharmacy, Rangsit University, Phatumthani,
Thailand (1st class honors).

B.Sc. in Pharmaceutical Science

SCHOLARSHIP

2009-2014 The Royal Golden Jubilee (RGJ) Ph.D. Scholarship from The
Thailand Research Fund, Thailand.